

การตรวจสอบทางทฤษฎีของสมบัติการรับรู้แก้สของแผ่นนาโนซิงก์ออกไซด์



นางสาวเบญจวรรณ แก้วรักษา

ศูนย์วิทยทรัพยากร
จุฬาลงกรณ์มหาวิทยาลัย

วิทยานิพนธ์นี้เป็นส่วนหนึ่งของการศึกษาตามหลักสูตรปริญญาวิทยาศาสตรมหาบัณฑิต

สาขาวิชาเคมี ภาควิชาเคมี

คณะวิทยาศาสตร์ จุฬาลงกรณ์มหาวิทยาลัย

ปีการศึกษา 2553

ลิขสิทธิ์ของจุฬาลงกรณ์มหาวิทยาลัย

THEORETICAL INVESTIGATION OF GAS-SENSING PROPERTIES OF ZnO
NANOSHEETS

Miss Benjawan Kaewrukso

ศูนย์วิทยทรัพยากร
จุฬาลงกรณ์มหาวิทยาลัย

A Thesis Submitted in Partial Fulfillment of the Requirements
for the Degree of Master of Science Program in Chemistry

Faculty of Science


Chulalongkorn University

Academic Year 2010

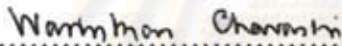
Copyright of Chulalongkorn University

Thesis Title THEORETICAL INVESTIGATION OF GAS-
SENSING PROPERTIES OF ZnO NANOSHEETS
By Miss Benjawan Kaewrukxa
Field of study Chemistry
Thesis Advisor Associate Professor Vithaya Ruangpornvisuti, Dr.rer.nat.


Accepted by the Faculty of Science, Chulalongkorn University in Partial
Fulfillment of the Requirements for the Master's Degree

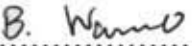

.....Dean of the Faculty of Science
(Professor Supot Hannongbua, Dr.rer.nat.)

THESIS COMMITTEE


.....Chairman
(Assistant Professor Warinthorn Chavasiri, Ph.D.)


.....Thesis Advisor
(Associate Professor Vithaya Ruangpornvisuti, Dr.rer.nat.)


.....Examiner
(Associate Professor Pornthep Sompornpisut, Ph.D.)


.....External Examiner
(Banchob Wann, Ph.D.)

เบญจวรรณ แก้วรักษา : การตรวจสอบทางทฤษฎีของสมบัติการรับรู้แก๊สของแผ่นนาโนซิงก์ออกไซด์. (THEORETICAL INVESTIGATION OF GAS-SENSING PROPERTIES OF ZnO NANOSHEETS) อ. ที่ปรึกษาวิทยานิพนธ์หลัก: รศ. ดร. วิทยา เรืองพรวิสุทธิ์, 87 หน้า.

ศึกษาทุกโครงสร้างที่เหมาะสมของการดูดซับโมเลกุลแก๊สได้แก่ ออกซิเจน คาร์บอนมอนอกไซด์ ไนตริกออกไซด์ ไนโตรเจนไดออกไซด์ ไนตรัสออกไซด์ แอมโมเนีย ไฮโดรเจน และน้ำ ที่ถูกดูดซับบนซิงก์ออกไซด์นาโนคลัสเตอร์ (ZnONC) ได้แก่ ชนิดคล้าย แอลูมิเนียม (AL-ZnONC) แนฟทาลีน (NLL-ZnONC) ไพรีน (PRL-ZnONC) และแผ่นนาโนซิงก์ออกไซด์ชนิดคล้ายกราฟีน (ZnOGLNS) ได้แก่ โคลโลนีน (CNL-ZnONS) และเซอควัมโคโรนีน (CCL-ZnONS) โดยการคำนวณด้วย B3LYP/LanL2DZ รายงานค่าพลังงานการดูดซับของโมเลกุลแก๊สเหล่านี้บน AL-ZnONC NLL-ZnONC PRL-ZnONC CNL-ZnOGLNS และ CCL-ZnOGLNSs พบว่าออกซิเจนเท่านั้นที่ถูกดูดซับทางเคมีด้วยอะตอมไฮโดรเจนของ ZnONCs และ ZnOGLNSs ในขณะที่แก๊สชนิดอื่นไม่ถูกดูดซับในการดูดซับทางกายภาพ โมเลกุลออกซิเจนเท่านั้นที่ถูกดูดซับบนระนาบของ ZnOGLNSs เนื่องจากค่าช่องว่างพลังงานของ ZnOGLNSs มีค่าลดลงมากหลังจากดูดซับโมเลกุล ออกซิเจน ไนตริกออกไซด์ หรือ ไนโตรเจนไดออกไซด์ ดังนั้น ZnOGLNSs สามารถนำไปเป็นวัสดุรับรู้แก๊สเหล่านี้ได้ พบว่าการดูดซับ คาร์บอนมอนอกไซด์ ไฮโดรเจน น้ำ แอมโมเนีย และไนตรัสออกไซด์บน ZnOGLNSs ก่อนข้างอ่อน ดังนั้น ZnOGLNSs เหล่านี้รับรู้แก๊สดังกล่าวได้ยาก

ศูนย์วิทยทรัพยากร จุฬาลงกรณ์มหาวิทยาลัย

ภาควิชา เคมี..... ภายมือชื่อนิสิต..... เณยพตท. แก้วรักษา.....
สาขาวิชา เคมี..... ภายมือชื่อ อ.ที่ปรึกษาวิทยานิพนธ์หลัก.....
ปีการศึกษา 2553.....

5272393023: MAJOR CHEMISTRY

KEYWORDS: ZnO-NANOCLUSTERS/ ZnO-NANOSHEETS/ DFT/ GAS-SENSING/ ADSORPTION

BENJAWAN KAEWRUKSA: THEORETICAL INVESTIGATION OF GAS-SENSING PROPERTIES OF ZnO NANOSHEETS. ADVISOR: ASSOC. PROF. VITHAYA RUANGPORNVISUTI, Dr.rer.nat. , 87 pp.

The structure optimizations of all configurations of gaseous O₂, CO, NO, NO₂, N₂O, NH₃, H₂ and H₂O molecules adsorbed on ZnO nanoclusters (ZnONCs), aromatic-like (AL-ZnONC), naphthalene-like (NLL-ZnONC), pyrene-like (PRL-ZnONC) and ZnO graphene-like nanosheets (ZnOGLNSs), coronene-like (CNL-ZnONS) and circumcoronene-like (CCL-ZnONS) were carried out using the B3LYP/LanL2DZ calculations. Adsorption energies of these gases on AL-ZnONC, NLL-ZnONC, PRL-ZnONC, CNL-ZnOGLNS and CCL-ZnOGLNS were reported. It was found that only O₂ was chemically adsorbed via the hydride atoms of zinc-hydride in the ZnONCs and ZnOGLNSs whereas the other gases are not. In terms of physisorptions, only O₂ molecule was adsorbed over the plane of ZnOGLNSs. As the energy gaps of ZnOGLNSs were largely reduced after adsorption of O₂, NO or NO₂, these ZnOGLNSs were therefore be the sensing materials for these gases. It was found that adsorption of CO, H₂, H₂O, NH₃ and N₂O on ZnOGLNSs were somewhat weak, and thus these ZnOGLNSs were hardly sensing to these gases.

Department: Chemistry.....
 Field of Study: Chemistry.....
 Academic Year: 2010.....

Student's Signature
 Advisor's Signature

ACKNOWLEDGEMENTS

This study was carried out at the Chemistry, Faculty of Science, Chulalongkorn University. I would like to express my sincere thank to advisor Associate Professor Dr. Vithaya Ruangpornvisuti for his very useful guidance, understanding, and constant support throughout the course of this research.

I would like to really thank Assist. Prof. Dr. Warinthorn Chavasiri, Associate Professor Dr. Pornthep Sompornpisut and Dr. Banchob Wannooand for kindly serving on my thesis committee. Their sincere suggestions are definitely imperative for accomplishing my thesis.

Special thanks to all members in Supramolecular Chemistry Research Unit for their kind help. I also would like thank all teaching staff and my friends for all their good suggestions, friendship and continuous encouragement.

Finally, I would like to thank my favorite family; my father and mother, my aunt, my grandmother, my sisters and my brother for their infinite love and for always supporting and trusting in my decisions. I am very proud to be a part of this beloved family.



ศูนย์วิทยทรัพยากร
จุฬาลงกรณ์มหาวิทยาลัย

CONTENTS

	Page
ABSTRACT IN THAI	iv
ABSTRACT IN ENGLISH	v
ACKNOWLEDGEMENTS	vi
CONTENTS	vii
LIST OF TABLES	x
LIST OF FIGURES	xiii
LIST OF ABBREVIATIONS AND SYMBOLS	xix
CHAPTER I INTRODUCTION	1
1.1 Background.....	1
1.2 Fundamentals of the zinc oxide structure.....	1
1.3 Literature reviews	3
1.4 Objective.....	5
CHAPTER II THEORETICAL BACKGROUND	6
2.1 <i>Ab Initio</i> method.....	6
2.1.1 The Hartree–Fock method	6
2.2 Density functional theory.....	9
2.2.1 The Kohn–Sham energy and the Kohn–Sham equations.....	10
2.2.1.1 The Kohn–Sham energy.....	10
2.2.1.2 The Kohn–Sham equations.....	12
2.2.2 Hybrid methods.....	14
2.3 Gaussian basis sets.....	15
2.3.1 Minimal basis sets.....	17
2.3.2 Split–valence basis sets.....	17
2.3.3 Polarized basis sets.....	18
2.3.4 Basis sets incorporating diffuse functions potentials.....	19
2.3.5 Effective core potentials.....	19

	Page
CHAPTER III DETAILS OF THE CALCULATIONS.....	20
3.1 Computational method.....	20
CHAPTER IV RESULTS AND DISCUSSION	23
4.1 The optimized structures and Zn–O bond strength.....	23
4.2 Adsorption of molecule gaseous on ZnO nanoclusters and ZnO nanosheets	24
4.2.1 Adsorption of oxygen molecule.....	24
4.2.1.1 Atomic charge distribution.....	28
4.2.1.2 Energy gap.....	29
4.2.2 Adsorption of carbon monoxide molecule.....	30
4.2.2.1 Adsorption energies of CO pointing with C–end.....	30
4.2.2.2 Adsorption energies of CO pointing with O–end.....	35
4.2.2.3 Bond types and maximum numbers of CO adsorption.....	36
4.2.2.4 Energy gap.....	37
4.2.3 Adsorption of water molecule.....	41
4.2.3.1 Adsorption energies of H ₂ O.....	41
4.2.4 Adsorption of ammonia molecule.....	47
4.2.4.1 Adsorption energies of NH ₃	47
4.2.5 Adsorption of hydrogen molecule.....	50
4.2.5.1 Adsorption energies of H ₂	50
4.2.6 Adsorption of nitric oxide molecule.....	54
4.2.6.1 Adsorption energies of NO pointing with N–end.....	54
4.2.6.2 Adsorption energies of NO pointing with O–end.....	60
4.2.6.3 Energy gap.....	62
4.2.7 Adsorption of nitrous oxide molecule.....	63
4.2.7.1 Adsorption energies of N ₂ O pointing with N–end.....	63
4.2.7.2 Adsorption energies of N ₂ O pointing with O–end.....	69
4.2.8 Adsorption of nitrogen dioxide molecule.....	71
4.2.8.1 Adsorption energies of NO ₂ pointing with N–end.....	71
4.2.8.2 Adsorption energies of NO ₂ pointing with O–end.....	77

	Page
CHAPTER V CONCLUSIONS	80
5.1 Conclusions.....	80
5.2 Suggestion for future work.....	80
REFERENCES	81
APPENDIX	85
APPENDIX A.....	86
VITAE	87



ศูนย์วิทยทรัพยากร
จุฬาลงกรณ์มหาวิทยาลัย

LIST OF TABLES

Table	Page
4.1 Adsorption energies (ΔE_{ads} in kcal/mol) of O_2 on ZnONCs and ZnOGLNSs, and energy gaps (ΔE_{GAP} in eV) of bare surfaces of ZnONCs, ZnOGLNSs, and their O_2 adsorption complexes, computed at the B3LYP/LanL2DZ level of theory.....	26
4.2 Adsorption energies (ΔE_{ads} in kcal/mol) of CO pointing its C-end toward surfaces of ZnONCs and ZnOGLNSs and energy gaps (ΔE_{GAP} in eV) of bare surfaces of ZnONCs, ZnOGLNSs and their CO adsorption complexes, computed at the B3LYP/LanL2DZ level of theory.....	34
4.3 Adsorption energies (ΔE_{ads} in kcal/mol) of CO pointing its O-end toward surfaces of ZnONCs and ZnOGLNSs and energy gaps (ΔE_{GAP} in eV) of bare surfaces of ZnONCs, ZnOGLNSs, computed at the B3LYP/LanL2DZ level of theory.....	37
4.4 Bond distances (in Å) between CO atoms and atoms of adsorption sites.....	39
4.5 Maximum number of CO adsorbed on ZnOGLNSs and their formulae.....	40
4.6 Adsorption energies (ΔE_{ads} in kcal/mol) of H_2O on ZnONCs and ZnOGLNSs, and energy gaps (ΔE_{GAP} in eV) of bare ZnONCs and ZnOGLNSs and their H_2O adsorption complexes, computed at the B3LYP/LanL2DZ level of theory.....	45
4.7 Bond distances between oxygen atom of H_2O and Zn atom of ZnOGLNSs.....	46
4.8 Adsorption energies (ΔE_{ads} in kcal/mol) of NH_3 on ZnONCs and ZnOGLNSs, and energy gaps (ΔE_{GAP} in eV) of the bare ZnONCs and ZnOGLNSs and their NH_3 adsorption complexes, computed at the B3LYP/LanL2DZ level of theory.....	50
4.9 Adsorption energies (ΔE_{ads} in kcal/mol) of H_2 on ZnONCs and ZnOGLNSs, and energy gaps (ΔE_{GAP} in eV) of the bare surfaces of ZnONCs, ZnOGLNSs, and their H_2 adsorption complexes, computed	

Table	Page
at the B3LYP/LanL2DZ level of theory.....	53
4.10 Adsorption energies (ΔE_{ads} in kcal/mol) of NO pointing its N-end toward surfaces of ZnONCs and ZnOGLNSs and energy gaps (ΔE_{GAP} in eV) of bare surfaces of ZnONCs, ZnOGLNSs and their NO adsorption complexes, computed at the B3LYP/LanL2DZ level of theory.....	59
4.11 Bond distances (in Å) between NO atoms and atoms of adsorption sites.....	60
4.12 Adsorption energies (ΔE_{ads} in kcal/mol) of NO pointing its O-end toward surfaces of ZnONCs and ZnOGLNSs and energy gaps (ΔE_{GAP} in eV) of bare surfaces of ZnONCs, ZnOGLNSs and their NO adsorption complexes, computed at the B3LYP/LanL2DZ level of theory.....	63
4.13 Adsorption energies (ΔE_{ads} in kcal/mol) of N ₂ O pointing its N-end toward surfaces of ZnONCs and ZnOGLNSs and energy gaps (ΔE_{GAP} in eV) of bare surfaces of ZnONCs, ZnOGLNSs and their N ₂ O adsorption complexes, computed at the B3LYP/LanL2DZ level of theory.....	68
4.14 Bond distances (in Å) between N ₂ O atoms and atoms of adsorption sites.....	69
4.15 Adsorption energies (ΔE_{ads} in kcal/mol) of N ₂ O pointing its O-end toward surfaces of ZnONCs and ZnOGLNSs and energy gaps (ΔE_{GAP} in eV) of bare surfaces of ZnONCs, ZnOGLNSs and their N ₂ O adsorption complexes, computed at the B3LYP/LanL2DZ level of theory.....	71
4.16 Adsorption energies (ΔE_{ads} in kcal/mol) of NO ₂ pointing its N-end toward surfaces of ZnONCs and ZnOGLNSs and energy gaps (ΔE_{GAP} in eV) of bare surfaces of ZnONCs, ZnOGLNSs and their NO ₂ adsorption complexes, computed at the B3LYP/LanL2DZ level of theory.....	76
4.17 Bond distances (in Å) between NO ₂ atoms and atoms of adsorption sites.....	77

Table	Page
4.18 Adsorption energies (ΔE_{ads} in kcal/mol) of NO_2 pointing its O-end toward surfaces of ZnONCs and ZnOGLNSs and energy gaps (ΔE_{GAP} in eV) of bare surfaces of ZnONCs, ZnOGLNSs and their NO_2 adsorption complexes, computed at the B3LYP/LanL2DZ level of theory.....	79



ศูนย์วิทยทรัพยากร
จุฬาลงกรณ์มหาวิทยาลัย

LIST OF FIGURES

Figure		Page
1.1	Stick-and-ball representation of ZnO crystal structures: (a) rocksalt, (b) zinc blende and (c) wurtzite. Gray and black balls denote Zn and O atoms, respectively.....	2
3.1	The B3LYP/LanL2DZ-optimized structures of (a) the AL-ZnONC, (b) NLL-ZnONC, (c) PRL-ZnONC, (d) CNL-ZnONS and (e) CCL-ZnONS and their energy gaps and molecular symmetries. The atomic labeling of their representative atoms depend on their molecular symmetries.....	21
3.2	The CNL-ZnONS selected as representative ZnO nanosheets shows the possible adsorption sites as over the hydrogen, zinc, gas molecules and hexagonal center of nanosheets.....	21
4.1	The B3LYP/LanL2DZ-optimized structures of (a) the AL-ZnONC, (b) NLL-ZnONC, (c) PRL-ZnONC, (d) CNL-ZnONS and (e) CCL-ZnONS and their energy gaps and molecular symmetries. The atomic labeling of their representative atoms depend on their molecular symmetries.....	24
4.2	Plots of oxygen molecules as minimum energy structures of their adsorptions on (a) the AL-ZnONC ($Zn_6O_6H_6$), (b) NLL-ZnONC ($Zn_{10}O_{10}H_{10}$) and (c) PRL-ZnONC ($Zn_{16}O_{16}H_{16}$). The molecules labeled with numbers represent the oxygen molecule interacting with ZnONCs as representative of molecular symmetry of AL-ZnONC (C_{3h}), NLL-ZnONC (C_{2v}) and PRL-ZnONC (C_{2v}). Adsorption energies in kcal/mol were presented.....	25
4.3	Plots of oxygen molecules as minimum energy structures of their adsorptions on (a) CNL-ZnONS ($Zn_{12}O_{12}H_{12}$) and (b) CCL-ZnONS ($Zn_{27}O_{27}H_{18}$) as minimum energy structures. The molecules labeled with numbers represent the oxygen molecule interacting with ZnONCs as representative of molecular symmetry of CNL-ZnONS (C_{3h}) and CCL-ZnONS (C_{3h}). Adsorption energies in kcal/mol were presented.....	25

Figure	Page
4.4 NBO charges (e) of oxygen and zinc atoms on the (a) AL–ZnONC, (b) NLL–ZnONC and (c) PRL–ZnONC.....	28
4.5 NBO charges (e) of oxygen and zinc atoms on the (a) CNL–ZnONS and (b) CCL–ZnONS.....	29
4.6 Plots of energy gaps of ZnO nanosheets against invert values of their termination–proton numbers (NTP).....	30
4.7 Plots of CO molecules as minimum energy structures of their adsorptions on (a) the AL–ZnONC ($Zn_3O_3H_6$), (b) NLL–ZnONC ($Zn_5O_5H_8$) and (c) PRL–ZnONC ($Zn_8O_8H_{10}$). Their left and right adsorption maps were CO adsorption on ZnONCs by pointing C–end and O–end toward the adsorption sites, respectively. The set of labeled molecules was representative of CO interacting with AL–ZnONC (C_{3h}), NLL–ZnONC (C_{2v}) and PRL–ZnONC (C_{2v}). Adsorption energies were presented in kcal/mol.....	31
4.8 Plots of CO molecules as minimum energy structures of their adsorptions on CNL–ZnONS ($Zn_{12}O_{12}H_{12}$) as adsorption configurations of CO with pointing its (a) C–end and (b) O–end toward the adsorption sites of the CNL–ZnONS. The set of labeled molecules was representative of CO adsorption interacting with CNL–ZnONS with C_{3h} symmetry. Adsorption energies were presented in kcal/mol.....	32
4.9 Plots of carbon monoxide molecules as minimum energy structures of their adsorptions on CCL–ZnONS ($Zn_{27}O_{27}H_{18}$) as (a) adsorption configurations of CO by pointing (a) C–end and (b) O–end toward the adsorption sites. The molecules labeled with numbers represent the oxygen molecule interacting with CCL–ZnONS of molecular symmetry of (C_{3h}). Adsorption energies were presented in kcal/mol.....	32
4.10 Plots of all possible adsorption energies of CO on all the ZnONC, PRL–ZnONC nanoclusters and PRL–ZnONC, CNL–ZnONS and CCL–ZnONS nanosheets against their bond distances. Four bond distances types [$\underline{CO}\cdots H$], [$\underline{CO}\cdots Zn$], [$\underline{CO}\cdots H$] and [$\underline{CO}\cdots Zn$], four	

Figure	Page
zones were found.....	38
4.11 The structure models of (a) C_{3h} symmetric ZnOGLNS(<i>i</i>) and (b) C_{2v} symmetric ZnOGLNS(<i>i</i>). The layer numbers of C_{3h} -ZnOGLNS(<i>i</i>) and C_{2v} -ZnOGLNS(<i>i</i>) defined as radial layer models of which the one layer structures (the most inner) were AL-ZnONC and PRL-ZnONC, respectively. The numbers labeled in the center of hexagonal rings indicate the number of most outer layer of the ZnOGLNS.....	38
4.12 The adsorption configurations of water adsorbed on (a) the AL-ZnONC, (b) NLL-ZnONC, (c) PRL-ZnONC, (d) CNL-ZnONS and (e) CCL-ZnONS. The bond distances bonds were in Å.....	41
4.13 Plots of water molecules as minimum energy structures of their adsorptions on (a) the AL-ZnONC ($Zn_3O_3H_6$), (b) NLL-ZnONC ($Zn_5O_5H_8$), (c) PRL-ZnONC ($Zn_8O_8H_{10}$), (d) CNL-ZnONS ($Zn_{12}O_{12}H_{12}$) and (e) CCL-ZnONS ($Zn_{27}O_{27}H_{18}$). The molecules labeled with numbers represent the water molecules interacting with ZnONCs and ZnOGLNSs as representative of molecular symmetries of AL-ZnONC (C_{3h}), NLL-ZnONC (C_{2v}), PRL-ZnONC (C_{2v}), CNL-ZnOGLNS (C_{3h}) and CCL-ZnOGLNS (C_{3h}). Adsorption energies in kcal/mol were presented.....	42
4.14 The adsorption configurations of ammonia adsorbed on (a) the AL- ZnONC, (b) NLL-ZnONC, (c) PRL-ZnONC, (d) CNL-ZnONS and (e) CCL-ZnONS. The bond distances, ($N_{NH_3} \cdots Zn$) were in Å.....	47
4.15 Plots of ammonia molecules as minimum energy structures of their adsorptions on (a) the AL-ZnONC, (b) NLL-ZnONC, (c) PRL-ZnONC, (d) CNL-ZnONS and (e) CCL-ZnONS. The molecules labeled with numbers represent the ammonia molecules interacting with ZnONCs and ZnOGLNSs as representative of their molecular symmetries. Adsorption energies in kcal/mol were presented.....	48

Figure	Page
4.16 Plots of H ₂ molecules as minimum energy structures of their adsorptions on (a) the AL–ZnONC, (b) NLL–ZnONC, (c) PRL–ZnONC, (d) CNL–ZnONS and (e) CCL–ZnONS. The molecules labeled with numbers represent the H ₂ molecules interacting with ZnONCs and ZnOGLNSs as representative of their molecular symmetries. Adsorption energies in kcal/mol were presented.....	52
4.17 Plots of NO molecules as minimum energy structures of their adsorptions on (a) the AL–ZnONC (Zn ₃ O ₃ H ₆), (b) NLL–ZnONC (Zn ₅ O ₅ H ₈) and (c) PRL–ZnONC (Zn ₈ O ₈ H ₁₀). Their left and right adsorption maps were NO adsorption on ZnONCs by pointing N–end and O–end toward the adsorption sites, respectively. The set of labeled molecules was representative of NO interacting with AL–ZnONC (C _{3h}), NLL–ZnONC (C _{2v}) and PRL–ZnONC (C _{2v}). Adsorption energies were presented in kcal/mol.....	55
4.18 Plots of NO molecules as minimum energy structures of their adsorptions on CNL–ZnONS (Zn ₁₂ O ₁₂ H ₁₂) as adsorption configurations of NO with pointing its (a) N–end and (b) O–end toward the adsorption sites of the CNL–ZnONS. The set of labeled molecules was representative of NO adsorption interacting with CNL–ZnONS with C _{3h} symmetry. Adsorption energies were presented in kcal/mol.....	56
4.19 Plots of NO molecules as minimum energy structures of their adsorptions on CCL–ZnONS (Zn ₂₇ O ₂₇ H ₁₈) as (a) adsorption configurations of NO by pointing (a) N–end and (b) O–end toward the adsorption sites. The molecules labeled with numbers represent the oxygen molecule interacting with CCL–ZnONS of molecular symmetry of (C _{3h}). Adsorption energies were presented in kcal/mol	56
4.20 Plots of N ₂ O molecules as minimum energy structures of their adsorptions on (a) the AL–ZnONC (Zn ₃ O ₃ H ₆), (b) NLL–ZnONC (Zn ₅ O ₅ H ₈) and (c) PRL–ZnONC (Zn ₈ O ₈ H ₁₀). Their left and right adsorption maps were N ₂ O adsorption on ZnONCs by pointing	

Figure	Page
N-end and O-end toward the adsorption sites, respectively. Their left and right adsorption maps were N ₂ O adsorption on ZnONCs by pointing N-end and O-end toward the adsorption sites, respectively. The set of labeled molecules was representative of N ₂ O interacting with AL-ZnONC (C _{3h}), NLL-ZnONC (C _{2v}) and PRL-ZnONC (C _{2v}). Adsorption energies were presented in kcal/mol.....	66
4.21 Plots of N ₂ O molecules as minimum energy structures of their adsorptions on CNL-ZnONS (Zn ₁₂ O ₁₂ H ₁₂) as adsorption configurations of N ₂ O with pointing its (a) N-end and (b) O-end toward the adsorption sites of the CNL-ZnONS. The set of labeled molecules was representative of N ₂ O adsorption interacting with CNL-ZnONS with C _{3h} symmetry. Adsorption energies were presented in kcal/mol.....	67
4.22 Plots of N ₂ O molecules as minimum energy structures of their adsorptions on CCL-ZnONS (Zn ₂₇ O ₂₇ H ₁₈) as (a) adsorption configurations of N ₂ O by pointing (a) N-end and (b) O-end toward the adsorption sites. The molecules labeled with numbers represent the N ₂ O molecule interacting with CCL-ZnONS of molecular symmetry of (C _{3h}). Adsorption energies were presented in kcal/mol.....	67
4.23 Plots of NO ₂ molecules as minimum energy structures of their adsorptions on (a) the AL-ZnONC (Zn ₃ O ₃ H ₆), (b) NLL-ZnONC (Zn ₅ O ₅ H ₈) and (c) PRL-ZnONC (Zn ₈ O ₈ H ₁₀). Their left and right adsorption maps were NO ₂ adsorption on ZnONCs by pointing N-end and O-end toward the adsorption sites, respectively. The set of labeled molecules was representative of NO ₂ interacting with AL-ZnONC (C _{3h}), NLL-ZnONC (C _{2v}) and PRL-ZnONC (C _{2v}). Adsorption energies were presented in kcal/mol.....	74
4.24 Plots of NO ₂ molecules as minimum energy structures of their adsorptions on CNL-ZnONS (Zn ₁₂ O ₁₂ H ₁₂) as adsorption configurations of NO ₂ with pointing its (a) N-end and (b) O-end	

Figure**Page**

- toward the adsorption sites of the CNL–ZnONS. The set of labeled molecules was representative of NO₂ adsorption interacting with CNL–ZnONS with C_{3h} symmetry. Adsorption energies were presented in kcal/mol..... 75
- 4.25 Plots of NO₂ molecules as minimum energy structures of their adsorptions on CCL–ZnONS (Zn₂₇O₂₇H₁₈) as (a) adsorption configurations of NO₂ by pointing (a) N–end and (b) O–end toward the adsorption sites. The molecules labeled with numbers represent the NO₂ molecule interacting with CCL–ZnONS of molecular symmetry of (C_{3h}). Adsorption energies were presented in kcal/mol..... 75

LIST OF ABBREVIATIONS AND SYMBOLS

Å	Angstrom
AL	Aromatic-like
B3LYP	Beck 3 Lee–Yang–Parr
<i>BS</i>	Bond strength
CCL	Circumcoronene-like
CNL	Coronene-like
$c_{\mu i}$	Coefficients
DFT	Density functional theory
<i>E</i>	Energy
ECP	Effective core potentials
\hat{H}	Hamiltonian operator
HF	Hartree–Fock
LCAO	Linear combination of atomic orbitals
LanL2DZ	Los Alamos National Laboratory 2 double Zeta
NBO	Natural bond orbital
NLL	Naphthalene-like
N_{hydride}	Number of hydride
N_o	Avogadro number
N_{TP}	Termination-proton numbers
PRL	Pyrene-like
$r_{\text{Zn-O}}$	Inter nuclear between zinc and oxygen atom
SCF	Self-consistent field
STO	Slater type orbital
ZnO	Zinc oxide
ZnONCs	Zinc oxide nanoclusters
ZnONSs	Zinc oxide nanosheets
ψ	Wave function
ϕ	Basis functions
ρ	Electron density

CHAPTER I

INTRODUCTION

1.1 Background

The crystal faces of zinc oxide (ZnO) have been studied by several experimental and theoretical techniques on adsorptions of H₂ [1–5], CO [6], H₂O [7–9], CO₂ [10], NH₃ [11], NO [12], NO₂ [12, 13], SO₂ [13] and N₂O [14]. ZnO materials have excellent performance in optics, electronics, photoelectronics [1] and piezoelectricity [2]. It can also be used as transducers and sensors due to their strong piezoelectricity. Different surfaces of the wurtzite ZnO [15, 16] and planar graphite-like structure [17] have been studied. A large number of different ZnO nanostructures such as nanorods [18], nanowires [19–21], nanocombs [22], nanorings [23] and nanotubes [24, 25] have been prepared and studied their properties. One dimensional ZnO nanotube, or nanorods, or nanowires ZnO were found that they have shown much higher sensitivity than polycrystalline ZnO at room temperature because of their higher surface-to-volume ratio and stronger dependence of electrical conductance on the amount of adsorbates [26–33]. However, since ultrawide ZnO nanosheets which have high specific surface area were synthesized, [34] they are expected to have the highest surface-to-volume ratio and can be used as gas sensors. Many synthesized ZnO nanosheets have been expected to be wurtzite or planar graphite-like structures [15, 16, 17] but they have never been expected to be graphene-like structures. Recently, the single ZnO monolayer with graphene-like structure (SZOML) was theoretically studied and its elastic, piezoelectric, electronic and optical properties were investigated from the first principles calculations [35]. Nevertheless, its chemical properties such adsorption of fundamental gases have almost never been studied.

1.2 Fundamentals of the zinc oxide structure [36]

Zinc oxide (ZnO) is a compound semiconductor whose ionicity resides at the borderline between the covalent and ionic semiconductors. The crystal structures of

ZnO are found as three structures namely rock salt, zinc blende and wurtzite as shown in Figure 1.1 (a), (b) and (c), respectively. The wurtzite ZnO structure is found to be the most stable phase. The zinc blende ZnO structure is found to be stabilized on cubic substrates.

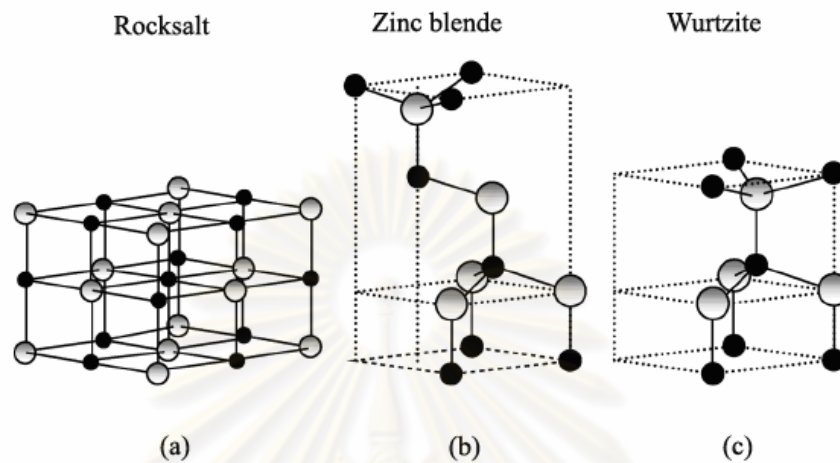


Figure 1.1 Stick-and-ball representation of ZnO crystal structures: (a) rocksalt, (b) zinc blende and (c) wurtzite. Gray and black balls denote Zn and O atoms, respectively.

Bulk ZnO is known as an ionic semiconductor with a wide band gap (3.4 eV). ZnO have been extensively studied for using as a gas sensor and biosensor due to its excellent compatibility of ZnO surface. However, it has been found that polycrystalline ZnO in forms of integrated film or ceramics shows only limited sensitivity for gas-sensor application. Additionally, high sensitivity of the thin-film gas sensors can be only realized at elevated temperatures. Alternatively, one dimensional (1D) ZnO nanotubes (NTs), nanorods (NRs), or nanowires (NWs) have shown much higher sensitivity than polycrystalline ZnO at room temperature. The reason is that their surface-to-volume ratio all high. Moreover, the gas sensors fabricated with the 1D ZnO nanostructures have shown some advantages over crystalline materials for examples low power consumption, light weight, and easy recovery capability.

1.3 Literature reviews

In the 2003, Meyer *et al.* [37] studied the adsorption of CO on different ideal, defect-free, ZnO surfaces. For the non-polar $(10\bar{1}0)$ surface they compared monolayer versus half-monolayer coverage and CO adsorption geometries with the C-atom ('C-down') and the O-atom ('O-down') coordinated to the surface. For the two polar surfaces, different adsorption sites were considered and they studied the influence of hydrogen coverage of the surface. The study indicated that CO only binds to Zn ions present at the non-polar $(10\bar{1}0)$ and the polar $(000\bar{1})$ -Zn surface and to the OH groups of the hydrogen saturated $(000\bar{1})$ -O surface. In all cases, the 'C-down' adsorption geometry was more stable than the 'O-down' configuration. The relaxation of the surfaces was a significant effect and the contribution to the adsorption energy is not negligible. No binding of CO to surface oxygen ions was found. Therefore, in the experiments where a chemisorption of CO on the $(000\bar{1})$ -O surface was observed, CO was either bound to defects sites and step edges or the surface was hydrogen-covered. Altogether, pronounced differences in the adsorption properties of CO were found for the four polar surface terminations. The finding of this study opens the possibility of employing CO as a probe molecule to identify surface terminations, and by comparing theoretical and experimental results, to validate microscopic models of the complex, inhomogeneous polar ZnO surfaces.

In the 2004, Martins *et al.* [11] studied the large cluster model approximately includes the surrounding effects. Fortunately, in the Morokumas ONIOM framework, a very large system was divided into three layers. Every layer was described by different levels of theory. High level methods especially those including electron correlation effects was applied to the small system, the chemically active part, while neighbors effects were described by lower level methods. Analysis of the interaction of small molecules with ZnO surfaces using the cluster model approach within the Oniom three layers methodology offer an opportunity to probe the validity of this methodology, as well as a better comprehension of the electronic and structural properties of adsorption of CO, H₂, H₂O, NH₃, and CO₂ species on ZnO surfaces. The results were indicated that the binding energies, orbital stabilization and geometries were comparable to the available experimental values. In general, the 6-31+G** basis

set level results for the binding energies, angles and orbital stabilization energies were in better agreement with the experimental values. The partial charge values calculated using the ChelpG methods were better agreement with the suggested experimental acid–basic properties for the oniom high layer.

In the 2010, Zhang *et al.* [38] performed spin–polarized density functional theory calculations with a plane–wave basis set, as implemented in the Vienna *ab initio* simulation package (VASP) to investigate the electronic and magnetic properties of hydrogenated monolayer ZnOGSs. The exchange correlation functional was described by the generalized gradient approximation (GGA) in the form of Perdew and Wang 91 (PW91). The relaxations were performed by computing the Hellmann–Feynman (H–F) forces. The analyses of the relative stability show that the H atoms preferred to adsorb on O atoms rather than Zn atoms, while the NH₂ functional groups tended to adsorb on Zn atoms rather than O atoms. The study indicated that the metallicity or magnetic semiconductor of ZnOGS could be realized experimentally through surface passivation. The various electronic and magnetic properties of the passivated ZnOGSs might motivate potential applications of ZnO nanostructures in nanoelectronics and spintronics.

In the 2010, He *et al.* [39] investigated the interaction of an Mn atom with a (9, 0) single–wall ZnO nanotube and with a graphitic ZnO sheet by first–principles spin–polarized calculations based on density functional theory (DFT). Following that, the adsorption of a single Mn atom at various sites on the outer and inner walls of the (9, 0) zigzag single–wall ZnO nanotube are discussed, respectively. In each case, the structural, electronic and magnetic properties of the Mn–doped (9, 0) single–wall ZnO nanotube were analyzed. The study indicated that the adsorption of an Mn atom on a graphitic ZnO sheet and a single–wall zigzag (9, 0) ZnO nanotube were studied by *ab initio* calculations. For the Mn–doped ZnO sheet, the most stable adsorption site was the H site. The Mn atom tended to push its three nearest–neighbor Zn atoms out of the plane so that it can form bonds with its three nearest–neighbor oxygen atoms. Similarly, the H configuration was also the most energetically favorable site for adsorption of a single Mn atom on the inner wall of the (9, 0) ZnO nanotube. The study provided some useful reference to the synthesis of ZnO nanotubes using TM atoms as catalysts and its potential applications.

1.4 Objective

In this study, the various sizes of ZnO nanoclusters (ZnONCs) and ZnO nanosheets (ZnONSs) *i.e.* ZnO nanoclusters of aromatic-like (AL-ZnONC, $Zn_3O_3H_6$), naphthalene-like (NLL-ZnONC, $Zn_5O_5H_8$), PRL-like (PRL-ZnONC, $Zn_8O_8H_{10}$), and ZnO nanosheets of coronene-like (CNL-ZnONS, $Zn_{12}O_{12}H_{12}$) and circumcoronene-like (CCL-ZnONS, $Zn_{27}O_{27}H_{18}$) and bond strength of their Zn–O bonds have been investigated. Adsorptions of gaseous oxygen, carbon monoxide, nitric oxide, nitrogen dioxide, nitrous oxide, ammonia, hydrogen and water molecules on the ZnONCs and ZnONSs and their electronic properties have been addressed by employing the calculations at the B3LYP/LanL2DZ level of theory.



CHAPTER II

THEORETICAL BACKGROUND

The main of quantum chemical investigations determine the energies of molecules using heavy computations based on approximate solutions of the quantum methods. Quantum chemistry is divided into semi-empirical, Hartree-Fock (HF) and density functional theory (DFT) methods that are also based on quantum mechanical principles to the explanation and prediction of chemical behavior. Quantum chemical studies relate to the ground state of individual atoms and molecules, to excited states, and to the transition states that occur during chemical reactions. Quantum chemical results include molecular structure, bond strengths and other characteristics of chemical bonds.

2.1 *Ab Initio* method

Ab initio quantum chemistry methods are computational methods based on quantum chemistry [40]. The simplest type of *ab initio* electronic structure calculation is the Hartree-Fock (HF), in which the instantaneous coulombic electron-electron repulsion is not specifically taken into account. Only its average effect is included in the calculation. This is a variational procedure therefore, the obtained approximate energies, expressed in terms of the system's wave function are always equal to or greater than the exact energy and tend to a limiting value called the Hartree-Fock limit as the size of the basis is increased [41].

2.1.1 The Hartree-Fock method [42]

The Schrödinger equation is deceptive in that, although it is mostly easy to write down for any collection of nuclei and electrons, it has proven to be insolvable except for the one-electron case (the hydrogen atom). To appreciate the convenient of quantum mechanical theory, it is necessary to make three approximations to the general multinuclear, multi-electron Schrödinger equation:

$$\hat{H}\Psi = E\Psi \quad (2.1)$$

where E is the total energy of the system and Ψ is the n -electron wave function that depends both on the identities and positions of the nuclei and on the total number of electrons. The Hamiltonian \hat{H} provides the recipe for specifying the kinetic and potential energies for each of the particles:

$$\begin{aligned} \hat{H} = & -\frac{\hbar^2}{2m_e} \sum_i^{\text{electrons}} \nabla_i^2 - \frac{\hbar^2}{2} \sum_A^{\text{nuclei}} \frac{1}{M_A} \nabla_A^2 - \frac{e^2}{4\pi\epsilon_0} \sum_i^{\text{electrons}} \sum_A^{\text{nuclei}} \frac{Z_A}{r_{iA}} \\ & + \frac{e^2}{4\pi\epsilon_0} \sum_{i>j}^{\text{electrons}} \sum_j^{\text{electrons}} \frac{1}{r_{ij}} + \frac{e^2}{4\pi\epsilon_0} \sum_{A>B}^{\text{nuclei}} \sum_B^{\text{nuclei}} \frac{Z_A Z_B}{R_{AB}} \end{aligned} \quad (2.2)$$

where Z is the nuclear charge, M_A is the mass of the electron, R_{AB} is the distance between nuclei A and B , r_{iA} is the distance between electrons i and j , r_{iA} is the distance between electron i and nucleus A , and ϵ_0 is the permittivity of free space.

The first approximation takes benefit of the fact that nuclei move much more slowly than do electrons. We assume that the nuclei are stationary which is known as the Born-Oppenheimer approximation. This assumption leads to a nuclear-nuclear coulombic energy term, the last term, which is constant. What results is the electronic Schrödinger equation:

$$\hat{H}^{\text{el}}\Psi^{\text{el}} = E^{\text{el}}\Psi^{\text{el}} \quad (2.3)$$

$$\hat{H} = -\frac{\hbar^2}{2m_e} \sum_i^{\text{electrons}} \nabla_i^2 - \frac{e^2}{4\pi\epsilon_0} \sum_i^{\text{electrons}} \sum_A^{\text{nuclei}} \frac{Z_A}{r_{iA}} + \frac{e^2}{4\pi\epsilon_0} \sum_{i>j}^{\text{electrons}} \sum_j^{\text{electrons}} \frac{1}{r_{ij}} \quad (2.4)$$

The nuclear-nuclear coulomb energy, the previous term in Equation (2.2) needs to be added to E^{el} to get the total energy. Note that nuclear mass does not appear in the electronic Schrödinger equation. To the extent that the Born-Oppenheimer approximation is suitable, this means that isotope effects on molecular properties must have a different origin.

Equation (2.3), like Equation (2.1), is insolvable for the general case and further approximations need to be made. The most obvious thing to do is to assume

that electrons move independently of each other, which is what is done in the Hartree–Fock approximation. In practice, this can be proficient by assuming that individual electrons are limited to functions called spin orbitals, χ_i . Each of the N electrons feels the presence of an average field made up of all of the other $(N-1)$ electrons. To ensure that the total wave function Ψ is anti-symmetric upon interchange of electron coordinates, it is written in the form of a single determinant called the Slater determinant:

$$\Psi = \frac{1}{\sqrt{N!}} \begin{vmatrix} \chi_1(1) & \chi_2(1) \dots & \chi_n(1) \\ \chi_1(2) & \chi_2(2) \dots & \chi_n(2) \\ \dots & \dots & \dots \\ \chi_1(N) & \chi_2(N) & \chi_N(N) \end{vmatrix} \quad (2.5)$$

Individual electrons are represented by different rows in the determinant, which means that interchanging the coordinates of two electrons is equivalent to interchanging two rows in the determinant, multiplying its value by -1 . Spin orbitals are the product of spatial functions or molecular orbitals, ψ_i , and spin functions, α or β . The fact that there are only two kinds of spin functions (α and β) leads to the conclusion that two electrons at most may occupy a given molecular orbital. Were a third electron to occupy the orbital, two rows in the determinant would be the same. Therefore, the value of the determinant would be zero. Thus, the perception that electrons are paired is really an artifact of the Hartree–Fock approximation. The set of molecular orbitals leading to the lowest energy is obtained by a process referred to as a self-consistent-field (SCF) procedure.

The Hartree–Fock approximation leads to a set of differential equations, the Hartree–Fock equations, each involving the coordinates of a single electron. Although they can be solved numerically, it is profitable to introduce an additional approximation in order to transform the Hartree–Fock equations into a set of algebraic equations. The basis for this approximation is the probability that the one-electron solutions for many-electron molecules will closely resemble the one-electron wave functions for hydrogen atom. The molecular orbitals ψ_i are expressed as linear combinations of a basis set of prescribed functions known as basis functions, ϕ :

$$\psi_i = \sum_{\mu}^{\text{basis functions}} c_{\mu i} \phi_{\mu} \quad (2.6)$$

In this equation, the coefficients $c_{\mu i}$ are the molecular orbital coefficients. Because the ϕ are usually centered at the nuclear positions, they are referred to as atomic orbitals, and equation (2.6) is called the linear combination of atomic orbitals (LCAO) approximation. Note that in the boundary of a complete basis set, the LCAO approximation is exact.

2.2 Density functional theory [42]

The Hartree–Fock model is now commonly known as density functional theory. It is based on the availability of an exact solution for an idealized many–electron problem, particularly an electron gas of uniform density. The part of this solution that relates only to the exchange and correlation contributions is extracted and then directly included into the SCF formalism much like Hartree–Fock formalism. Because the new exchange and correlation terms get from idealized problems, density functional models, unlike configuration interaction and Møller–Plesset models, do not limit to the exact solution of the Schrödinger equation. In a sense, they are empirical in that they integrate external data. For this finding, important to the development of practical density set model, Walter Kohn was awarded the Nobel Prize in chemistry in 1998.

The Hartree–Fock energy may be written as a sum of the kinetic energy, E_T , the electron–nuclear potential energy, E_V , and coulomb, E_J , and exchange, E_K , components of the electron–electron interaction energy:

$$E^{\text{HF}} = E_T + E_V + E_J + E_K \quad (2.7)$$

The first three of these terms take over directly to density functional models, whereas the Hartree–Fock exchange energy is replaced by so–called exchange/correlation energy, E_{XC} , the form of which follows from the solution of the idealized electron gas problem:

$$E^{\text{DFT}} = E_{\text{T}} + E_{\text{v}} + E_{\text{J}} + E_{\text{XC}} \quad (2.8)$$

except for E_{T} , all components depend on the total electron density, $\rho(r)$:

$$\rho(r) = 2 \sum_i^{\text{orbitals}} |\psi_i(r)|^2 \quad (2.9)$$

the ψ_i are orbitals, strictly similar to molecular orbitals in Hartree–Fock theory.

2.2.1 The Kohn–Sham energy and the Kohn–Sham equations [43]

The first Kohn–Sham theorem tells us that it is worth looking for a way to calculate molecular properties from the electron density. The second theorem suggests that a variation approach might yield a way to calculate the energy and electron density (the electron density, in turn, could be used to calculate other properties). The two basis ideas behind the Kohn–Sham approach to DFT are (1) to express the molecular energy as a sum of term, only one of which, a relatively small term, involves the unknown functional. Thus even somewhat large errors in this term will not introduce large errors into the total energy (2) to use an initial guess of the electron density ρ in the Kohn–Sham equations to calculate an initial guess of the Kohn–Sham orbitals. The final Kohn–Sham orbitals are used to calculate an electron density that in turn is used to calculate the energy.

2.2.1.1 The Kohn–Sham energy

The ideal energy is that of an ideal system, a fictitious non–interacting reference system, defined as one in which the electrons do not interact and in which the ground state electron density ρ_{r} is exactly the same as in our real ground state system, $\rho_{\text{r}} = \rho_0$. The electronic energy of the molecule is the total internal frozen–nuclei energy can be found by adding the internuclear repulsions and the 0 K total internal energy by further adding the zero–point energy.

The ground state electronic energy of our real molecule is the sum of the electron kinetic energy, the nucleus–electron attraction potential energies, and the

electron–electron repulsion potential energies and each is a functional of the ground–state electron density

$$E_0 = \langle T[\rho_0] \rangle + \langle V_{ne}[\rho_0] \rangle + \langle V_{ee}[\rho_0] \rangle \quad (2.10)$$

Focusing on the middle term, the nucleus–electron potential energy is the sum over all $2n$ electrons of the potential corresponding to attraction of an electron for all the nuclei A

$$\langle V_{ne} \rangle = \sum_{i=1}^{2n} \sum_{\text{nuclei } A} -\frac{Z_A}{r_{iA}} = \sum_{i=1}^{2n} v(r_i) \quad (2.11)$$

where $v(r_i)$ is the external potential for the attraction of electron i to the nuclei. The density function ρ can be introduced into $\langle V_{ne} \rangle$ by using that

$$\int \Psi \sum_{i=1}^{2n} f(r_i) \Psi dt = \int \rho(r) f(r) dr \quad (2.12)$$

where $f(r_i)$ is a function of the coordinates of the $2n$ electrons of a system and Ψ is the total wave function from equations (2.11) and (2.12), invoking the notion of expectation value $\langle V_{ne} \rangle = \langle \Psi | \hat{V}_{ne} | \Psi \rangle$, and since $\hat{V} = V_x$, and get,

$$E_0 = \int \rho_0(r) v(r) dr + \langle T[\rho_0] \rangle + \langle V_{ee}[\rho_0] \rangle \quad (2.13)$$

that can not known the function in $\langle T[\rho_0] \rangle$ and $\langle V_{ee}[\rho_0] \rangle$. The Kohn and Sham to introduced the idea of a reference system of non–interacting electrons. Let us to define the quantity $\Delta \langle T[\rho_0] \rangle$ as the deviation of the real kinetic energy from that of the reference system.

$$\Delta \langle T[\rho_0] \rangle \equiv \langle T[\rho_0] \rangle - \langle T_r[\rho_0] \rangle \quad (2.14)$$

Let us next define $\Delta\langle V_{ee} \rangle$ as the deviation of the real electron–electron repulsion energy from classical charged–cloud coulomb repulsion energy. This typical electrostatic repulsion energy is the summation of the repulsion energies for pairs of infinitesimal volume elements $\rho(r_1)dr_1$ and $\rho(r_2)dr_2$ divided by distance r_{12} , multiplied by one–half. The sum infinitesimals is an integral and so

$$\Delta\langle V_{ee}[\rho_0] \rangle = \langle V_{ee}[\rho_0] \rangle - \frac{1}{2} \iint \frac{\rho_0(r_1)\rho_0(r_2)}{r_{12}} dr_1 dr_2 \quad (2.15)$$

Actually, the classical charged–cloud repulsion is somewhat inappropriate for electrons in that smearing an electron out into a cloud forces it to repel itself, as any two regions of the cloud interact repulsively. This physically incorrect electron self–interacting will be compensated for by a good exchange–correlation functional can be written as

$$E_0 = \int \rho_0(r) v(r) dr + \langle T[\rho_0] \rangle + \frac{1}{2} \iint \frac{\rho_0(r_1)\rho_0(r_2)}{r_{12}} + \Delta\langle T[\rho_0] \rangle + \Delta\langle V_{ee}[\rho_0] \rangle \quad (2.16)$$

The sum of the kinetic energy deviation from the reference system and the electron–electron repulsion energy deviation from the classical system is called the exchange–correlation energy, E_{xc}

$$E_{xc}[\rho_0] \equiv \Delta\langle T[\rho_0] \rangle + \Delta\langle V_{ee}[\rho_0] \rangle \quad (2.17)$$

The $\Delta\langle T \rangle$ term represents the kinetic correlation energy of the electrons and the $\langle \Delta V_{ee} \rangle$ term the potential correlation energy and the exchange energy, although exchange and correlation energy in DFT do have exactly.

2.2.1.2 The Kohn–Sham equations [43]

The Kohn–Sham equations are theorem obtained by utilizing the variation principle, which the second Hohenberg–Kohn theorem assures applies to DFT. They

use the fact that the electron density of the reference system, which is the same as that of our real system, is given by

$$\rho_0 = \rho_r = \sum_{i=1}^{2n} |\psi_i^{\text{KS}}(1)|^2 \quad (2.18)$$

where the ψ_i^{KS} are the Kohn–Sham spatial orbital. Substituting the above appearance for the orbitals into the energy and varying E_0 with respect to the ψ_i^{KS} subject to the restriction that these remain orthonormal lead to the Kohn–Sham equations, procedure is similar to that used in deriving the Hartree–Fock equations,

$$\left[-\frac{1}{2} \nabla_i^2 - \sum_{\text{nuclei A}} \frac{Z_A}{r_{iA}} + \int \frac{\rho(r_2)}{r_{12}} dr_2 + v_{\text{xc}}(1) \right] \psi_i^{\text{KS}}(1) = \varepsilon_i^{\text{KS}} \psi_i^{\text{KS}}(1) \quad (2.19)$$

where $\varepsilon_i^{\text{KS}}$ are the Kohn–Sham energy levels and $v_{\text{xc}}(1)$ is the exchange correlation potential, arbitrarily designated here for electron number 1, since the Kohn–Sham equations are a set of one–electron equations with the subscript i running from 1 to n , over all the $2n$ electron in the system. The exchange correlation potential is defined as the functional derivative of $E_{\text{xc}}[\rho_0(r)]$ with respect to $\rho(r)$

$$v_{\text{xc}}(r) = \frac{\delta E_{\text{xc}}[\rho(r)]}{\delta \rho(r)} \quad (2.20)$$

We need the derivative v_{xc} for, and the exchange–correlation function itself for the energy equation. The Kohn–Sham equations can be written as

$$\hat{h}^{\text{KS}}(1) \psi_i^{\text{KS}}(1) = \varepsilon_i^{\text{KS}} \psi_i^{\text{KS}}(1) \quad (2.21)$$

The Kohn–Sham operator \hat{h}^{KS} is defined by equation (2.19). The difference between DFT methods is the choice of the functional from of the exchange–correlation energy. Functional forms are often designed to have a certain limiting behavior, and correct parameters to known perfect data. Which functional is the better

will have to be settled by comparing the performance with experiments or high-level wave mechanics calculations.

2.2.2 Hybrid methods

Hybrid functional increase the DFT exchange–correlation energy with a term calculated from Hartree–Fock theory. The Kohn–Sham orbitals are quit similar to the HF orbitals give an expression, based on Kohn–Sham orbitals, for the HF exchange energy

$$E_x^{\text{HF}} = - \sum_{i=1}^n \sum_{j=1}^n \left\langle \psi_i^{\text{KS}}(1) \psi_i^{\text{KS}}(2) \left| \frac{1}{r_{ij}} \right| \psi_i^{\text{KS}}(2) \psi_j^{\text{KS}}(1) \right\rangle \quad (2.22)$$

Since the Kohn–Sham Slater determinant is an exact representation of the wave function of the non–interacting electron reference system, E_x^{HF} is the exact exchange energy for a system of non–interacting electron with electron density equal to real system. Including in a LSDA gradient–corrected DFT expression for E_{xc} ($E_{xc}=E_x+E_c$) a weighted involvement of the expression for E_x^{HF} give a HF/DFT exchange–correlation functional, commonly called a Hybrid DFT functional. The most popular hybrid functional at present is based on an exchange–energy functional developed by Becke and Steven *et al.* modified introduction of the LYP correlation–energy functional. This exchange–correlation functional, called the Becke3LYP or B3LYP functional is

$$E_{xc}^{\text{B3LYP}} = (1-a_0-a_x)E_x^{\text{LSDA}} + a_0E_x^{\text{HF}} + a_xE_x^{\text{B88}} + (1-a_c)E_x^{\text{VWN}} + a_cE_c^{\text{LYP}} \quad (2.23)$$

Here E_x^{LSDA} is the kind accurate pure DFT LSDA non–gradient–corrected exchange functional, E_x^{HF} is the Kohn–Sham orbitals based HF exchange energy functional, E_x^{B88} is the Becke 88 exchange functional

$$E_x^{\text{B88}} = E_x^{\text{LDA}} + \Delta E_x^{\text{B88}}$$

$$\Delta E_x^{\text{B88}} = -\beta\rho^{1/3} \frac{x^2}{1 + 6\beta x \sinh^{-1} x}$$

the β parameter is determined by fitting to known atomic data and x is a dimension gradient variable. The E_x^{VWN} is the Vosko, Wilk, Nusair function (VWN) can be written

$$E_x^{\text{VWN}} = E_x^{\text{LDA}} (1 + ax^2 + bx^4 + cx^6)^{1/5}$$

$$x = \frac{|\nabla\rho|}{\rho^{4/3}}$$

which forms part of the perfect functional for the homogeneous electron gas of the LDA and LSDA, and E_c^{LYP} is the LYP correlation functional. The parameters a_0 , a_x and a_c are those that give the best fit of the calculated energy to molecular atomization energies. This is thus gradient-corrected hybrid functional.

2.3 Gaussian basis sets

The LCAO approximation requires the use of a basis set made up of a finite number of well-defined functions centered on each atom. The apparent choice for the functions would be those corresponding closely to the exact solution of the hydrogen atom, that is, a polynomial in the Cartesian coordinates multiplying an exponential in r . However, the use of these functions was not cost effective, and early numerical calculations were carried out using nodeless Slater-type orbitals (STOs), defined by

$$\phi(r, \theta, \phi) = \frac{(2\zeta/a_0)^{n+1/2}}{[(2n)!]^{1/2}} r^{n-1} e^{-\zeta r/a_0} Y_l^m(\theta, \phi) \quad (2.24)$$

The symbols n , m , and l denote the usual quantum numbers and ζ are the effective nuclear charge. Use of these so-called Slater functions was entertained sincerely in the years immediately following the introduction of the Roothaan-Hall equations, but soon abandoned because they lead to integrals that are difficult if not impossible to

evaluate analytically. Further work showed that the cost of calculations can be further reduced if the AOs are expanded in terms of Gaussian functions, which have the form

$$g_{ijk}(r) = N x^i y^j z^k e^{-\alpha r^2} \quad (2.25)$$

In this equation, x , y , and z are the position coordinates measured from the nucleus of an atom; i , j , and k are nonnegative integers, and α is an orbital exponent. An s -type function is generated if one of i , j , and k is 1 and the remaining two are 0; and a d -type function (second order Gaussian) is generated by all combinations that give $i + j + k = 2$. Note that this guidelines leads to six rather than five d -type functions, but appropriate combinations of these six functions give the usual five d -type functions and a sixth function that has s symmetry.

Gaussian functions lead to integrals that are easily evaluated. With the experiment of so-called semi-empirical models, which do not actually entail evaluation of large numbers of difficult integrals, all practical quantum chemical models now make use of Gaussian functions.

Given the different radial dependence of STOs and Gaussian functions, it is not obvious at first glance that Gaussian functions are appropriate choices for AOs. The solution to this problem is to approximate the STOs by a linear combination of Gaussian functions having different α values, rather than by a single Gaussian function.

In practice, instead of taking character Gaussian functions as members of the basis set, a normalized linear combination of Gaussian functions with fixed coefficients is constructed to provide a best fit to an AO. The value of each coefficient is optimized either by seeking minimum atom energies or by comparing calculated and experimental results for representative molecules. These linear combinations are called contracted functions. The contracted functions become the elements of basis set. Although the coefficients in the contracted functions are fixed, the coefficient $c_{\mu i}$ in Equation (2.6) is variable and optimized in the solution of the Schrödinger equation.

2.3.1 Minimal basis sets

Although there is no limit to the number of functions that can be located on an atom, there is a minimum number. The minimum number is the number of functions required to grasp all the electrons of the atom while still maintaining its overall spherical character. This simplest representation or minimal basis set involves a single (1s) function for hydrogen and helium, a set of five functions (1s, 2s, 2p_x, 2p_y, 2p_z) for lithium to neon, and a set of nine functions (1s, 2s, 2p_x, 2p_y, 2p_z, 3s, 3p_x, 3p_y, 3p_z) for sodium to argon. Note that although 2p functions are not occupied in the lithium atoms (and 3p functions are not occupied in the sodium or magnesium atoms), they are needed to provide proper descriptions of the bonding in molecular systems.

The minimal basis sets have been devised, perhaps the most widely used and widely documented is the STO–3G basis set. Here, each of the basis functions is extended in terms of three Gaussian functions, where the values of the Gaussian exponents and the linear coefficient have been determined by least squares as best fits to Slater–type (exponential) functions.

$$\begin{aligned}\varphi(2s) &= d_{1s}e^{-\alpha_{1s}r} + d_{2s}e^{-\alpha_{2s}r} + d_{3s}e^{-\alpha_{3s}r} \\ \phi(2p_x) &= d_{1p_x}e^{-\alpha_{1p}r} + d_{2p_x}e^{-\alpha_{2p}r} + d_{3p_x}e^{-\alpha_{3p}r} \\ \phi(2p_y) &= d_{1p_y}e^{-\alpha_{1p}r} + d_{2p_y}e^{-\alpha_{2p}r} + d_{3p_y}e^{-\alpha_{3p}r} \\ \phi(2p_z) &= d_{1p_z}e^{-\alpha_{1p}r} + d_{2p_z}e^{-\alpha_{2p}r} + d_{3p_z}e^{-\alpha_{3p}r}\end{aligned}$$

2.3.2 Split–valence basis sets

A Split–valence basis sets represents core atomic orbitals by one set of functions and valence atomic orbitals by two sets of functions, 1s, 2sⁱ, 2p_xⁱ, 2p_yⁱ, 2p_zⁱ, 2s^o, 2p_x^o, 2p_y^o, 2p_z^o for lithium to neon and 1s, 2s, 2p_x, 2p_y, 2p_z, 3sⁱ, 3p_xⁱ, 3p_yⁱ, 3p_zⁱ, 3s^o, 3p_x^o, 3p_y^o, 3p_z^o for sodium to argon. Note that the valence 2s (3s) functions are also split into inner and outer components, and that hydrogen atoms are also represented by inner and outer valence (1s) functions. Among the simplest split–valence basis sets are 3–21G and 6–31G. Each core atomic orbital in the 3–21G basis set is expanded in terms of three Gaussians, whereas basis functions representing

inner and outer components of valence atomic orbitals are expanded in terms of two and one Gaussians, respectively. The 6-31G basis sets are similarly constructed, with core orbitals represented in terms of six Gaussians and valence orbitals split into three and one Gaussian components. Expansion coefficients and Gaussian exponents for 3-21G and 6-31G basis sets have been determined by Hartree-Fock energy minimization on atomic ground states.

2.3.3 Polarized basis sets

The second shortcoming of a minimal (or split-valence) basis set, namely, that the basis functions are centered on atoms rather than between atoms, can be addressed by providing *d*-type functions on main-group elements (where the valence orbitals are of *s* and *p* type), and *p*-type functions on hydrogen (where the valence orbital is of *s* type). This allows displacement of electron distributions away from the nuclear positions.

The inclusion of polarization functions can be thought about either in terms of hybrid orbitals, for example, *pd* and *sp* hybrids, or otherwise in terms of a Taylor series expansion of a function (*d* functions are the first derivatives of *p* functions and *p* functions are the first derivatives of *s* functions). Although the first way of thinking is quite familiar to chemists (Pauling hybrids), the second offers the advantage of significant what steps might be taken next to effect further development, that is, adding second, third, and so on derivatives.

Among the simplest polarization basis sets is 6-31G*, constructed from 6-31G by adding a set of *d*-type polarization functions written in terms of a single Gaussian for each heavy (non-hydrogen) atom. A set of six second-order Gaussians is added in the case of 6-31G*. Gaussian exponents for polarization functions have been selected to give the lowest energies for representative molecules. Polarization of the *s* orbitals on hydrogen atoms is necessary for an accurate description of the bonding in many systems (particularly those in which hydrogen is a bridging atom). The 6-31G* basis set is identical to 6-31G, except that it also provides *p*-type polarization functions for hydrogen.

2.3.4 Basis sets incorporating diffuse functions

Calculations involving anions, for example, absolute acidity calculations, and calculations of molecules in excited states and of UV adsorption spectra often posture special problems. This is because the highest energy electrons for such species may only be loosely related with specific atoms (or pairs of atoms). In these situations, basis sets may need to be supplemented by diffuse functions, such as diffuse *s*- and *p*-type functions, on heavy (non-hydrogen) atoms (designated with a plus sign as 6-31+G* and 6-31+G**). It may also be enviable to provide hydrogens with diffuse *s*-type functions (designated by two plus signs as in 6-31 ++G* and 6-31 ++G**).

2.3.5 Effective core potentials

The use of effective core potentials (ECP) has been the important success in the molecular orbital calculations involving transition metals. ECP is simply a group of potential functions that substitute the inner shell electrons and orbitals that are normally implicit to have minor effects on the formation of chemical bonds. Calculations of the valence electrons using ECP can be carried out at a fraction of the computational cost that is required for an all electron (AE) calculation, while the overall quality of computation does not differ much from the AE calculations. Combined with the use of dependable basis sets, it appears to be the most dominant and reasonable method for dealing with molecules containing heavy transition metals. Following this approach, the LanL2DZ basis set [38-40] was employed for geometry optimization. The LanL2DZ basis sets (a split valence basis) are one of the double basis sets which were used for determining only valence electron in order to be easy in calculation. It contains effective core potential representations of electrons near the nuclei for post-third-row atoms. The reliability of this basis set has been confirmed by the accuracy of calculation results compared with experimental data as well as those from a more expensive all electron basis set.

CHAPTER III

DETAILS OF THE CALCULATIONS

3.1 Computational method

Structure optimizations of gaseous oxygen, carbon monoxide, nitric oxide, nitrogen dioxide, nitrous oxide, ammonia, hydrogen and water molecules adsorption configurations on the various sizes of hydrogen-terminated ZnONCs and ZnOGLNSs namely aromatic-like (AL-ZnONC, $Zn_3O_3H_6$), naphthalene-like (NLL-ZnONC, $Zn_5O_5H_8$), pyrene-like (PRL-ZnONC, $Zn_8O_8H_{10}$), coronene-like (CNL-ZnOGLNS, $Zn_{12}O_{12}H_{12}$) and circumcoronene-like (CCL-ZnOGLNS, $Zn_{27}O_{27}H_{18}$) were carried out using density functional theory (DFT) approach. The calculations have been performed with hybrid density functional B3LYP, the Becke's three-parameter exchange functional [36] with the Lee-Yang-Parr correlation functional [37], using the Los Alamos LanL2DZ split-valence basis set [38-40]. All calculations were performed with the GAUSSIAN 03 program [44].

The B3LYP/LanL2DZ-optimized structures of the AL-ZnONC, NLL-ZnONC, and PRL-ZnONC nanoclusters and the CNL-ZnOGLNS and CCL-ZnOGLNS nanosheets obtained from the full geometry optimizations were shown in Figure 3.1. The molecular symmetries for the AL-ZnONC (C_{3h}), NLL-ZnONC (C_{2v}), PRL-ZnONC (C_{2v}), CNL-ZnOGLNS (C_{3h}) and CCL-ZnOGLNS (C_{3h}) were not obtained from the calculations but assumed based on group theory using their optimized geometries which were hardly distorted. Numbers of various gaseous molecules adsorption positions of gas molecules adsorbed on nanosheets were one third for C_{2v} symmetry and one sixth for C_{3h} symmetry of the whole adsorption area. Therefore, only one third and one sixth of adsorption area of nanosheets have been investigated as representative area for the C_{2v} and C_{3h} symmetries, respectively and the whole adsorption positions have been generated from their symmetrical operation.

Initial positions of gas molecules adsorbed on the studied ZnO nanoclusters and nanosheets have been examined by lining up the gas molecules bond parallel to every bond types, the Zn-O, Zn-H and O-H bonds with all possible directions of gas molecules above the hexagonal structure of ZnOGLNSs and perpendicular to

hydrogen, oxygen atoms, zinc atoms and center of the their hexagon as illustrated in Figure 3.2 which the CNL–ZnOGLNS was selected as representative ZnO nanosheets.

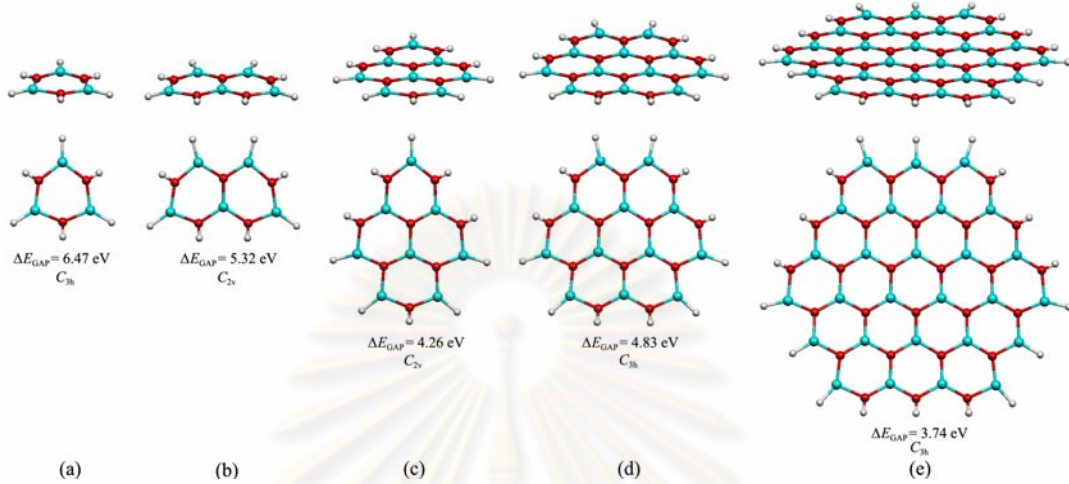


Figure 3.1 The B3LYP/LanL2DZ-optimized structures of (a) the AL–ZnONC, (b) NLL–ZnONC, (c) PRL–ZnONC, (d) CNL–ZnONS and (e) CCL–ZnONS and their energy gaps and molecular symmetries. The atomic labeling of their representative atoms depend on their molecular symmetries.

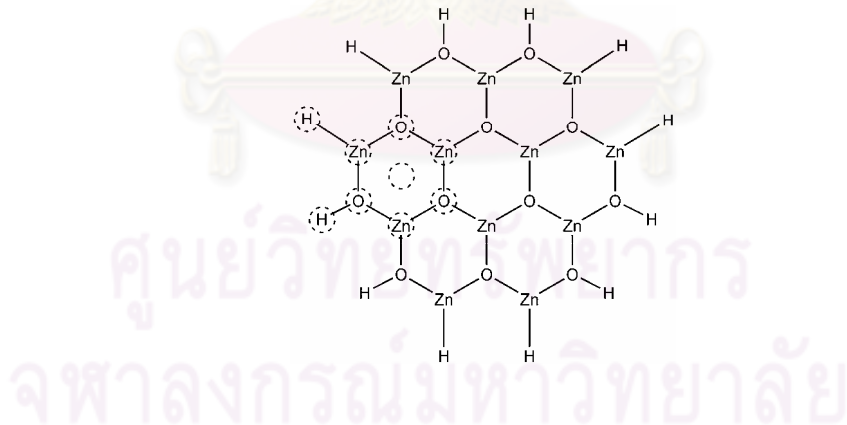


Figure 3.2 The CNL–ZnONS selected as representative ZnO nanosheets shows the possible adsorption sites as over the hydrogen, zinc, oxygen atoms and hexagonal center of nanosheets.

The adsorption energy (ΔE_{ads}) for gas molecules adsorbed on the clean surface of ZnOGLNS has been computed by the following equation:

$$\Delta E_{ads} = E_{gas/ZnOGLNS} - (E_{gas} + E_{ZnOGLNS}) \quad (3.1)$$

where $E_{\text{gas/ZnOGLNS}}$ is the total energy of gas molecules adsorbed on the ZnOGLNS surface, E_{gas} and E_{ZnOGLNS} are the total energies of the isolated gas molecules and clean surface of ZnOGLNS, respectively.

The bond strength (BS in kcal/mol) of Zn–O bond in bare ZnO nanosheets has been computed using the coulomb's law as following equation:

$$BS = \frac{5.52 \times 10^{-22} \times N_0 q_{\text{Zn}} q_{\text{O}}}{r_{\text{Zn-O}}} \quad (3.2)$$

where N_0 is an Avogadro number, q_{Zn} and q_{O} are electronic charges (e) of zinc and oxygen atoms, respectively and $r_{\text{Zn-O}}$ (Å) is distance between zinc and oxygen atoms.



ศูนย์วิทยทรัพยากร
จุฬาลงกรณ์มหาวิทยาลัย

CHAPTER IV

RESULTS AND DISCUSSION

In the present study, the adsorption of gaseous oxygen, carbon monoxide, nitric oxide, nitrogen dioxide, nitrous oxide, ammonia, hydrogen and water molecules on the ZnO nanoclusters (ZnONCs) and ZnO nanosheets (ZnONSs) *i.e.* ZnO nanoclusters of aromatic-like (AL-ZnONC, $Zn_3O_3H_6$), naphthalene-like (NLL-ZnONC, $Zn_5O_5H_8$), pyrene-like PRL-like (PRL-ZnONC, $Zn_8O_8H_{10}$), and ZnO nanosheets of coronene-like (CNL-ZnONS, $Zn_{12}O_{12}H_{12}$) and circumcoronene-like (CCL-ZnONS, $Zn_{27}O_{27}H_{18}$) and their electronic properties have been investigated. The details of results and discussion were shown below.

4.1 The optimized structures and Zn–O bond strength

The B3LYP/LanL2DZ-optimized structures of the AL-ZnONC, NLL-ZnONC, and PRL-ZnONC nanoclusters and the CNL-ZnOGLNS and CCL-ZnOGLNS nanosheets obtained by all-atom geometry optimization method were shown in Figure 4.1. The molecular symmetries for B3LYP/LanL2DZ-optimized structures of the AL-ZnONC (C_{3h}), NLL-ZnONC (C_{2v}), PRL-ZnONC (C_{2v}), CNL-ZnOGLNS (C_{3h}) and CCL-ZnOGLNS (C_{3h}) were obtained by assumption of their perfect geometries; their optimized geometries were hardly distorted as shown in Figure 2.1. The bond strengths of outer Zn–O bonds of all the ZnONCs and ZnOGLNSs were much weaker than inner Zn–O bonds. All the ZnONCs and ZnOGLNSs, the bond strengths of their outer Zn–O bonds which zinc were terminated by hydrogen atom, were found within the energy range of –301.88 to –316.65 kcal/mol. The bond strengths of the most inner Zn–O bonds of ZnOGLNSs computed using equation (3.2) were in order: CCL-ZnOGLNS (–487.10 kcal/mol) > CNL-ZnOGLNS (–485.52 kcal/mol) > PRL-ZnONC (–474.93 kcal/mol).

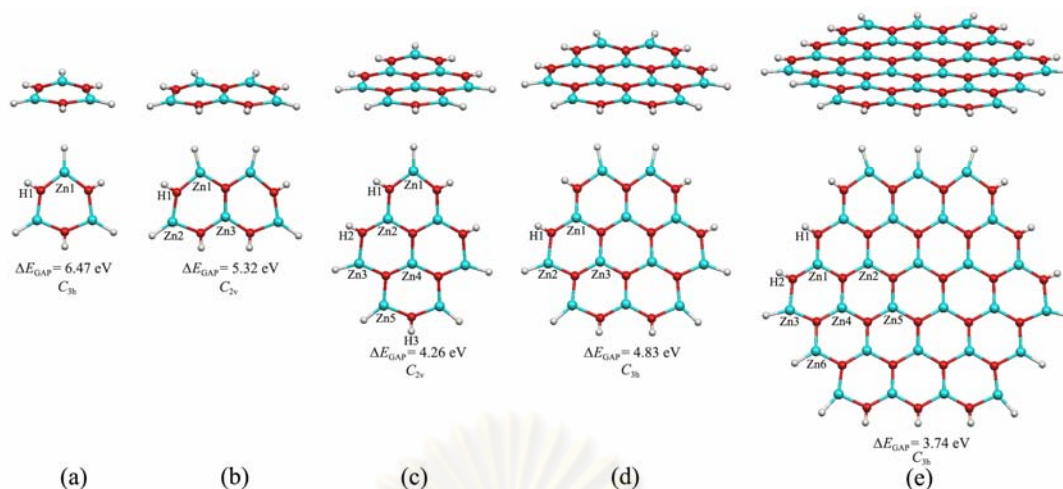


Figure 4.1 The B3LYP/LanL2DZ-optimized structures of (a) the AL-ZnONC, (b) NLL-ZnONC, (c) PRL-ZnONC, (d) CNL-ZnONS and (e) CCL-ZnONS and their energy gaps and molecular symmetries. The atomic labeling of their representative atoms depend on their molecular symmetries.

4.2 Adsorption of molecule gaseous on ZnO nanoclusters and ZnO nanosheets

4.2.1 Adsorption of oxygen molecule

Geometry configurations of oxygen adsorptions on the rigid structures of the AL-ZnONC, NLL-ZnONC, and PRL-ZnONC nanoclusters and the CNL-ZnOGLNS and CCL-ZnOGLNS nanosheets were obtained as shown in Figures 4.2 and 4.3. The number of energy minima of oxygen adsorptions on the AL-ZnONC of nine configurations was found for each side of its molecular planes. These energy minima were obtained from the structure optimizations of interaction configurations within one third of each side of the AL-ZnONC molecular area and oxygen adsorptions over the whole AL-ZnONC molecular area were generated using C_{3h} symmetrical operation. The most stable configuration of oxygen adsorption on the AL-ZnONC was represented by the configuration of oxygen #1 of which the adsorption energy was -29.87 kcal/mol ($O-H = 1.00$ Å). Adsorption energies of oxygen on studied nanoclusters and nanosheets were shown in Table 4.1.

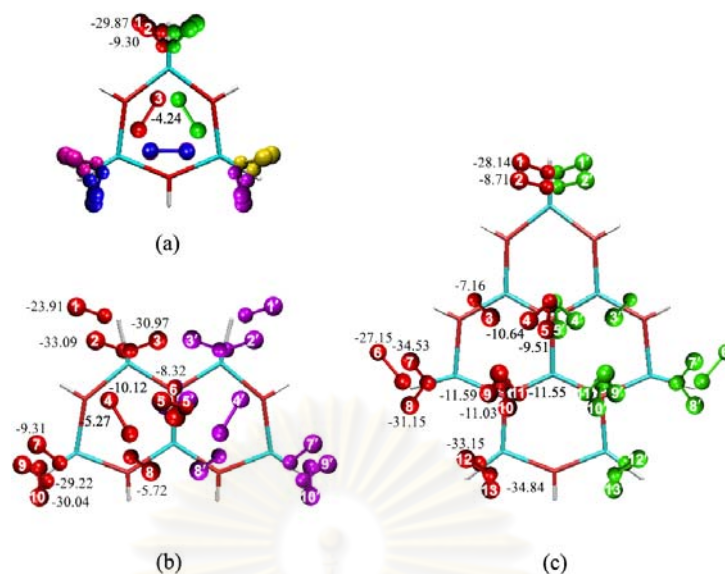


Figure 4.2 Plots of oxygen molecules as minimum energy structures of their adsorptions on (a) the AL-ZnONC ($\text{Zn}_3\text{O}_3\text{H}_6$), (b) NLL-ZnONC ($\text{Zn}_5\text{O}_5\text{H}_8$) and (c) PRL-ZnONC ($\text{Zn}_8\text{O}_8\text{H}_{10}$). The molecules labeled with numbers represent the oxygen molecule interacting with ZnONCs as representative of molecular symmetry of AL-ZnONC (C_{3h}), NLL-ZnONC (C_{2v}) and PRL-ZnONC (C_{2v}). Adsorption energies in kcal/mol were presented.

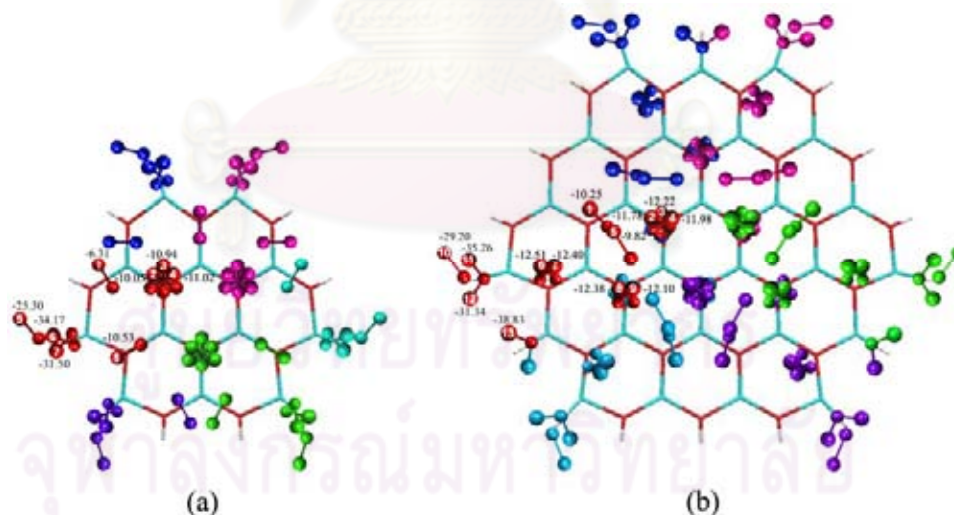


Figure 4.3 Plots of oxygen molecules as minimum energy structures of their adsorptions on (a) CNL-ZnONS ($\text{Zn}_{12}\text{O}_{12}\text{H}_{12}$) and (b) CCL-ZnONS ($\text{Zn}_{27}\text{O}_{27}\text{H}_{18}$) as minimum energy structures. The molecules labeled with numbers represent the oxygen molecule interacting with ZnONCs as representative of molecular symmetry of CNL-ZnONS (C_{3h}) and CCL-ZnONS (C_{3h}). Adsorption energies in kcal/mol were presented.

Table 4.1 Adsorption energies (ΔE_{ads} in kcal/mol) of O_2 on ZnONCs and ZnOGLNSs, and energy gaps (ΔE_{GAP} in eV) of bare surfaces of ZnONCs, ZnOGLNSs, and their O_2 adsorption complexes, computed at the B3LYP/LanL2DZ level of theory.

ZnOGLNSs/oxygen adsorption	ΔE_{ads} (kcal/mol)	ΔE_{GAP} (eV)
AL-ZnONC:		6.47
$\text{O}_2 + \text{AL-ZnONC} \rightarrow \text{O}_2/\text{AL-ZnONC}$ (1)	-29.87	3.50
$\text{O}_2 + \text{AL-ZnONC} \rightarrow \text{O}_2/\text{AL-ZnONC}$ (2)	-9.30	2.14
$\text{O}_2 + \text{AL-ZnONC} \rightarrow \text{O}_2/\text{AL-ZnONC}$ (3)	-4.24	1.49
NLL-ZnONC:		5.32
$\text{O}_2 + \text{NLL-ZnONC} \rightarrow \text{O}_2/\text{NLL-ZnONC}$ (1)	-23.91	2.55
$\text{O}_2 + \text{NLL-ZnONC} \rightarrow \text{O}_2/\text{NLL-ZnONC}$ (2)	-33.09	3.41
$\text{O}_2 + \text{NLL-ZnONC} \rightarrow \text{O}_2/\text{NLL-ZnONC}$ (3)	-30.97	3.35
$\text{O}_2 + \text{NLL-ZnONC} \rightarrow \text{O}_2/\text{NLL-ZnONC}$ (4)	-5.27	1.25
$\text{O}_2 + \text{NLL-ZnONC} \rightarrow \text{O}_2/\text{NLL-ZnONC}$ (5)	-10.12	2.01
$\text{O}_2 + \text{NLL-ZnONC} \rightarrow \text{O}_2/\text{NLL-ZnONC}$ (6)	-8.32	2.06
$\text{O}_2 + \text{NLL-ZnONC} \rightarrow \text{O}_2/\text{NLL-ZnONC}$ (7)	-9.31	2.12
$\text{O}_2 + \text{NLL-ZnONC} \rightarrow \text{O}_2/\text{NLL-ZnONC}$ (8)	-5.72	0.87
$\text{O}_2 + \text{NLL-ZnONC} \rightarrow \text{O}_2/\text{NLL-ZnONC}$ (9)	-29.22	3.46
$\text{O}_2 + \text{NLL-ZnONC} \rightarrow \text{O}_2/\text{NLL-ZnONC}$ (10)	-30.04	3.50
PRL-ZnONC:		4.26
$\text{O}_2 + \text{PRL-ZnONC} \rightarrow \text{O}_2/\text{PRL-ZnONC}$ (1)	-28.14	2.73
$\text{O}_2 + \text{PRL-ZnONC} \rightarrow \text{O}_2/\text{PRL-ZnONC}$ (2)	-8.71	1.03
$\text{O}_2 + \text{PRL-ZnONC} \rightarrow \text{O}_2/\text{PRL-ZnONC}$ (3)	-7.16	0.54
$\text{O}_2 + \text{PRL-ZnONC} \rightarrow \text{O}_2/\text{PRL-ZnONC}$ (4)	-10.64	1.16
$\text{O}_2 + \text{PRL-ZnONC} \rightarrow \text{O}_2/\text{PRL-ZnONC}$ (5)	-9.51	0.99
$\text{O}_2 + \text{PRL-ZnONC} \rightarrow \text{O}_2/\text{PRL-ZnONC}$ (6)	-27.15	2.48
$\text{O}_2 + \text{PRL-ZnONC} \rightarrow \text{O}_2/\text{PRL-ZnONC}$ (7)	-34.53	3.33
$\text{O}_2 + \text{PRL-ZnONC} \rightarrow \text{O}_2/\text{PRL-ZnONC}$ (8)	-31.15	3.18
$\text{O}_2 + \text{PRL-ZnONC} \rightarrow \text{O}_2/\text{PRL-ZnONC}$ (9)	-11.59	1.82
$\text{O}_2 + \text{PRL-ZnONC} \rightarrow \text{O}_2/\text{PRL-ZnONC}$ (10)	-11.03	1.92
$\text{O}_2 + \text{PRL-ZnONC} \rightarrow \text{O}_2/\text{PRL-ZnONC}$ (11)	-11.55	1.86
$\text{O}_2 + \text{PRL-ZnONC} \rightarrow \text{O}_2/\text{PRL-ZnONC}$ (12)	-33.15	3.35
$\text{O}_2 + \text{PRL-ZnONC} \rightarrow \text{O}_2/\text{PRL-ZnONC}$ (13)	-34.84	3.32
CNL-ZnONS:		4.83
$\text{O}_2 + \text{CNL-ZnONS} \rightarrow \text{O}_2/\text{CNL-ZnONS}$ (1)	-6.31	1.06
$\text{O}_2 + \text{CNL-ZnONS} \rightarrow \text{O}_2/\text{CNL-ZnONS}$ (2)	-10.05	1.95
$\text{O}_2 + \text{CNL-ZnONS} \rightarrow \text{O}_2/\text{CNL-ZnONS}$ (3)	-10.94	1.90
$\text{O}_2 + \text{CNL-ZnONS} \rightarrow \text{O}_2/\text{CNL-ZnONS}$ (4)	-11.02	1.92
$\text{O}_2 + \text{CNL-ZnONS} \rightarrow \text{O}_2/\text{CNL-ZnONS}$ (5)	-25.30	2.39
$\text{O}_2 + \text{CNL-ZnONS} \rightarrow \text{O}_2/\text{CNL-ZnONS}$ (6)	-34.17	3.34
$\text{O}_2 + \text{CNL-ZnONS} \rightarrow \text{O}_2/\text{CNL-ZnONS}$ (7)	-31.50	3.27
$\text{O}_2 + \text{CNL-ZnONS} \rightarrow \text{O}_2/\text{CNL-ZnONS}$ (8)	-10.53	2.15
CCL-ZnONS:		3.74
$\text{O}_2 + \text{CCL-ZnONS} \rightarrow \text{O}_2/\text{CCL-ZnONS}$ (1)	-10.25	1.08
$\text{O}_2 + \text{CCL-ZnONS} \rightarrow \text{O}_2/\text{CCL-ZnONS}$ (2)	-11.78	1.41
$\text{O}_2 + \text{CCL-ZnONS} \rightarrow \text{O}_2/\text{CCL-ZnONS}$ (3)	-12.22	1.41
$\text{O}_2 + \text{CCL-ZnONS} \rightarrow \text{O}_2/\text{CCL-ZnONS}$ (4)	-11.98	1.41
$\text{O}_2 + \text{CCL-ZnONS} \rightarrow \text{O}_2/\text{CCL-ZnONS}$ (5)	-9.82	0.90
$\text{O}_2 + \text{CCL-ZnONS} \rightarrow \text{O}_2/\text{CCL-ZnONS}$ (6)	-12.51	1.51
$\text{O}_2 + \text{CCL-ZnONS} \rightarrow \text{O}_2/\text{CCL-ZnONS}$ (7)	-12.40	1.62
$\text{O}_2 + \text{CCL-ZnONS} \rightarrow \text{O}_2/\text{CCL-ZnONS}$ (8)	-12.38	1.46
$\text{O}_2 + \text{CCL-ZnONS} \rightarrow \text{O}_2/\text{CCL-ZnONS}$ (9)	-12.10	1.55
$\text{O}_2 + \text{CCL-ZnONS} \rightarrow \text{O}_2/\text{CCL-ZnONS}$ (10)	-29.20	2.51
$\text{O}_2 + \text{CCL-ZnONS} \rightarrow \text{O}_2/\text{CCL-ZnONS}$ (11)	-35.26	3.22
$\text{O}_2 + \text{CCL-ZnONS} \rightarrow \text{O}_2/\text{CCL-ZnONS}$ (12)	-31.34	3.03
$\text{O}_2 + \text{CCL-ZnONS} \rightarrow \text{O}_2/\text{CCL-ZnONS}$ (13)	-38.83	2.95

Due to the NLL-ZnONC and PRL-ZnONC nanoclusters were in C_{2v} symmetry, the numbers of oxygen adsorptions on each side of their molecular planes were nineteen and twenty six configurations, respectively, see Figure 4.2(b) and (c). Five different types of adsorption sites of oxygen chemisorbed ($O-H = 1.01 \text{ \AA}$) [45] on the NLL-ZnONC were located in vicinity of hydrogen of zinc hydride and the positions of adsorbed oxygen were the oxygen #1 -23.91 kcal/mol ($O-H = 1.00 \text{ \AA}$), #2 -33.09 kcal/mol ($O-H = 1.00 \text{ \AA}$), #3 -30.97 kcal/mol ($O-H = 1.00 \text{ \AA}$), #9 -29.22 kcal/mol ($O-H = 1.00 \text{ \AA}$) and #10 -30.04 kcal/mol ($O-H = 1.00 \text{ \AA}$). Six different types of adsorption sites of oxygen chemisorbed on the PRL-ZnONC were also located in vicinity of hydrogen of zinc hydride and the positions of adsorbed oxygen were the oxygen #1 -28.14 kcal/mol ($O-H = 1.00 \text{ \AA}$), #6 -27.15 kcal/mol ($O-H = 1.00 \text{ \AA}$), #7 -34.53 kcal/mol ($O-H = 1.00 \text{ \AA}$), #8 -31.15 kcal/mol ($O-H = 1.00 \text{ \AA}$) and #12 -33.15 kcal/mol ($O-H = 1.00 \text{ \AA}$) and #13 -34.83 kcal/mol ($O-H = 1.00 \text{ \AA}$).

The CNL-ZnOGLNS and CCL-ZnOGLNS were in C_{3h} symmetry, the numbers of oxygen adsorptions on each side of their molecular planes were forty two and seventy two configurations, respectively, see Figure 4.3. Three different types of adsorption sites of oxygen chemisorbed on the CNL-ZnOGLNS which were the oxygen #5 -25.30 kcal/mol ($O-H = 1.00 \text{ \AA}$), #6 -34.17 kcal/mol ($O-H = 1.00 \text{ \AA}$) and #7 -31.50 kcal/mol ($O-H = 1.00 \text{ \AA}$). Four different types of adsorption sites of oxygen chemisorbed on the CCL-ZnOGLNS as the positions of oxygen #10 -29.20 kcal/mol ($O-H = 1.02 \text{ \AA}$), #11 -35.26 kcal/mol ($O-H = 1.02 \text{ \AA}$), #12 -31.34 kcal/mol ($O-H = 1.02 \text{ \AA}$) and #13 -38.83 kcal/mol ($O-H = 1.02 \text{ \AA}$). It can be concluded that the chemisorption of oxygen on any large ZnOGLNSs occurred on the hydride adsorption site of ZnOGLNSs edge. Type number of chemisorption of oxygen on large C_{3h} -symmetrical ZnOGLNSs was the number of hydride of zinc hydride (N_{hydride}) on each edge plus two, $N_{\text{hydride}}+2$. The Figure 4.3 showed that the oxygen adsorptions on the central ring of the CCL-ZnOGLNS, the adsorbed oxygen were located at positions above the oxygen in CCL-ZnOGLNS hexagonal ring by pointing its oxygen atom toward the nanosheet oxygen with slightly tilt direction. Nevertheless, the oxygen adsorptions occurring on oxygen of the CCL-ZnOGLNS hexagonal rings closed to the central hexagonal ring also show their adsorption position above the nanosheet oxygen, see Figure 4.3(b). This suggests that the oxygen adsorptions on large ZnOGLNSs over hexagonal ring in central region, adsorbed

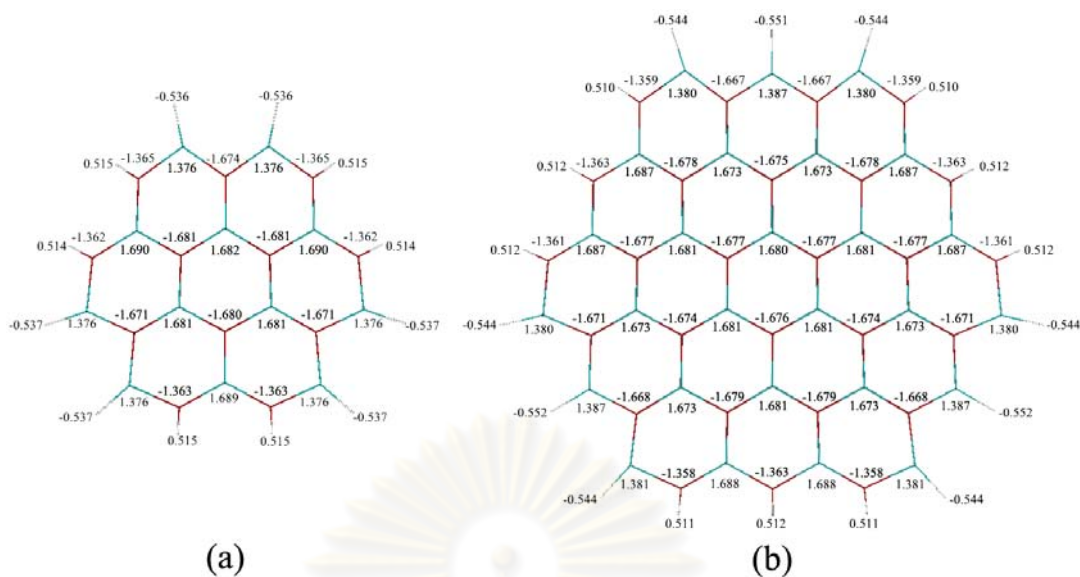


Figure 4.5 NBO charges (e) of oxygen and zinc atoms on the (a) CNL-ZnONS and (b) CCL-ZnONS.

4.2.1.2 Energy gap

The energy gaps of the clean ZnOGLNSs and their oxygen-adsorption complexes were shown in Table 4.1. The energy gaps of clean ZnOGLNSs were in order: AL-ZnONC (6.47 eV) > NLL-ZnONC (5.32 eV) > CNL-ZnOGLNS (4.83 eV) > PRL-ZnONC (4.26 eV) > CCL-ZnOGLNS (3.74 eV). In all cases, the energy gaps of clean ZnOGLNSs were higher than those values of their corresponding O₂ adsorption complexes, see Table 4.1. This suggests that the ZnOGLNSs were oxygen sensitive materials and could be developed as oxygen sensor based on electrical conductivity. It appears that the energy gap of ZnOGLNS was an inverse function of its size except PRL-ZnONC which was more active than expectation. However, the energy gap of large ZnO nanosheet should be converted into a single value which can be determined using periodic boundary condition (PBC) method; band gap of the wurtzite ZnO was found to be ≈ 3.3 eV [46]. Inverted values of termination-proton numbers (N_{TP}) for AL-ZnONC ($N_{TP} = 6$), NLL-ZnONC ($N_{TP} = 8$), PRL-ZnONC ($N_{TP} = 10$), CNL-ZnOGLNS ($N_{TP} = 12$), and CCL-ZnOGLNS ($N_{TP} = 18$) plotted against their energy gaps were shown in Figure 4.6. It shows that the energy gap of large ZnOGLNSs converted to a single value while the inverse value of N_{TP} approached to zero.

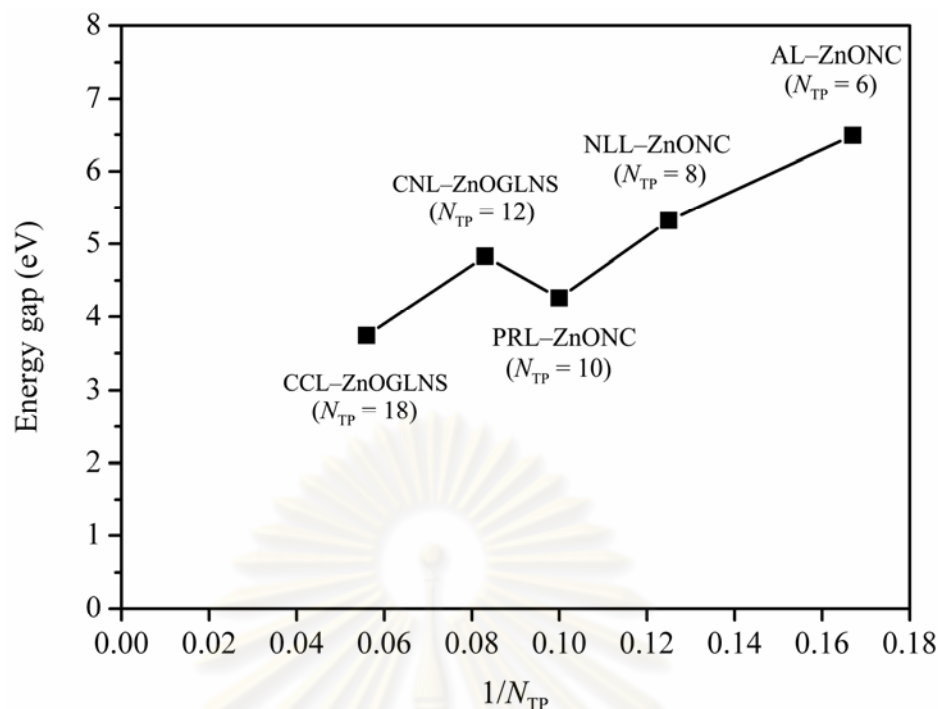


Figure 4.6 Plots of energy gaps of ZnO nanosheets against invert values of their termination–proton numbers (N_{TP}).

4.2.2 Adsorption of carbon monoxide molecule

4.2.2.1 Adsorption energies of CO pointing with C–end

Geometry configurations of CO adsorptions on the rigid structures of the AL–ZnONC, NLL–ZnONC, and PRL–ZnONC nanoclusters, shown in Figure 4.7 and the CNL–ZnONS, shown in Figure 4.8 and CCL–ZnONS nanosheets, shown in Figure 4.9, were obtained. The CO adsorption configurations of CO pointing with C–end to adsorption sites of nanoclusters were shown in left side of Figure 4.7 and to adsorption sites of the CNL–ZnONS and CCL–ZnONS nanosheets were shown in Figures 4.8(a) and 4.9(a), respectively.

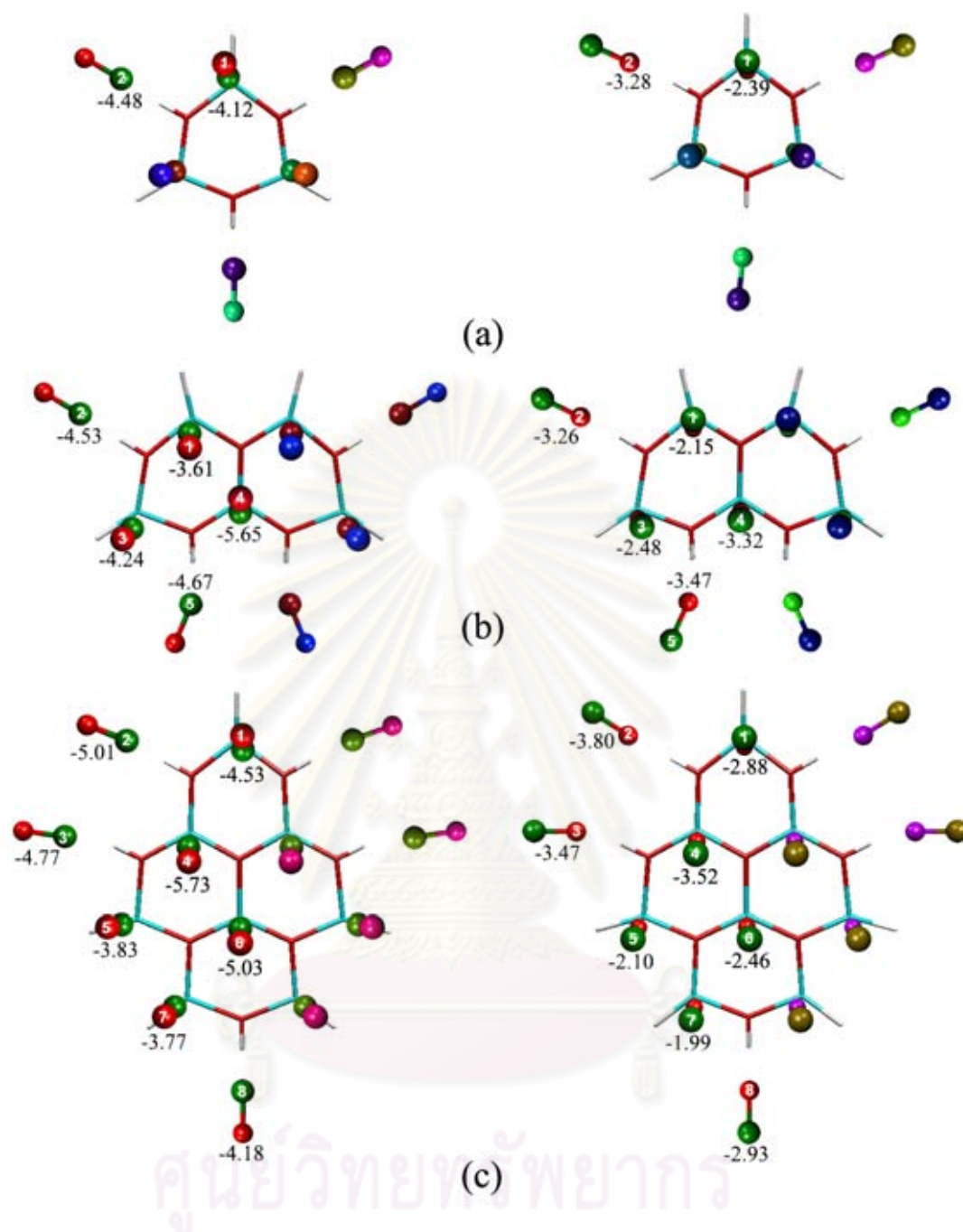


Figure 4.7 Plots of CO molecules as minimum energy structures of their adsorptions on (a) the AL-ZnONC ($\text{Zn}_3\text{O}_3\text{H}_6$), (b) NLL-ZnONC ($\text{Zn}_5\text{O}_5\text{H}_8$) and (c) PRL-ZnONC ($\text{Zn}_8\text{O}_8\text{H}_{10}$). Their left and right adsorption maps were CO adsorption on ZnONCs by pointing C-end and O-end toward the adsorption sites, respectively. The set of labeled molecules was representative of CO interacting with AL-ZnONC (C_{3h}), NLL-ZnONC (C_{2v}) and PRL-ZnONC (C_{2v}). Adsorption energies were presented in kcal/mol.

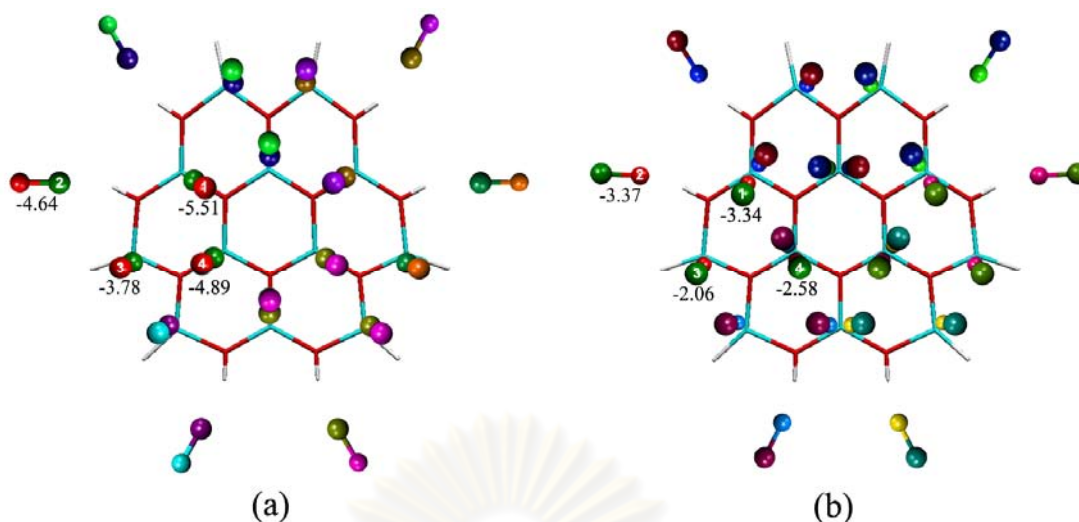


Figure 4.8 Plots of CO molecules as minimum energy structures of their adsorptions on CNL-ZnONS (Zn₁₂O₁₂H₁₂) as adsorption configurations of CO with pointing its (a) C-end and (b) O-end toward the adsorption sites of the CNL-ZnONS. The set of labeled molecules was representative of CO adsorption interacting with CNL-ZnONS with C_{3h} symmetry. Adsorption energies were presented in kcal/mol.

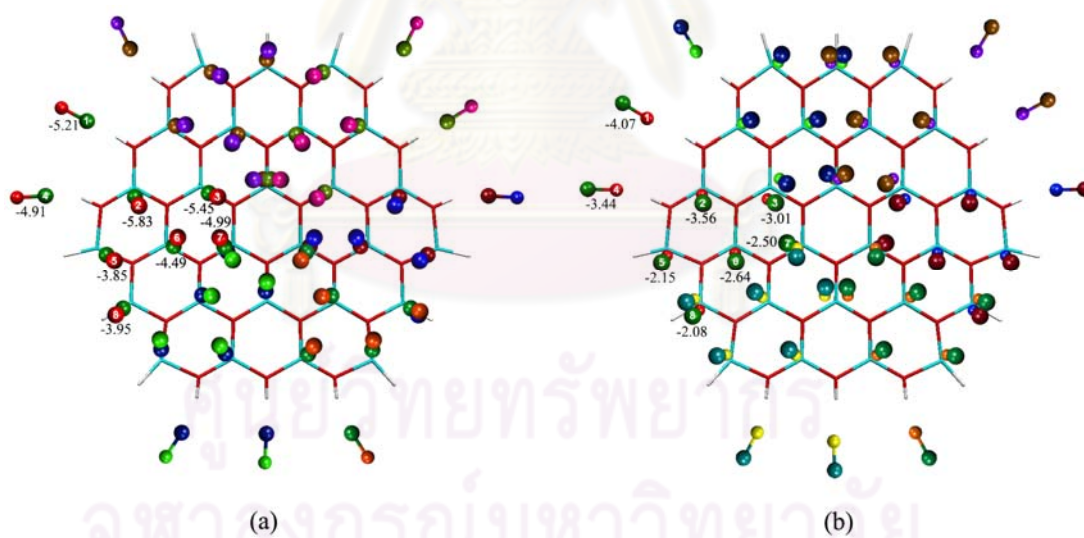


Figure 4.9 Plots of carbon monoxide molecules as minimum energy structures of their adsorptions on CCL-ZnONS (Zn₂₇O₂₇H₁₈) as (a) adsorption configurations of CO by pointing (a) C-end and (b) O-end toward the adsorption sites. The molecules labeled with numbers represent the oxygen molecule interacting with CCL-ZnONS of molecular symmetry of (C_{3h}). Adsorption energies were presented in kcal/mol.

The number of energy minima of CO adsorptions on the AL–ZnONC of six configurations was found for each side of its molecular planes. These energy minima were obtained from the structure optimizations of interaction configurations within one third of each side of the AL–ZnONC molecular area and CO adsorptions over the whole AL–ZnONC molecular area were generated using C_{3h} symmetrical operation. The most stable configuration of CO adsorption on the AL–ZnONC was represented by the configuration of CO #2 of which the adsorption energy was -4.48 kcal/mol. Adsorption energies of CO on studied nanoclusters and nanosheets were shown in Table 4.2.

As the NLL–ZnONC and PRL–ZnONC nanoclusters were in C_{2v} symmetry, the numbers of CO adsorptions on each side of their molecular planes were nine and thirteen configurations, as shown in the left sides of Figure 4.7(b) and (c), respectively. There were five types of adsorption positions on the NLL–ZnONC which were composed of adsorption position CO #1 (-3.61 kcal/mol), #2 (-4.53 kcal/mol), #3 (-4.24 kcal/mol), #4 (-5.65 kcal/mol) and #5 (-4.67 kcal/mol). There were eight types of adsorption positions on the PRL–ZnONC which were composed of adsorption positions CO #1 (-4.53 kcal/mol), #2 (-5.01 kcal/mol), #3 (-4.77 kcal/mol), #4 (-5.73 kcal/mol), #5 (-3.83 kcal/mol), #6 (-5.03 kcal/mol), #7 (-3.77 kcal/mol) and #8 (-4.18 kcal/mol).

The CNL–ZnONS and CCL–ZnONS were in C_{3h} symmetry, the numbers of CO adsorptions on each side of their molecular planes were eighteen and thirty nine configurations as shown in Figure 4.8(a) and Figure 4.9(a) respectively. There were four types of adsorption positions on the CNL–ZnONS which were composed of adsorption position CO #1 (-5.51 kcal/mol), #2 (-4.64 kcal/mol), #3 (-3.78 kcal/mol) and #4 (-4.89 kcal/mol). There were eight types of adsorption positions on the CCL–ZnONS which were composed of adsorption positions CO #1 (-5.21 kcal/mol), #2 (-5.83 kcal/mol), #3 (-5.45 kcal/mol), #4 (-4.91 kcal/mol), #5 (-3.85 kcal/mol), #6 (-4.49 kcal/mol), #7 (-4.99 kcal/mol) and #8 (-3.95 kcal/mol).

The adsorption energies of CO adsorption by pointing C–end towards to adsorption atoms on AL–ZnONC, NLL–ZnONC, PRL–ZnONC, CNL–ZnONS and CCL–ZnONS were within the ranges of -4.12 to -4.48 , -3.61 to -4.72 , -3.77 to -4.72 , -3.78 to -5.51 and -3.85 to -5.83 kcal/mol, respectively. On the same position of CO adsorptions either on nanoclusters or nanosheets, the adsorption energies of CO of which the C–end pointing towards the nanosheets atoms were more stable than the

O–end by within 1.14 to 2.57 kcal/mol. The CO adsorptions with pointing C–end towards atoms of the ZnOGLNSs were categorized into two bond types, [CO⋯H] and [CO⋯Zn]. The [CO⋯H] bond occurred when the CO adsorption with pointing C–end toward hydroxyl hydrogen of the ZnOGLNSs to which the molecular axis of CO was nearly parallel to the molecular plane. But the [CO⋯H] bond occurred when the CO adsorption with pointing C–end towards Zn atom of the ZnOGLNS to which the molecular axis of CO was nearly perpendicular to the molecular plane.

Table 4.2 Adsorption energies (ΔE_{ads} in kcal/mol) of CO pointing its C–end toward surfaces of ZnONCs and ZnOGLNSs and energy gaps (ΔE_{GAP} in eV) of bare surfaces of ZnONCs, ZnOGLNSs and their CO adsorption complexes, computed at the B3LYP/LanL2DZ level of theory.

ZnOGLNSs/carbon monoxide adsorption	ΔE_{ads} (kcal/mol)	E_{GAP} (eV)
AL-ZnONC:		6.47
<u>CO</u> + AL-ZnONC → <u>CO</u> /AL-ZnONC(1)	-4.12	5.02
<u>CO</u> + AL-ZnONC → <u>CO</u> /AL-ZnONC(2)	-4.48	5.03
NLL-ZnONC:		5.32
<u>CO</u> + NLL-ZnONC → <u>CO</u> /NLL-ZnONC (1)	-3.61	4.72
<u>CO</u> + NLL-ZnONC → <u>CO</u> /NLL-ZnONC (2)	-4.53	4.88
<u>CO</u> + NLL-ZnONC → <u>CO</u> /NLL-ZnONC (3)	-4.24	4.71
<u>CO</u> + NLL-ZnONC → <u>CO</u> /NLL-ZnONC (4)	-5.65	4.54
<u>CO</u> + NLL-ZnONC → <u>CO</u> /NLL-ZnONC (5)	-4.67	4.36
PRL-ZnONC:		4.26
<u>CO</u> + PRL-ZnONC → <u>CO</u> /PRL-ZnONC (1)	-4.53	3.82
<u>CO</u> + PRL-ZnONC → <u>CO</u> /PRL-ZnONC (2)	-5.01	3.70
<u>CO</u> + PRL-ZnONC → <u>CO</u> /PRL-ZnONC (3)	-4.77	4.28
<u>CO</u> + PRL-ZnONC → <u>CO</u> /PRL-ZnONC (4)	-5.73	3.82
<u>CO</u> + PRL-ZnONC → <u>CO</u> /PRL-ZnONC (5)	-3.83	4.26
<u>CO</u> + PRL-ZnONC → <u>CO</u> /PRL-ZnONC (6)	-5.03	4.28
<u>CO</u> + PRL-ZnONC → <u>CO</u> /PRL-ZnONC (7)	-3.77	4.22
<u>CO</u> + PRL-ZnONC → <u>CO</u> /PRL-ZnONC (8)	-4.18	4.21
CNL-ZnONS:		4.83
<u>CO</u> + CNL-ZnONS → <u>CO</u> /CNL-ZnONS (1)	-5.51	4.52
<u>CO</u> + CNL-ZnONS → <u>CO</u> /CNL-ZnONS (2)	-4.64	4.76
<u>CO</u> + CNL-ZnONS → <u>CO</u> /CNL-ZnONS (3)	-3.78	4.79
<u>CO</u> + CNL-ZnONS → <u>CO</u> /CNL-ZnONS (4)	-4.89	4.59
CCL-ZnONS:		3.74
<u>CO</u> + CCL-ZnONS → <u>CO</u> /CCL-ZnONS (1)	-5.21	3.37
<u>CO</u> + CCL-ZnONS → <u>CO</u> /CCL-ZnONS (2)	-5.83	3.70
<u>CO</u> + CCL-ZnONS → <u>CO</u> /CCL-ZnONS (3)	-5.45	3.73
<u>CO</u> + CCL-ZnONS → <u>CO</u> /CCL-ZnONS (4)	-4.91	3.76
<u>CO</u> + CCL-ZnONS → <u>CO</u> /CCL-ZnONS (5)	-3.85	3.74
<u>CO</u> + CCL-ZnONS → <u>CO</u> /CCL-ZnONS (6)	-4.49	3.71
<u>CO</u> + CCL-ZnONS → <u>CO</u> /CCL-ZnONS (7)	-4.99	3.75
<u>CO</u> + CCL-ZnONS → <u>CO</u> /CCL-ZnONS (8)	-3.95	3.72

4.2.2.2 Adsorption energies of CO pointing with O-end

The CO adsorption configurations of CO pointing with O-end to adsorption sites of nanoclusters were shown in right side of Figure 4.7 and to adsorption sites of the CNL-ZnONS and CCL-ZnONS nanosheets were shown in Figures 4.8(b) and 4.9(b), respectively.

The number of energy minima of CO adsorptions on the AL-ZnONC of six configurations was found for each side of its molecular planes. These energy minima were obtained from the structure optimizations of interaction configurations within one third of each side of the AL-ZnONC molecular area and CO adsorptions over the whole AL-ZnONC molecular area were generated using C_{3h} symmetrical operation. The most stable configuration of CO adsorption on the AL-ZnONC was represented by the configuration of CO #2 of which the adsorption energy was -3.28 kcal/mol. Adsorption energies of CO on studied nanoclusters and nanosheets were shown in Table 4.3.

As the NLL-ZnONC and PRL-ZnONC nanoclusters were in C_{2v} symmetry, the numbers of CO adsorptions on each side of their molecular planes were nine and thirteen configurations, as shown in the right sides of Figure 4.7(b) and (c), respectively. There were five types of adsorption positions on the NLL-ZnONC which were composed of adsorption position CO #1 (-2.15 kcal/mol), #2 (-3.26 kcal/mol), #3 (-2.48 kcal/mol) and #4 (-3.32 kcal/mol) and #5 (-3.47 kcal/mol). There were eight types of adsorption positions on the PRL-ZnONC which were composed of adsorption positions CO #1 (-2.88 kcal/mol), #2 (-3.80 kcal/mol), #3 (-3.47 kcal/mol), #4 (-3.52 kcal/mol), #5 (-2.10 kcal/mol), #6 (-2.46 kcal/mol), #7 (-1.99 kcal/mol) and #8 (-2.93 kcal/mol).

The CNL-ZnONS and CCL-ZnONS were in C_{3h} symmetry, the numbers of CO adsorptions on each side of their molecular planes were thirty four and forty five configurations as shown in Figures 4.8(b) and 4.9(b) respectively. There were four types of adsorption positions on the CNL-ZnONS which were composed of adsorption position CO #1 (-3.34 kcal/mol), #2 (-3.37 kcal/mol), #3 (-2.06 kcal/mol) and #4 (-2.58 kcal/mol). There were eight types of adsorption positions on the CCL-ZnONS which were composed of adsorption positions CO #1 (-4.07 kcal/mol), #2 (-3.56 kcal/mol), #3 (-3.01 kcal/mol), #4 (-3.44 kcal/mol), #5 (-2.15 kcal/mol), #6 (-2.64 kcal/mol), #7 (-2.50 kcal/mol) and #8 (-2.08 kcal/mol).

The adsorption energies of CO adsorption with pointing O-end towards to adsorption atoms on AL-ZnONC, NLL-ZnONC, PRL-ZnONC, CNL-ZnONS and CCL-ZnONS were within the ranges of -2.39 to -3.47, -1.99 to -3.80, -2.06 to -3.37, -2.06 to -3.37 and -2.08 to -4.07 kcal/mol, respectively.

4.2.2.3 Bond types and maximum numbers of CO adsorption

The bond distances between atoms of CO atoms and atoms of adsorption sites were shown in Table 4.4. Plots of all possible adsorption energies of CO on all ZnONC, PRL-ZnONC nanoclusters and PRL-ZnONC, CNL-ZnONS and CCL-ZnONS nanosheets against their bond distances were shown in Figure 4.10. It shows that the four types of bonds [CO...H], [CO...Zn], [OC...H] and [OC...Zn], separated as four zones were found. The bond distances of four types, [CO...H], [CO...Zn], [OC...H] and [OC...Zn] were within the ranges of 2.21 to 2.24 Å, 2.04 to 2.07 Å, 2.61 to 2.80 Å and 2.62 to 2.96 Å which their corresponding adsorption energies were within the ranges of -4.18 to -5.21, -3.61 to -5.83, -2.93 to -4.07 and -1.99 to -3.52 kcal/mol, respectively. The numbers of bonds of four types were 8, 8, 18 and 18 for [CO...H], [CO...Zn], [OC...H] and [OC...Zn], respectively. The maximum numbers of CO adsorbed on ZnOGLNSs and their formulae were shown in Table 4.5. It shows formulae to compute the maximum numbers for CO adsorbed on the C_{3h} and C_{2v} symmetric ZnOGLNS(i) modeled structures as defined in Figure 4.11, respectively. The C_{3h} -ZnOGLNS(i) and C_{2v} -ZnOGLNS(i) were the radial layer extended structures of AL-ZnONC and PRL-ZnONC, respectively. Therefore, the one layer structures for the C_{3h} -ZnOGLNS(i) and C_{2v} -ZnOGLNS(i) were the AL-ZnONC and PRL-ZnONC, respectively. The maximum numbers for CO adsorbed on the C_{3h} ZnOGLNS(i) and C_{2v} -ZnOGLNS(i) were $6 \sum_{i=1}^i (2i-1) + 3i$ and $2 \sum_{i=1}^i (6i+1) + 2i + 3$, respectively. The maximum numbers for CO adsorbed on the C_{3h} -ZnOGLNS(i) and C_{2v} ZnOGLNS(i) were computed from $n_{MAX} = 2x + \frac{1}{2}y$, where x and y were numbers of zinc and hydrogen atoms in their ZnOGLNSs, respectively.

4.2.2.4 Energy gap

The energy gaps of CO adsorptions either with pointing C-end or O-end on the AL-ZnONC or PRL-ZnONC were higher than the corresponding bare sheets. For CO adsorptions on the large nanosheets, PRL-ZnONC, CNL-ZnONS and CCL-ZnONS, their energy gaps were slightly changed but some of energy gaps of adsorption states were slightly higher than their corresponding clean nanosheets. It means that CO adsorptions on the large nanosheets were quite stable and they can be used as CO storage materials.

Table 4.3 Adsorption energies (ΔE_{ads} in kcal/mol) of CO pointing its O-end toward surfaces of ZnONCs and ZnOGLNSs and energy gaps (ΔE_{GAP} in eV) of bare surfaces of ZnONCs, ZnOGLNSs, computed at the B3LYP/LanL2DZ level of theory.

ZnOGLNSs/carbon monoxide adsorption	ΔE_{ads} (kcal/mol)	E_{GAP} (eV)
AL-ZnONC:		6.47
CO + AL-ZnONC → CO/AL-ZnONC (1)	-2.39	5.12
CO + AL-ZnONC → CO/AL-ZnONC (2)	-3.28	5.13
NLL-ZnONC:		5.32
CO + NLL-ZnONC → CO/NLL-ZnONC (1)	-2.15	4.99
CO + NLL-ZnONC → CO/NLL-ZnONC (2)	-3.26	4.94
CO + NLL-ZnONC → CO/NLL-ZnONC (3)	-2.48	4.80
CO + NLL-ZnONC → CO/NLL-ZnONC (4)	-3.32	4.59
CO + NLL-ZnONC → CO/NLL-ZnONC (5)	-3.47	4.52
PRL-ZnONC:		4.26
CO + PRL-ZnONC → CO/PRL-ZnONC (1)	-2.88	3.96
CO + PRL-ZnONC → CO/PRL-ZnONC (2)	-3.80	3.85
CO + PRL-ZnONC → CO/PRL-ZnONC (3)	-3.47	4.27
CO + PRL-ZnONC → CO/PRL-ZnONC (4)	-3.52	3.93
CO + PRL-ZnONC → CO/PRL-ZnONC (5)	-2.10	4.28
CO + PRL-ZnONC → CO/PRL-ZnONC (6)	-2.46	4.28
CO + PRL-ZnONC → CO/PRL-ZnONC (7)	-1.99	4.19
CO + PRL-ZnONC → CO/PRL-ZnONC (8)	-2.93	4.21
CNL-ZnONS:		4.83
CO + CNL-ZnONS → CO/CNL-ZnONS (1)	-3.34	4.61
CO + CNL-ZnONS → CO/CNL-ZnONS (2)	-3.37	4.80
CO + CNL-ZnONS → CO/CNL-ZnONS (3)	-2.06	4.79
CO + CNL-ZnONS → CO/CNL-ZnONS (4)	-2.58	4.71
CCL-ZnONS:		3.74
CO + CCL-ZnONS → CO/CCL-ZnONS (1)	-4.07	3.56
CO + CCL-ZnONS → CO/CCL-ZnONS (2)	-3.56	3.76
CO + CCL-ZnONS → CO/CCL-ZnONS (3)	-3.01	3.76
CO + CCL-ZnONS → CO/CCL-ZnONS (4)	-3.44	3.75
CO + CCL-ZnONS → CO/CCL-ZnONS (5)	-2.15	3.75
CO + CCL-ZnONS → CO/CCL-ZnONS (6)	-2.64	3.75
CO + CCL-ZnONS → CO/CCL-ZnONS (7)	-2.50	3.77
CO + CCL-ZnONS → CO/CCL-ZnONS (8)	-2.08	3.69

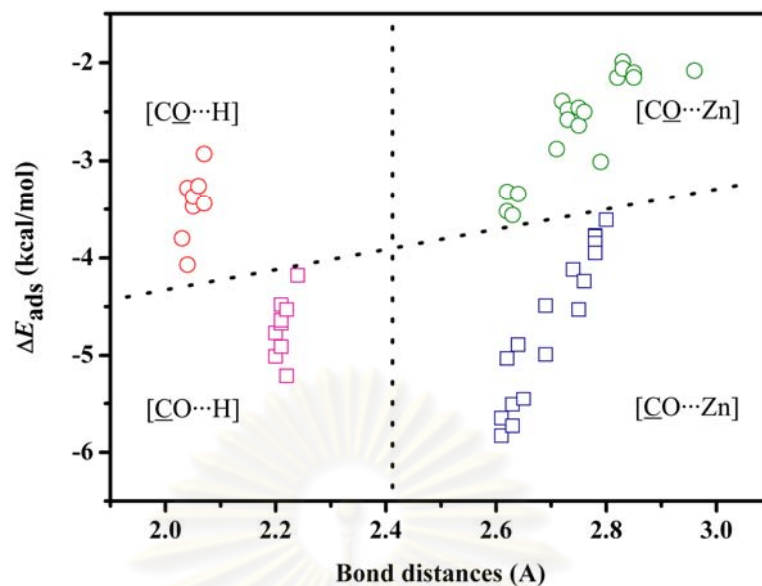


Figure 4.10 Plots of all possible adsorption energies of CO on all the ZnONC, PRL–ZnONC nanoclusters and PRL–ZnONC, CNL–ZnONS and CCL–ZnONS nanosheets against their bond distances. Four bond distances types $[\underline{\text{C}}\text{O}\cdots\text{H}]$, $[\underline{\text{C}}\text{O}\cdots\text{Zn}]$, $[\underline{\text{C}}\text{O}\cdots\text{H}]$ and $[\underline{\text{C}}\text{O}\cdots\text{Zn}]$, separated as four zones were found.

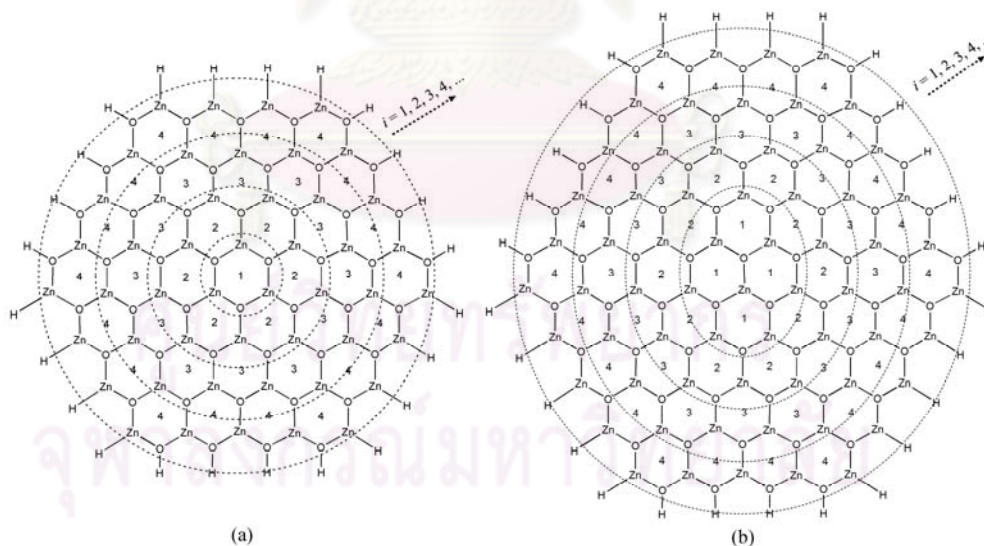


Figure 4.11 The structure models of (a) C_{3h} symmetric ZnOGLNS(i) and (b) C_{2v} symmetric ZnOGLNS(i). The layer numbers of C_{3h} –ZnOGLNS(i) and C_{2v} –ZnOGLNS(i) defined as radial layer models of which the one layer structures (the most inner) were AL–ZnONC and PRL–ZnONC, respectively. The numbers labeled

in the center of hexagonal rings indicate the number of most outer layer of the ZnOGLNS.

Table 4.4 Bond distances (in Å) between CO atoms and atoms of adsorption sites.

ZnOGLNSs	[<u>CO</u> ...S] ^a		[<u>CO</u> ...S] ^a	
AL-ZnONC:				
	<u>CO</u> ...Zn1	2.74	<u>CO</u> ...Zn1	2.72
	<u>CO</u> ...H1	2.21	<u>CO</u> ...H1	2.04
NLL-ZnONC:				
	<u>CO</u> ...Zn1	2.80	<u>CO</u> ...Zn1	2.82
	<u>CO</u> ...H1	2.22	<u>CO</u> ...H1	2.06
	<u>CO</u> ...Zn2	2.76	<u>CO</u> ...Zn2	2.73
	<u>CO</u> ...Zn3	2.61	<u>CO</u> ...Zn3	2.62
PRL-ZnONC:				
	<u>CO</u> ...Zn1	2.75	<u>CO</u> ...Zn1	2.71
	<u>CO</u> ...H1	2.20	<u>CO</u> ...H1	2.03
	<u>CO</u> ...H2	2.20	<u>CO</u> ...H2	2.05
	<u>CO</u> ...Zn2	2.63	<u>CO</u> ...Zn2	2.62
	<u>CO</u> ...Zn3	2.78	<u>CO</u> ...Zn3	2.85
	<u>CO</u> ...Zn4	2.62	<u>CO</u> ...Zn4	2.75
	<u>CO</u> ...Zn5	2.78	<u>CO</u> ...Zn5	2.83
	<u>CO</u> ...H3	2.24	<u>CO</u> ...H3	2.07
CNL-ZnONS:				
	<u>CO</u> ...Zn1	2.63	<u>CO</u> ...Zn1	2.64
	<u>CO</u> ...H1	2.21	<u>CO</u> ...H1	2.05
	<u>CO</u> ...Zn2	2.78	<u>CO</u> ...Zn2	2.83
	<u>CO</u> ...Zn3	2.64	<u>CO</u> ...Zn3	2.73
CCL-ZnONS:				
	<u>CO</u> ...H1	2.22	<u>CO</u> ...H1	2.04
	<u>CO</u> ...Zn1	2.61	<u>CO</u> ...Zn1	2.63
	<u>CO</u> ...Zn2	2.65	<u>CO</u> ...Zn2	2.79
	<u>CO</u> ...H2	2.21	<u>CO</u> ...H2	2.07
	<u>CO</u> ...Zn3	2.78	<u>CO</u> ...Zn3	2.85
	<u>CO</u> ...Zn4	2.69	<u>CO</u> ...Zn4	2.75
	<u>CO</u> ...Zn5	2.69	<u>CO</u> ...Zn5	2.76
	<u>CO</u> ...Zn6	2.78	<u>CO</u> ...Zn6	2.96

^a Atom S stands for atomic adsorption site, CO and CO were carbon dioxide molecules pointing their C and O atoms toward atom S in the nanoclusters or nanosheets, respectively. Atomic positions of S atom were shown in Figure 4.1

Table 4.5 Maximum number of CO adsorbed on ZnOGLNSs and their formulae.

ZnOGLNSs	Symmetries	Clusters	Maximum number of adsorbed CO, $n_{\text{MAX}}^{\text{a}}$ (molecules)
AL-ZnONC	C_{3h}	$\text{Zn}_3\text{O}_3\text{H}_6$	9
NLL-ZnONC	C_{2v}	$\text{Zn}_5\text{O}_5\text{H}_8$	14
PRL-ZnONC	C_{2v}	$\text{Zn}_8\text{O}_8\text{H}_{10}$	21
CNL-ZnONS	C_{3h}	$\text{Zn}_{12}\text{O}_{12}\text{H}_{12}$	30
CCL-ZnONS	C_{3h}	$\text{Zn}_{27}\text{O}_{27}\text{H}_{18}$	63
ZnOGLNSs of large number of layers:			
$C_{3h}\text{-ZnOGLNS}(i)^{\text{b}}$	C_{3h}	$\text{Zn}_x\text{O}_x\text{H}_y^{\text{c}}$	$6 \sum_{i=1}^i (2i-1) + 3i$
$C_{2v}\text{-ZnOGLNS}(i)^{\text{d}}$	C_{2v}	$\text{Zn}_x\text{O}_x\text{H}_y^{\text{e}}$	$2 \sum_{i=1}^i (6i+1) + 2i + 3$

^a Computed from, $n_{\text{MAX}} = 2x + \frac{1}{2}y$, where x and y were numbers of zinc and hydrogen atoms in their ZnOGLNSs.

^b i -layer ZnOGLNS defined in Figure 4.11(a), where i was a number of radial layers of the $C_{3h}\text{-ZnOGLNS}(i)$ modeled structure.

^c $x = 3 \sum_{i=1}^i (2i-1)$ and $y = 6i$, where i was a number of radial layers of the $C_{3h}\text{-ZnOGLNS}(i)$ modeled structure.

^d i -layer ZnOGLNS defined in Figure 4.11(b), where i was a number of radial layers of the $C_{2v}\text{-ZnOGLNS}(i)$ modeled structure.

^e $x = 1 + \sum_{i=1}^i (6i+1)$ and $y = 6i+4$, where i was a number of radial layers of the $C_{2v}\text{-ZnOGLNS}(i)$ modeled structure.

4.2.3 Adsorption of water molecule

4.2.3.1 Adsorption energies of H₂O

The B3LYP/LanL2DZ-optimized structures of adsorption configurations of H₂O adsorbed on the rigid structures of the AL-ZnONC, NLL-ZnONC, PRL-ZnONC, CNL-ZnONS and CCL-ZnONS were shown in Figure 4.12. These adsorption structures were symmetrically representative of all possible water adsorptions on the whole nanosheets of AL-ZnONC, NLL-ZnONC, PRL-ZnONC, CNL-ZnONS and CCL-ZnONS. Due to the adsorption configurations of water adsorbed on the ZnONCs and ZnOGLNs and their molecular symmetries, all water molecules as minimum energy structures of their adsorptions can be plotted as shown in Figure 4.13.

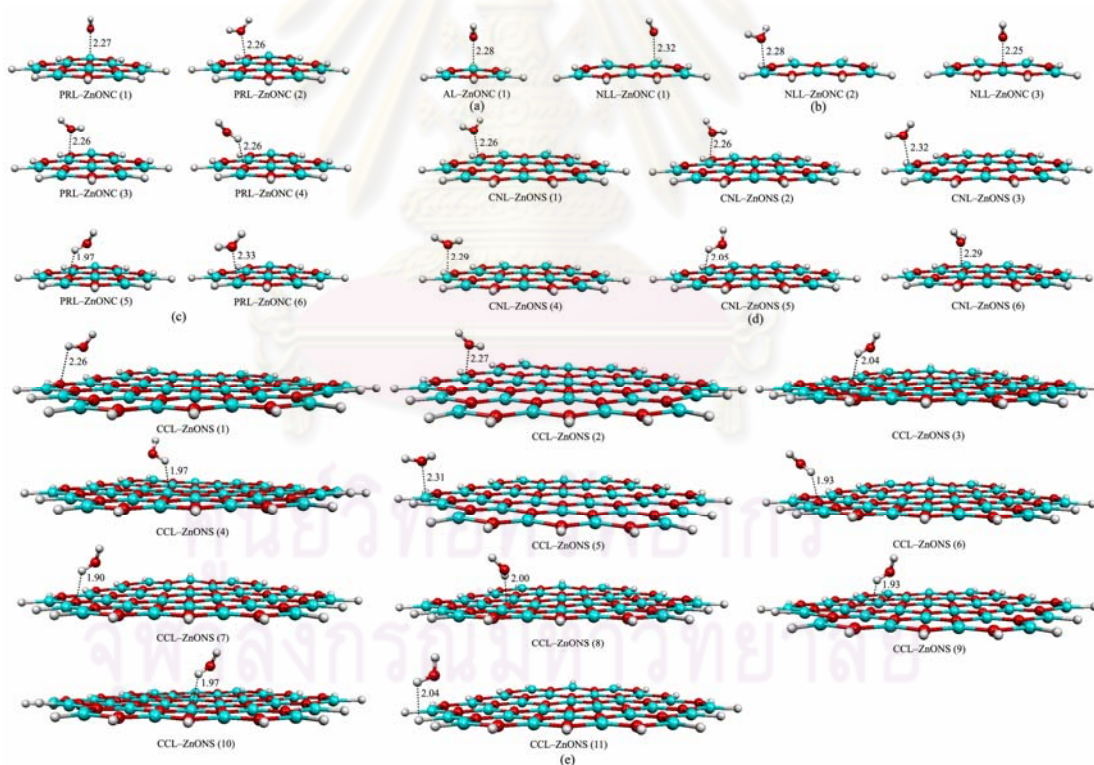


Figure 4.12 The adsorption configurations of water adsorbed on (a) the AL-ZnONC, (b) NLL-ZnONC, (c) PRL-ZnONC, (d) CNL-ZnONS and (e) CCL-ZnONS. The bond distances bonds were in Å.

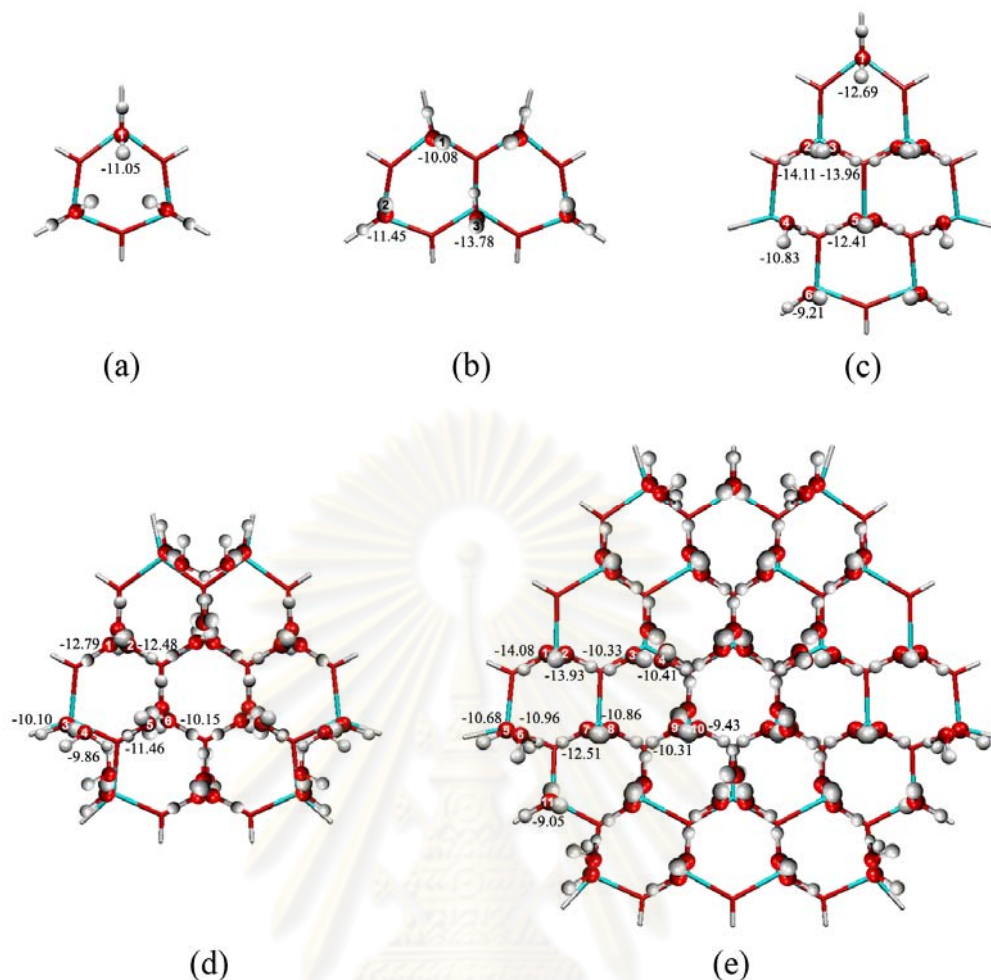


Figure 4.13 Plots of water molecules as minimum energy structures of their adsorptions on (a) the AL-ZnONC ($\text{Zn}_3\text{O}_3\text{H}_6$), (b) NLL-ZnONC ($\text{Zn}_5\text{O}_5\text{H}_8$), (c) PRL-ZnONC ($\text{Zn}_8\text{O}_8\text{H}_{10}$), (d) CNL-ZnONS ($\text{Zn}_{12}\text{O}_{12}\text{H}_{12}$) and (e) CCL-ZnONS ($\text{Zn}_{27}\text{O}_{27}\text{H}_{18}$). The molecules labeled with numbers represent the water molecules interacting with ZnONCs and ZnOGLNSs as representative of molecular symmetries of AL-ZnONC (C_{3h}), NLL-ZnONC (C_{2v}), PRL-ZnONC (C_{2v}), CNL-ZnOGLNS (C_{3h}) and CCL-ZnOGLNS (C_{3h}). Adsorption energies in kcal/mol were presented.

There was one type (called type I) of adsorption configuration of H_2O on the AL-ZnONC. The water adsorption, type I occurred by the water pointing its oxygen and hydrogen toward zinc and hydride hydrogen atoms of the surface, see Figure 4.12(a). The number of energy minima of H_2O adsorptions on the AL-ZnONC of three configurations was found for each side of its molecular planes. These energy minima were obtained from the structure optimizations of interaction configurations within one third of each side of the AL-ZnONC molecular area and H_2O adsorptions

over the whole AL–ZnONC molecular area were generated using C_{3h} symmetrical operation. The adsorption energy of H_2O on the AL–ZnONC was -11.05 kcal/mol as shown in Figure 4.12(a) and Table 4.6.

The adsorption configurations of H_2O on NLL–ZnONC of two types, type I and type II were found. The type II was the water adsorption by pointing its oxygen and hydrogen toward zinc and inner oxygen atoms of the surface, see Figure 4.12(b). The water adsorptions of type I were composed of adsorption position H_2O #1 (-10.08 kcal/mol, type I) and H_2O #2 (-11.45 kcal/mol, type I) and type II was H_2O #3 (-13.78 kcal/mol, type II).

There were four types of water adsorptions on the PRL–ZnONC which were composed of six adsorption positions H_2O #1 (-12.69 kcal/mol, type I), #2 (-14.11 kcal/mol, type II), #3 (-13.96 kcal/mol, type III), #4 (-10.83 kcal/mol, type IV), #5 (-12.41 kcal/mol, type III) and #6 (-9.21 kcal/mol, type I). The type I, the water adsorption by pointing its oxygen atom towards the zinc surface atom and its hydrogen atom towards the hydride–hydrogen surface atom were the adsorption position #1 and #6. The type II was the water adsorption with pointing its oxygen towards the zinc surface atom and its hydrogen atom towards the outer oxygen atom which corresponds to the adsorption position #2. The type III was the water adsorption with pointing its oxygen towards the zinc surface atom and its hydrogen atom towards the inner oxygen atom which corresponds to the adsorption positions #3 and #5. The type IV was the water adsorption with pointing its oxygen towards the zinc surface atom and its hydrogen atom towards the outer oxygen atom which corresponds to the adsorption position #4.

The CNL–ZnONS and CCL–ZnONS which were in C_{3h} symmetry, the numbers of H_2O adsorptions on each side of their molecular planes were six and eleven configurations as shown in Figure 4.12(d) and (e), respectively. Definition of types I, II, III and IV as used for the AL–ZnONC, NLL–ZnONC and PRL–ZnONC, we can therefore apply the same definition for the CNL–ZnONS and CCL–ZnONS as follows.

The four types of water adsorptions on the CNL–ZnONS were also composed of six adsorption positions of H_2O #1 (-12.79 kcal/mol, type II), #2 (-12.48 kcal/mol, type III), #3 (-10.10 kcal/mol, type I), #4 (-9.86 kcal/mol, type IV), #5 (-11.46 kcal/mol, type III) and #6 (-10.15 kcal/mol, type III). The four types of water adsorptions on the CCL–ZnONS were composed of eleven adsorption positions of

H₂O #1 (-14.08 kcal/mol, type II), #2 (-13.93 kcal/mol, type III), #3 (-10.33 kcal/mol, type III), #4 (-10.41 kcal/mol, type III), #5 (-10.68 kcal/mol, type I), #6 (-10.96 kcal/mol, type IV), #7 (-12.51 kcal/mol, type III), #8 (-10.86 kcal/mol, type III), #9 (-10.31 kcal/mol, type III), #10 (-9.43 kcal/mol, type III) and #11 (-9.05 kcal/mol, type I).

There were three bond types, types [H₂O...O], [H₂O...H_{hydride}] and [H₂O...Zn] of all the adsorption energies of H₂O on the AL-ZnONC, NLL-ZnONC, PRL-ZnONC, CNL-ZnONS and CCL-ZnONS as shown in Figure 4.14. It shows that bond distances of the bond types [H₂O...O], [H₂O...H_{hydride}] caused by interaction between partial positive charge of water hydrogen atom and partial negative charge of surface atoms (oxygen and hydride hydrogen atoms) were a little bit shorter than the bond distance of the bond type [H₂O...Zn] which caused by interaction between water oxygen and zinc surface atom, as listed in Table 4.7.

The energy gaps (ΔE_{GAP}) of the adsorption complexes H₂O with the AL-ZnONC, NLL-ZnONC, PRL-ZnONC, CNL-ZnONS and CCL-ZnONS were not much different from their corresponding bwere surfaces as shown in Table 4.6.

Table 4.6 Adsorption energies (ΔE_{ads} in kcal/mol) of H_2O on ZnONCs and ZnOGLNSs, and energy gaps (ΔE_{GAP} in eV) of bare ZnONCs and ZnOGLNSs and their H_2O adsorption complexes, computed at the B3LYP/LanL2DZ level of theory.

ZnOGLNSs/water adsorption	ΔE_{ads} (kcal/mol)	E_{GAP} (eV)
AL-ZnONC:		6.47
$\text{H}_2\text{O} + \text{AL-ZnONC} \rightarrow \text{H}_2\text{O/AL-ZnONC}$ (1)	-11.05	6.19
NLL-ZnONC:		5.32
$\text{H}_2\text{O} + \text{NLL-ZnONC} \rightarrow \text{H}_2\text{O/NLL-ZnONC}$ (1)	-10.08	4.99
$\text{H}_2\text{O} + \text{NLL-ZnONC} \rightarrow \text{H}_2\text{O/NLL-ZnONC}$ (2)	-11.45	5.31
$\text{H}_2\text{O} + \text{NLL-ZnONC} \rightarrow \text{H}_2\text{O/NLL-ZnONC}$ (3)	-13.78	5.66
PRL-ZnONC:		4.26
$\text{H}_2\text{O} + \text{PRL-ZnONC} \rightarrow \text{H}_2\text{O/PRL-ZnONC}$ (1)	-12.69	4.49
$\text{H}_2\text{O} + \text{PRL-ZnONC} \rightarrow \text{H}_2\text{O/PRL-ZnONC}$ (2)	-14.11	4.57
$\text{H}_2\text{O} + \text{PRL-ZnONC} \rightarrow \text{H}_2\text{O/PRL-ZnONC}$ (3)	-13.96	4.52
$\text{H}_2\text{O} + \text{PRL-ZnONC} \rightarrow \text{H}_2\text{O/PRL-ZnONC}$ (4)	-10.83	4.38
$\text{H}_2\text{O} + \text{PRL-ZnONC} \rightarrow \text{H}_2\text{O/PRL-ZnONC}$ (5)	-12.41	4.51
$\text{H}_2\text{O} + \text{PRL-ZnONC} \rightarrow \text{H}_2\text{O/PRL-ZnONC}$ (6)	-9.21	3.98
CNL-ZnONS:		4.83
$\text{H}_2\text{O} + \text{CNL-ZnONS} \rightarrow \text{H}_2\text{O/CNL-ZnONS}$ (1)	-12.79	4.88
$\text{H}_2\text{O} + \text{CNL-ZnONS} \rightarrow \text{H}_2\text{O/CNL-ZnONS}$ (2)	-12.48	4.74
$\text{H}_2\text{O} + \text{CNL-ZnONS} \rightarrow \text{H}_2\text{O/CNL-ZnONS}$ (3)	-10.10	4.48
$\text{H}_2\text{O} + \text{CNL-ZnONS} \rightarrow \text{H}_2\text{O/CNL-ZnONS}$ (4)	-9.86	4.35
$\text{H}_2\text{O} + \text{CNL-ZnONS} \rightarrow \text{H}_2\text{O/CNL-ZnONS}$ (5)	-11.46	4.96
$\text{H}_2\text{O} + \text{CNL-ZnONS} \rightarrow \text{H}_2\text{O/CNL-ZnONS}$ (6)	-10.15	4.84
CCL-ZnONS:		3.74
$\text{H}_2\text{O} + \text{CCL-ZnONS} \rightarrow \text{H}_2\text{O/CCL-ZnONS}$ (1)	-14.08	3.76
$\text{H}_2\text{O} + \text{CCL-ZnONS} \rightarrow \text{H}_2\text{O/CCL-ZnONS}$ (2)	-13.93	3.73
$\text{H}_2\text{O} + \text{CCL-ZnONS} \rightarrow \text{H}_2\text{O/CCL-ZnONS}$ (3)	-10.33	3.69
$\text{H}_2\text{O} + \text{CCL-ZnONS} \rightarrow \text{H}_2\text{O/CCL-ZnONS}$ (4)	-10.41	3.65
$\text{H}_2\text{O} + \text{CCL-ZnONS} \rightarrow \text{H}_2\text{O/CCL-ZnONS}$ (5)	-10.68	3.72
$\text{H}_2\text{O} + \text{CCL-ZnONS} \rightarrow \text{H}_2\text{O/CCL-ZnONS}$ (6)	-10.96	3.72
$\text{H}_2\text{O} + \text{CCL-ZnONS} \rightarrow \text{H}_2\text{O/CCL-ZnONS}$ (7)	-12.51	3.76
$\text{H}_2\text{O} + \text{CCL-ZnONS} \rightarrow \text{H}_2\text{O/CCL-ZnONS}$ (8)	-10.86	3.69
$\text{H}_2\text{O} + \text{CCL-ZnONS} \rightarrow \text{H}_2\text{O/CCL-ZnONS}$ (9)	-10.31	3.74
$\text{H}_2\text{O} + \text{CCL-ZnONS} \rightarrow \text{H}_2\text{O/CCL-ZnONS}$ (10)	-9.43	3.67
$\text{H}_2\text{O} + \text{CCL-ZnONS} \rightarrow \text{H}_2\text{O/CCL-ZnONS}$ (11)	-9.05	3.57

Table 4.7 Bond distances between oxygen atom of H₂O and Zn atom of ZnOGLNSs.

ZnOGLNSs	H ₂ O adsorbate ^a		
AL-ZnONC:	AL-ZnONC (1)	H ₂ O...Zn1	2.28
NLL-ZnONC:	NLL-ZnONC (1)	H ₂ O...Zn1	2.32
	NLL-ZnONC (2)	H ₂ O...Zn2	2.28
	NLL-ZnONC (3)	H ₂ O...Zn3	2.25
PRL-ZnONC:	PRL-ZnONC (1)	H ₂ O...Zn1	2.27
	PRL-ZnONC (2)	H ₂ O...Zn2	2.26
	PRL-ZnONC (3)	H ₂ O...Zn3	2.26
	PRL-ZnONC (4)	H ₂ O...O4	1.97
	PRL-ZnONC (5)	H ₂ O...O4	1.97
	PRL-ZnONC (6)	H ₂ O...Zn5	2.33
CNL-ZnONS:	CNL-ZnONS (1)	H ₂ O...Zn1	2.26
	CNL-ZnONS (2)	H ₂ O...Zn1	2.26
	CNL-ZnONS (3)	H ₂ O...Zn2	2.32
	CNL-ZnONS (4)	H ₂ O...Zn2	2.29
	CNL-ZnONS (5)	H ₂ O...O3	2.05
	CNL-ZnONS (6)	H ₂ O...Zn3	2.29
CCL-ZnONS:	CCL-ZnONS (1)	H ₂ O...Zn1	2.26
	CCL-ZnONS (2)	H ₂ O...Zn1	2.27
	CCL-ZnONS (3)	H ₂ O...O2	2.04
	CCL-ZnONS (4)	H ₂ O...O3	1.97
	CCL-ZnONS (5)	H ₂ O...Zn3	2.31
	CCL-ZnONS (6)	H ₂ O...O4	1.93
	CCL-ZnONS (7)	H ₂ O...O4	1.90
	CCL-ZnONS (8)	H ₂ O...O5	2.00
	CCL-ZnONS (9)	H ₂ O...O5	1.93
	CCL-ZnONS (10)	H ₂ O...O3	1.97
	CCL-ZnONS (11)	H ₂ O...H3	2.04

^a H₂O...Zn, H₂O...O and H₂O...H denote as bond distances between water oxygen and surface Zn atom, between water hydrogen and O surface atom, and water hydrogen and hydride hydrogen surface atom, Zn, O and H surface atoms are labeled as shown in Figure 4.1.

4.2.4 Adsorption of ammonia molecule

4.2.4.1 Adsorption energies of NH₃

The B3LYP/LanL2DZ-optimized structures of adsorption configurations of NH₃ adsorbed on the rigid structures of the AL-ZnONC, NLL-ZnONC, PRL-ZnONC, CNL-ZnONS and CCL-ZnONS were shown in Figure 4.14. These adsorption structures were symmetrically representative of all possible ammonia adsorptions on the whole nanosheets of AL-ZnONC, NLL-ZnONC, PRL-ZnONC, CNL-ZnONS and CCL-ZnONS. Due to the adsorption configurations of ammonia adsorbed on the ZnONCs and ZnOGLNSs and their molecular symmetries, all ammonia molecules as minimum energy structures of their adsorptions can be plotted as shown in Figure 4.15.

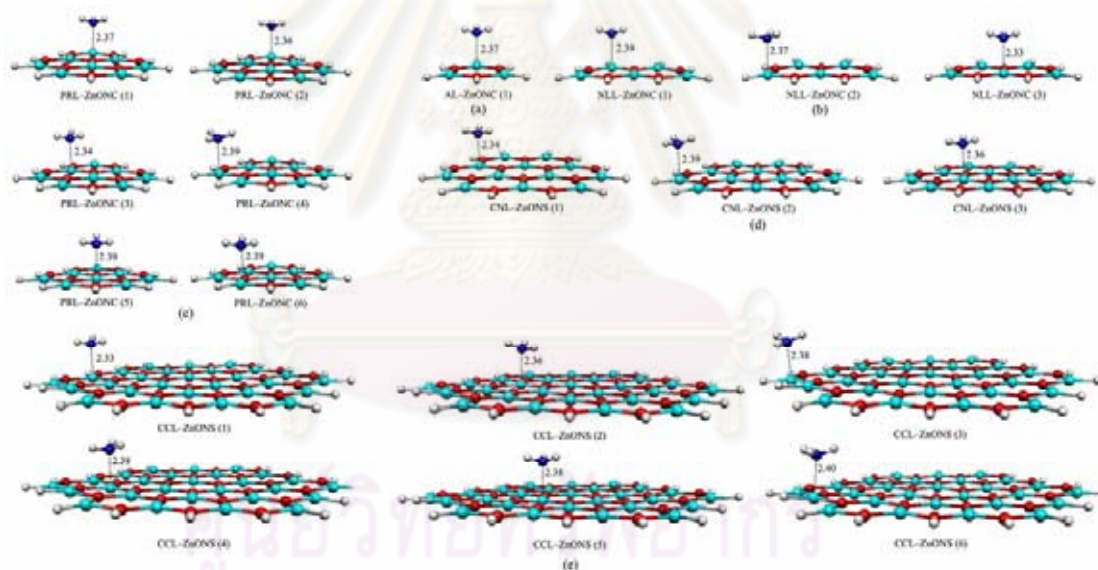


Figure 4.14 The adsorption configurations of ammonia adsorbed on (a) the AL-ZnONC, (b) NLL-ZnONC, (c) PRL-ZnONC, (d) CNL-ZnONS and (e) CCL-ZnONS. The bond distances, ($N_{\text{NH}_3} \cdots \text{Zn}$) were in Å.

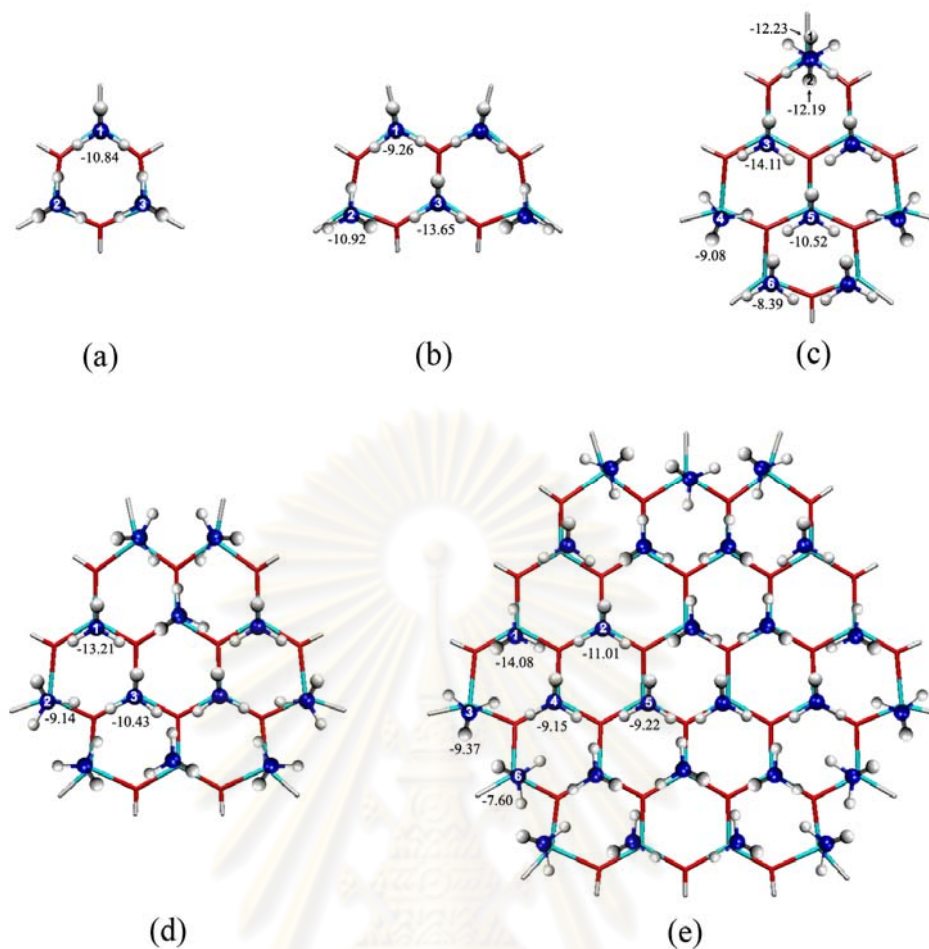


Figure 4.15 Plots of ammonia molecules as minimum energy structures of their adsorptions on (a) the AL-ZnONC, (b) NLL-ZnONC, (c) PRL-ZnONC, (d) CNL-ZnONS and (e) CCL-ZnONS. The molecules labeled with numbers represent the ammonia molecules interacting with ZnONCs and ZnOGLNSs as representative of their molecular symmetries. Adsorption energies in kcal/mol were presented.

The adsorption bonds of NH_3 adsorbed on the AL-ZnONC and NLL-ZnONC take place as one type called type I. The adsorption energies of NH_3 adsorbed on the AL-ZnONC was -10.84 kcal/mol and on the NLL-ZnONC were -9.26 , -10.92 and -13.65 kcal/mol as shown in Figure 4.14(a), 4.14(b) and Table 4.8. The ammonia adsorption of type I occurred by the ammonia pointing its nitrogen towards zinc surface atom and all three hydrogen atoms align on three $[\text{Zn}\cdots\text{O}]$ bonds of ZnONCs as shown in Figure 4.15(a) and 4.15(b).

The adsorption bonds of NH_3 adsorbed on the PRL-ZnONC occur as type I and another type which forms staggered configuration between N-H bond of

ammonia and Zn–O of the surface was defined as type II bond. The bonds of type II for the NH₃ adsorbed on the PRL–ZnONC were the adsorption position of ammonia #2 and #4. The adsorption positions of NH₃ on the PRL–ZnONC occurring as type I bond were #1 (–12.23 kcal/mol), #3 (–14.11 kcal/mol), #5 (–10.52 kcal/mol) and #6 (–8.39 kcal/mol) and as type II were #2 (–12.19 kcal/mol) and #4 (–9.08 kcal/mol).

Due to the adsorptions of NH₃ on the CNL–ZnONS and CCL–ZnONS, bonds of types I and II were also found. The types I and II bonds for all the NH₃ adsorbed either on the CNL–ZnONS or CCL–ZnONS obviously occur over the zinc surface as shown in Figure 4.14(d) and (e). The adsorption representatives of NH₃ on the CNL–ZnONS were three adsorption positions #1 (–13.21 kcal/mol, type I), #2 (–9.14 kcal/mol, type II) and #3 (–10.43 kcal/mol, type I) as shown in Figure 4.15(d). For the adsorption representatives of NH₃ on the CCL–ZnONS were six adsorption positions #1 (–14.08 kcal/mol, type I), #2 (–11.01 kcal/mol, type I), #3 (–9.37 kcal/mol, type II), #4 (–9.15 kcal/mol, type I), #5 (–9.22 kcal/mol, type I) and #6 (–7.60 kcal/mol, type II) as shown in Figure 4.15(e). Due to plots of ammonia molecules as minimum energy structures of their adsorptions on the CNL–ZnONS and CCL–ZnONS shown in Figure 4.15(d) and 4.15(e), it can therefore be concluded that the NH₃ adsorptions on all the Zn surface atoms were caused by the bonding of type I except that NH₃ adsorptions on terminal Zn atoms were caused by the bonding of type II. Nevertheless, all the NH₃ adsorbed on the ZnONCs and ZnOGLNSs occur by pointing its nitrogen toward Zn surface atom and this orientation was somewhat perpendicular to the surface planes of the nanosheets, as shown in Figure 4.14.

The energy gaps (ΔE_{GAP}) of the adsorption complexes NH₃ with the AL–ZnONC, NLL–ZnONC, PRL–ZnONC, CNL–ZnONS and CCL–ZnONS were also not much different from their corresponding bare surfaces as shown in Table 4.8.

Table 4.8 Adsorption energies (ΔE_{ads} in kcal/mol) of NH_3 on ZnONCs and ZnOGLNSs, and energy gaps (E_{GAP} in eV) of the bare ZnONCs and ZnOGLNSs and their NH_3 adsorption complexes, computed at the B3LYP/LanL2DZ level of theory.

ZnOGLNSs/ammonia adsorption	ΔE_{ads} (kcal/mol)	E_{GAP} (eV)
AL-ZnONC:		
$\text{NH}_3 + \text{AL-ZnONC} \rightarrow \text{NH}_3/\text{AL-ZnONC}(1)$	-10.84	6.47
NLL-ZnONC:		
$\text{NH}_3 + \text{NLL-ZnONC} \rightarrow \text{NH}_3/\text{NLL-ZnONC}(1)$	-9.26	5.86
$\text{NH}_3 + \text{NLL-ZnONC} \rightarrow \text{NH}_3/\text{NLL-ZnONC}(2)$	-10.92	5.32
$\text{NH}_3 + \text{NLL-ZnONC} \rightarrow \text{NH}_3/\text{NLL-ZnONC}(3)$	-13.65	4.59
PRL-ZnONC:		
$\text{NH}_3 + \text{PRL-ZnONC} \rightarrow \text{NH}_3/\text{PRL-ZnONC}(1)$	-12.23	4.47
$\text{NH}_3 + \text{PRL-ZnONC} \rightarrow \text{NH}_3/\text{PRL-ZnONC}(2)$	-12.19	4.47
$\text{NH}_3 + \text{PRL-ZnONC} \rightarrow \text{NH}_3/\text{PRL-ZnONC}(3)$	-14.11	4.54
$\text{NH}_3 + \text{PRL-ZnONC} \rightarrow \text{NH}_3/\text{PRL-ZnONC}(4)$	-9.08	3.92
$\text{NH}_3 + \text{PRL-ZnONC} \rightarrow \text{NH}_3/\text{PRL-ZnONC}(5)$	-10.52	4.31
$\text{NH}_3 + \text{PRL-ZnONC} \rightarrow \text{NH}_3/\text{PRL-ZnONC}(6)$	-8.39	3.59
CNL-ZnONS:		
$\text{NH}_3 + \text{CNL-ZnONS} \rightarrow \text{NH}_3/\text{CNL-ZnONS}(1)$	-13.21	4.83
$\text{NH}_3 + \text{CNL-ZnONS} \rightarrow \text{NH}_3/\text{CNL-ZnONS}(2)$	-9.14	4.85
$\text{NH}_3 + \text{CNL-ZnONS} \rightarrow \text{NH}_3/\text{CNL-ZnONS}(3)$	-10.43	4.10
CCL-ZnONS:		
$\text{NH}_3 + \text{CCL-ZnONS} \rightarrow \text{NH}_3/\text{CCL-ZnONS}(1)$	-14.08	4.89
$\text{NH}_3 + \text{CCL-ZnONS} \rightarrow \text{NH}_3/\text{CCL-ZnONS}(2)$	-11.01	3.74
$\text{NH}_3 + \text{CCL-ZnONS} \rightarrow \text{NH}_3/\text{CCL-ZnONS}(3)$	-9.37	3.76
$\text{NH}_3 + \text{CCL-ZnONS} \rightarrow \text{NH}_3/\text{CCL-ZnONS}(4)$	-9.15	3.77
$\text{NH}_3 + \text{CCL-ZnONS} \rightarrow \text{NH}_3/\text{CCL-ZnONS}(5)$	-9.22	3.39
$\text{NH}_3 + \text{CCL-ZnONS} \rightarrow \text{NH}_3/\text{CCL-ZnONS}(6)$	-7.60	3.71
		3.80
		3.07

4.2.5 Adsorption of hydrogen molecule

4.2.5.1 Adsorption energies of H_2

These adsorption structures were symmetrically representative of all possible H_2 adsorptions on the whole nanosheets of AL-ZnONC, NLL-ZnONC, PRL-ZnONC, CNL-ZnONS and CCL-ZnONS. Due to the adsorption configurations of H_2 adsorbed on the ZnONCs and ZnOGLNSs and their molecular symmetries, all H_2 molecules as minimum energy structures of their adsorptions can be plotted as shown in Figure 4.16. The number of energy minima of H_2 adsorptions on the AL-ZnONC of thirty configurations was found for each side of its molecular planes. These energy minima were obtained from the structure optimizations of interaction configurations within one third of each side of the AL-ZnONC molecular area and hydrogen adsorptions over the whole AL-ZnONC molecular area were generated using C_{3h} symmetrical operation. The adsorption energies of H_2 on the AL-ZnONC were composed of five adsorption positions H_2 #1 (-0.13 kcal/mol), #2 (-0.34 kcal/mol),

#3 (-0.52 kcal/mol), #4 (-0.47 kcal/mol) and #5 (-0.45 kcal/mol) as shown in Table 4.9.

The NLL-ZnONC and PRL-ZnONC nanocluster were in C_{2v} symmetry, the numbers of H_2 adsorptions on each side of their molecular planes were twenty two and thirty one configurations, respectively, see Figure 4.16(b) and (c). There were twelve type of adsorption positions on the NLL-ZnONC which were composed of H_2 adsorption positions H_2 #1 (-0.42 kcal/mol), #2 (-0.23 kcal/mol), #3 (-0.69 kcal/mol), #4 (-0.51 kcal/mol), #6 (-0.64 kcal/mol), #7 (-0.46 kcal/mol), #8 (-0.28 kcal/mol), #9 (-0.52 kcal/mol), #10 (-0.55 kcal/mol), #11 (-0.60 kcal/mol) and #12 (-0.62 kcal/mol). There were eighteen type of adsorption positions on the PRL-ZnONC which were composed of adsorption positions H_2 #1 (-0.33 kcal/mol), #2 (-0.52 kcal/mol), #3 (-0.80 kcal/mol), #4 (-0.58 kcal/mol), #5 (-0.52 kcal/mol), #6 (-0.72 kcal/mol), #7 (-0.70 kcal/mol), #8 (-0.71 kcal/mol), #9 (-0.75 kcal/mol), #10 (-0.46 kcal/mol), #11 (-0.37 kcal/mol), #12 (-0.74 kcal/mol), #13 (-0.33 kcal/mol), #14 (-0.44 kcal/mol), #15 (-0.33 kcal/mol), #16 (-0.53 kcal/mol), #17 (-0.57 kcal/mol) and #18 (-0.63 kcal/mol).

The CNL-ZnONS and CCL-ZnONS which were in C_{3h} symmetry, the numbers of H_2 adsorptions on each side of their molecular planes were fifty four and one seventy seven configurations, respectively, see Figure 4.16(d) and (e). The H_2 adsorptions on The CNL-ZnONS were also composed of nine adsorption positions H_2 #1 (-0.64 kcal/mol), #2 (-0.65 kcal/mol), #3 (-0.57 kcal/mol), #4 (-0.47 kcal/mol) and #5 (-0.85 kcal/mol) #6 (-0.38 kcal/mol), #7 (-0.29 kcal/mol), #8 (-0.70 kcal/mol) and #9 (-0.48 kcal/mol). The CCL-ZnONS were composed of eighteen adsorption positions H_2 #1 (-0.95 kcal/mol), #2 (-0.78 kcal/mol), #3 (-0.74 kcal/mol), #4 (-0.78 kcal/mol) and #5 (-0.71 kcal/mol) #6 (-0.76 kcal/mol), #7 (-0.37 kcal/mol), #8 (-1.13 kcal/mol), #9 (-0.56 kcal/mol), #10 (-0.96 kcal/mol), #11 (-0.64 kcal/mol), #12 (-0.46 kcal/mol), #13 (-0.97 kcal/mol), #14 (-0.75 kcal/mol), #15 (-1.03 kcal/mol), #16 (-0.67 kcal/mol), #17 (-0.71 kcal/mol) and #18 (-0.54 kcal/mol).

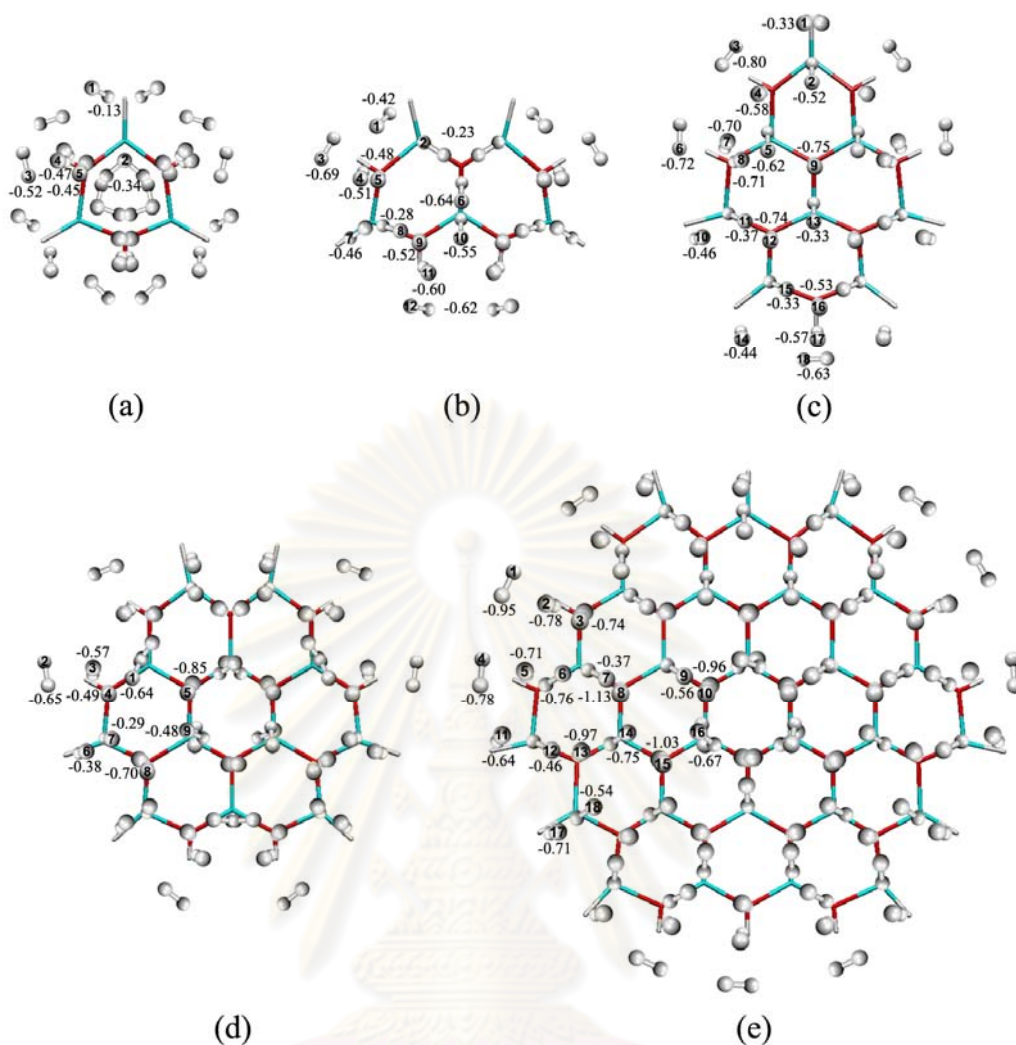


Figure 4.16 Plots of H₂ molecules as minimum energy structures of their adsorptions on (a) the AL-ZnONC, (b) NLL-ZnONC, (c) PRL-ZnONC, (d) CNL-ZnONS and (e) CCL-ZnONS. The molecules labeled with numbers represent the H₂ molecules interacting with ZnONCs and ZnOGLNSs as representative of their molecular symmetries. Adsorption energies in kcal/mol were presented.

Table 4.9 Adsorption energies (ΔE_{ads} in kcal/mol) of H_2 on ZnONCs and ZnOGLNSs, and energy gaps (ΔE_{GAP} in eV) of the bare surfaces of ZnONCs, ZnOGLNSs, and their H_2 adsorption complexes, computed at the B3LYP/LanL2DZ level of theory.

ZnOGLNSs/hydrogen adsorption	ΔE_{ads} (kcal/mol)	E_{GAP} (eV)
AL-ZnONC:		
$\text{H}_2 + \text{AL-ZnONC} \rightarrow \text{H}_2/\text{AL-ZnONC}$ (1)	-0.13	6.49
$\text{H}_2 + \text{AL-ZnONC} \rightarrow \text{H}_2/\text{AL-ZnONC}$ (2)	-0.34	6.50
$\text{H}_2 + \text{AL-ZnONC} \rightarrow \text{H}_2/\text{AL-ZnONC}$ (3)	-0.52	6.49
$\text{H}_2 + \text{AL} \rightarrow \text{H}_2/\text{AL}$ (4)	-0.47	6.48
$\text{H}_2 + \text{AL} \rightarrow \text{H}_2/\text{AL}$ (5)	-0.45	6.48
NPL-ZnONC:		
$\text{H}_2 + \text{NLL-ZnONC} \rightarrow \text{H}_2/\text{NLL-ZnONC}$ (1)	-0.42	5.33
$\text{H}_2 + \text{NLL-ZnONC} \rightarrow \text{H}_2/\text{NLL-ZnONC}$ (2)	-0.23	5.32
$\text{H}_2 + \text{NLL-ZnONC} \rightarrow \text{H}_2/\text{NLL-ZnONC}$ (3)	-0.69	5.32
$\text{H}_2 + \text{NLL-ZnONC} \rightarrow \text{H}_2/\text{NLL-ZnONC}$ (4)	-0.51	5.32
$\text{H}_2 + \text{NLL-ZnONC} \rightarrow \text{H}_2/\text{NLL-ZnONC}$ (5)	-0.48	5.32
$\text{H}_2 + \text{NLL-ZnONC} \rightarrow \text{H}_2/\text{NLL-ZnONC}$ (6)	-0.64	5.36
$\text{H}_2 + \text{NLL-ZnONC} \rightarrow \text{H}_2/\text{NLL-ZnONC}$ (7)	-0.46	5.33
$\text{H}_2 + \text{NLL-ZnONC} \rightarrow \text{H}_2/\text{NLL-ZnONC}$ (8)	-0.28	5.34
$\text{H}_2 + \text{NLL-ZnONC} \rightarrow \text{H}_2/\text{NLL-ZnONC}$ (9)	-0.52	5.33
$\text{H}_2 + \text{NLL-ZnONC} \rightarrow \text{H}_2/\text{NLL-ZnONC}$ (10)	-0.55	5.36
$\text{H}_2 + \text{NLL-ZnONC} \rightarrow \text{H}_2/\text{NLL-ZnONC}$ (11)	-0.60	5.36
$\text{H}_2 + \text{NLL-ZnONC} \rightarrow \text{H}_2/\text{NLL-ZnONC}$ (12)	-0.62	5.36
PRL-ZnONC:		
$\text{H}_2 + \text{PRL-ZnONC} \rightarrow \text{H}_2/\text{PRL-ZnONC}$ (1)	-0.33	4.26
$\text{H}_2 + \text{PRL-ZnONC} \rightarrow \text{H}_2/\text{PRL-ZnONC}$ (2)	-0.52	4.28
$\text{H}_2 + \text{PRL-ZnONC} \rightarrow \text{H}_2/\text{PRL-ZnONC}$ (3)	-0.80	4.30
$\text{H}_2 + \text{PRL-ZnONC} \rightarrow \text{H}_2/\text{PRL-ZnONC}$ (4)	-0.58	4.27
$\text{H}_2 + \text{PRL-ZnONC} \rightarrow \text{H}_2/\text{PRL-ZnONC}$ (5)	-0.62	4.31
$\text{H}_2 + \text{PRL-ZnONC} \rightarrow \text{H}_2/\text{PRL-ZnONC}$ (6)	-0.72	4.28
$\text{H}_2 + \text{PRL-ZnONC} \rightarrow \text{H}_2/\text{PRL-ZnONC}$ (7)	-0.70	4.29
$\text{H}_2 + \text{PRL-ZnONC} \rightarrow \text{H}_2/\text{PRL-ZnONC}$ (8)	-0.71	4.29
$\text{H}_2 + \text{PRL-ZnONC} \rightarrow \text{H}_2/\text{PRL-ZnONC}$ (9)	-0.75	4.28
$\text{H}_2 + \text{PRL-ZnONC} \rightarrow \text{H}_2/\text{PRL-ZnONC}$ (10)	-0.46	4.27
$\text{H}_2 + \text{PRL-ZnONC} \rightarrow \text{H}_2/\text{PRL-ZnONC}$ (11)	-0.37	4.27
$\text{H}_2 + \text{PRL-ZnONC} \rightarrow \text{H}_2/\text{PRL-ZnONC}$ (12)	-0.74	4.27
$\text{H}_2 + \text{PRL-ZnONC} \rightarrow \text{H}_2/\text{PRL-ZnONC}$ (13)	-0.33	4.28
$\text{H}_2 + \text{PRL-ZnONC} \rightarrow \text{H}_2/\text{PRL-ZnONC}$ (14)	-0.44	4.27
$\text{H}_2 + \text{PRL-ZnONC} \rightarrow \text{H}_2/\text{PRL-ZnONC}$ (15)	-0.33	4.26
$\text{H}_2 + \text{PRL-ZnONC} \rightarrow \text{H}_2/\text{PRL-ZnONC}$ (16)	-0.53	4.27
$\text{H}_2 + \text{PRL-ZnONC} \rightarrow \text{H}_2/\text{PRL-ZnONC}$ (17)	-0.57	4.27
$\text{H}_2 + \text{PRL-ZnONC} \rightarrow \text{H}_2/\text{PRL-ZnONC}$ (18)	-0.63	4.25
CNL-ZnONS:		
$\text{H}_2 + \text{CNL-ZnONS} \rightarrow \text{H}_2/\text{CNL-ZnONS}$ (1)	-0.64	4.86
$\text{H}_2 + \text{CNL-ZnONS} \rightarrow \text{H}_2/\text{CNL-ZnONS}$ (2)	-0.65	4.85
$\text{H}_2 + \text{CNL-ZnONS} \rightarrow \text{H}_2/\text{CNL-ZnONS}$ (3)	-0.57	4.85
$\text{H}_2 + \text{CNL-ZnONS} \rightarrow \text{H}_2/\text{CNL-ZnONS}$ (4)	-0.49	4.84
$\text{H}_2 + \text{CNL-ZnONS} \rightarrow \text{H}_2/\text{CNL-ZnONS}$ (5)	-0.85	4.85
$\text{H}_2 + \text{CNL-ZnONS} \rightarrow \text{H}_2/\text{CNL-ZnONS}$ (6)	-0.38	4.84
$\text{H}_2 + \text{CNL-ZnONS} \rightarrow \text{H}_2/\text{CNL-ZnONS}$ (7)	-0.29	4.85
$\text{H}_2 + \text{CNL-ZnONS} \rightarrow \text{H}_2/\text{CNL-ZnONS}$ (8)	-0.70	4.84
$\text{H}_2 + \text{CNL-ZnONS} \rightarrow \text{H}_2/\text{CNL-ZnONS}$ (9)	-0.48	4.85

Table 4.9 (cont.) Adsorption energies (ΔE_{ads} in kcal/mol) of H_2 on ZnONCs and ZnOGLNSs, and energy gaps (ΔE_{GAP} in eV) of the bare surfaces of ZnONCs, ZnOGLNSs, and their H_2 adsorption complexes, computed at the B3LYP/LanL2DZ level of theory.

ZnOGLNSs/hydrogen adsorption	ΔE_{ads} (kcal/mol)	E_{GAP} (eV)
<i>CCL-ZnONS:</i>		
$\text{H}_2 + \text{CCL-ZnONS} \rightarrow \text{H}_2/\text{CCL-ZnONS}$ (1)	-0.95	3.74
$\text{H}_2 + \text{CCL-ZnONS} \rightarrow \text{H}_2/\text{CCL-ZnONS}$ (2)	-0.78	3.76
$\text{H}_2 + \text{CCL-ZnONS} \rightarrow \text{H}_2/\text{CCL-ZnONS}$ (3)	-0.74	3.75
$\text{H}_2 + \text{CCL-ZnONS} \rightarrow \text{H}_2/\text{CCL-ZnONS}$ (4)	-0.78	3.75
$\text{H}_2 + \text{CCL-ZnONS} \rightarrow \text{H}_2/\text{CCL-ZnONS}$ (5)	-0.71	3.75
$\text{H}_2 + \text{CCL-ZnONS} \rightarrow \text{H}_2/\text{CCL-ZnONS}$ (6)	-0.76	3.76
$\text{H}_2 + \text{CCL-ZnONS} \rightarrow \text{H}_2/\text{CCL-ZnONS}$ (7)	-0.37	3.75
$\text{H}_2 + \text{CCL-ZnONS} \rightarrow \text{H}_2/\text{CCL-ZnONS}$ (8)	-1.13	3.75
$\text{H}_2 + \text{CCL-ZnONS} \rightarrow \text{H}_2/\text{CCL-ZnONS}$ (9)	-0.56	3.76
$\text{H}_2 + \text{CCL-ZnONS} \rightarrow \text{H}_2/\text{CCL-ZnONS}$ (10)	-0.96	3.75
$\text{H}_2 + \text{CCL-ZnONS} \rightarrow \text{H}_2/\text{CCL-ZnONS}$ (11)	-0.64	3.75
$\text{H}_2 + \text{CCL-ZnONS} \rightarrow \text{H}_2/\text{CCL-ZnONS}$ (12)	-0.46	3.75
$\text{H}_2 + \text{CCL-ZnONS} \rightarrow \text{H}_2/\text{CCL-ZnONS}$ (13)	-0.97	3.75
$\text{H}_2 + \text{CCL-ZnONS} \rightarrow \text{H}_2/\text{CCL-ZnONS}$ (14)	-0.75	3.75
$\text{H}_2 + \text{CCL-ZnONS} \rightarrow \text{H}_2/\text{CCL-ZnONS}$ (15)	-1.03	3.75
$\text{H}_2 + \text{CCL-ZnONS} \rightarrow \text{H}_2/\text{CCL-ZnONS}$ (16)	-0.67	3.76
$\text{H}_2 + \text{CCL-ZnONS} \rightarrow \text{H}_2/\text{CCL-ZnONS}$ (17)	-0.71	3.75
$\text{H}_2 + \text{CCL-ZnONS} \rightarrow \text{H}_2/\text{CCL-ZnONS}$ (18)	-0.54	3.75

The energy gaps (ΔE_{GAP}) of the adsorption complexes H_2 with the AL-ZnONC, NLL-ZnONC, PRL-ZnONC, CNL-ZnONS and CCL-ZnONS were also not much different from their corresponding bare surfaces as shown in Table 4.10.

4.2.6 Adsorption of nitric oxide molecule

4.2.6.1 Adsorption energies of NO pointing with N-end

Geometry configurations of NO adsorptions on the rigid structures of the AL-ZnONC, NLL-ZnONC, and PRL-ZnONC nanoclusters, shown in Figure 4.17 and the CNL-ZnONS, shown in Figure 4.18 and CCL-ZnONS nanosheets, shown in Figure 4.19. The calculated adsorption energy values of the minimum energy structures of NO on nanoclusters and nanosheets were shown in Table 4.10. The NO adsorption configurations of NO pointing with N-end to adsorption sites of nanoclusters were shown in left side of Figure 4.18 and to adsorption sites of the CNL-ZnONS and CCL-ZnONS nanosheets were shown in Figures 4.18(a) and 4.19(a), respectively.

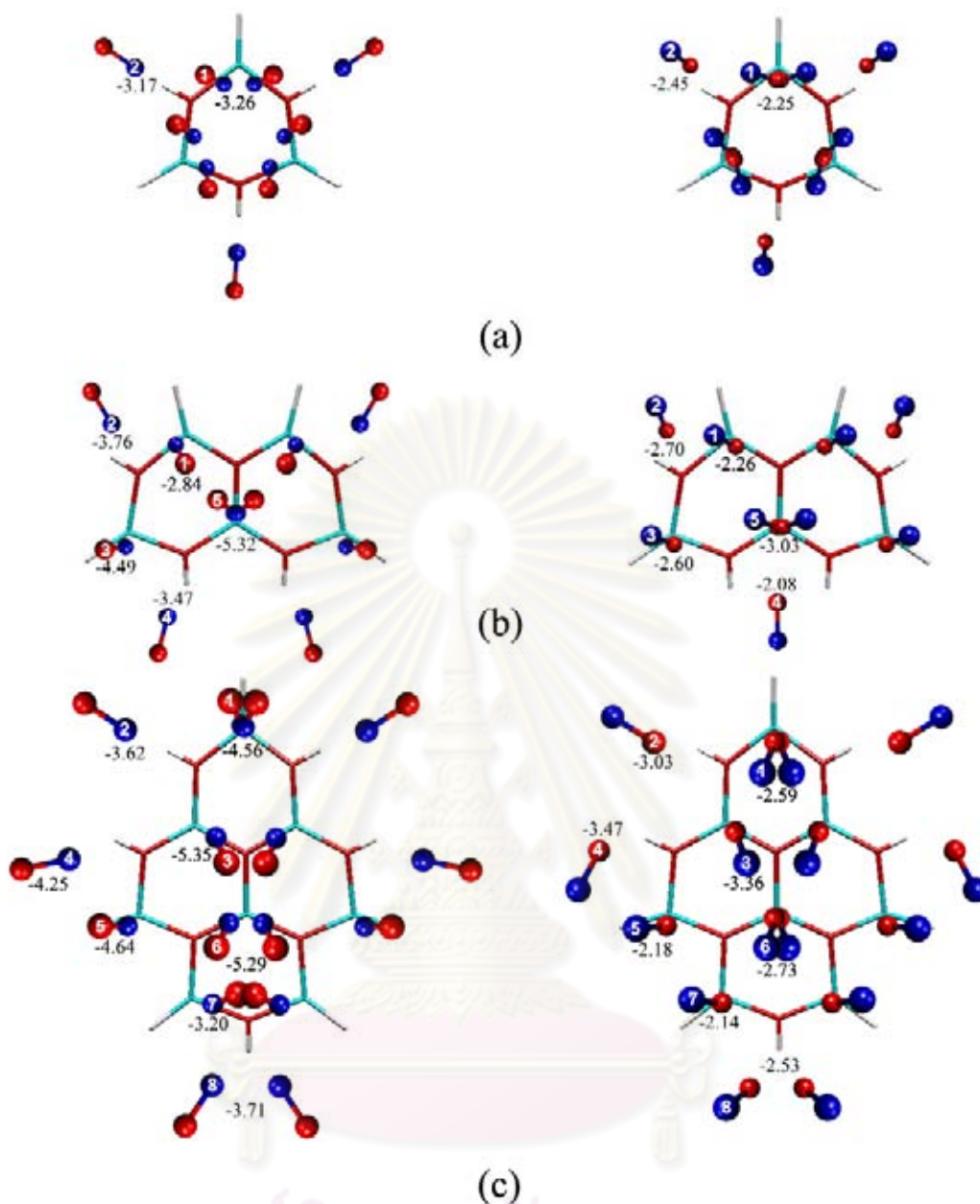


Figure 4.17 Plots of NO molecules as minimum energy structures of their adsorptions on (a) the AL-ZnONC ($\text{Zn}_3\text{O}_3\text{H}_6$), (b) NLL-ZnONC ($\text{Zn}_5\text{O}_5\text{H}_8$) and (c) PRL-ZnONC ($\text{Zn}_8\text{O}_8\text{H}_{10}$). Their left and right adsorption maps were NO adsorption on ZnONCs by pointing N-end and O-end toward the adsorption sites, respectively. The set of labeled molecules was representative of NO interacting with AL-ZnONC (C_{3h}), NLL-ZnONC (C_{2v}) and PRL-ZnONC (C_{2v}). Adsorption energies were presented in kcal/mol.

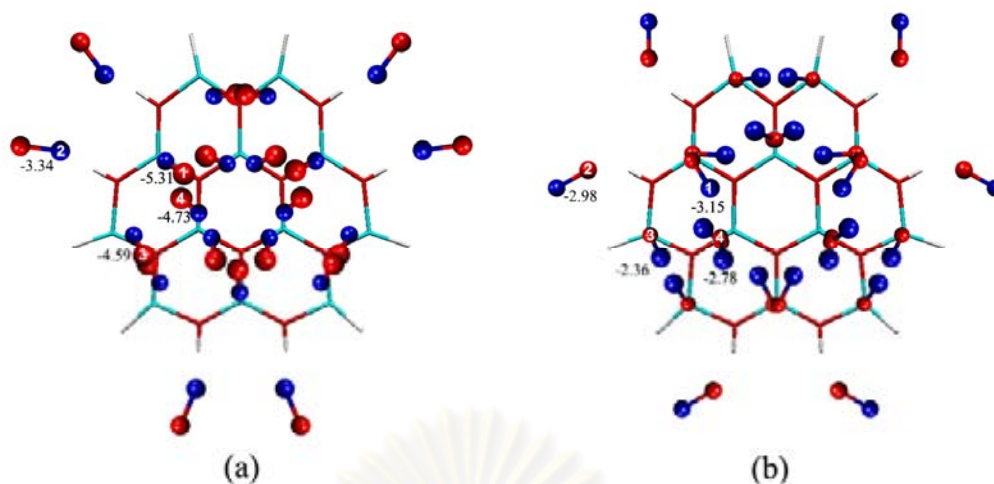


Figure 4.18 Plots of NO molecules as minimum energy structures of their adsorptions on CNL-ZnONS (Zn₁₂O₁₂H₁₂) as adsorption configurations of NO with pointing its (a) N-end and (b) O-end toward the adsorption sites of the CNL-ZnONS. The set of labeled molecules was representative of NO adsorption interacting with CNL-ZnONS with C_{3h} symmetry. Adsorption energies were presented in kcal/mol.

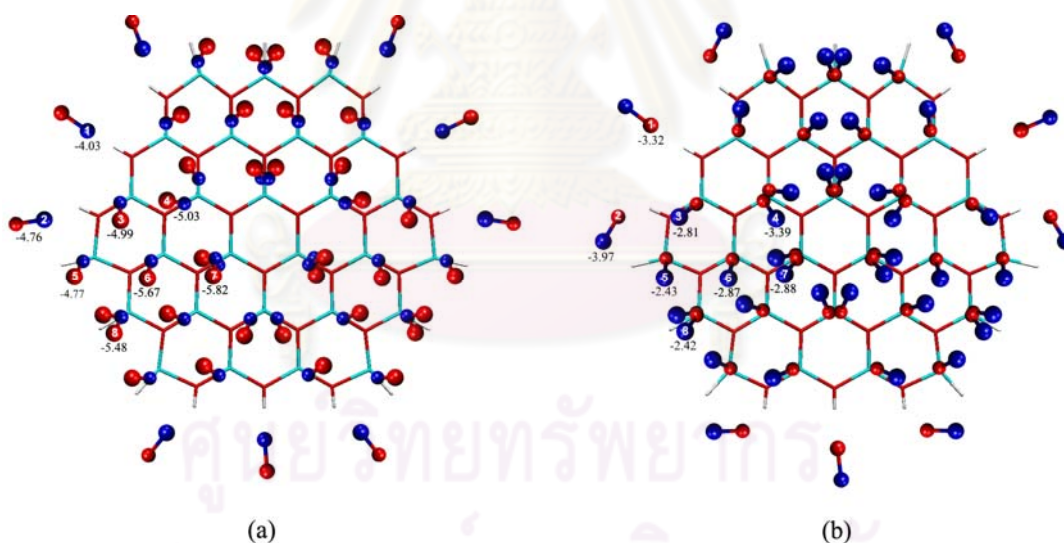


Figure 4.19 Plots of NO molecules as minimum energy structures of their adsorptions on CCL-ZnONS (Zn₂₇O₂₇H₁₈) as (a) adsorption configurations of NO by pointing (a) N-end and (b) O-end toward the adsorption sites. The molecules labeled with numbers represent the oxygen molecule interacting with CCL-ZnONS of molecular symmetry of (C_{3h}). Adsorption energies were presented in kcal/mol.

The number of energy minima of NO adsorptions on the AL–ZnONC of nine configurations was found for each side of its molecular planes. These energy minima were obtained from the structure optimizations of interaction configurations within one third of each side of the AL–ZnONC molecular area and NO adsorptions over the whole AL–ZnONC molecular area were generated using C_{3h} symmetrical operation. The most stable configuration of NO adsorption on the AL–ZnONC was represented by the configuration of NO #2 of which the adsorption energy was -3.26 kcal/mol, shows the N atom of NO pointing to a surface Zn atom ($\underline{\text{NO}}\cdots\text{H1}$) at a distance of 2.15 Å, show in Table 4.11.

As the NLL–ZnONC and PRL–ZnONC nanoclusters were in C_{2v} symmetry, the numbers of NO adsorptions on each side of their molecular planes were ten and sixteen configurations, as shown in the left sides of Figure 4.17(b) and (c), respectively. There were four types of adsorption positions on the NLL–ZnONC which were composed of adsorption position NO #1 (-2.84 kcal/mol), #2 (-3.76 kcal/mol), #3 (-4.49 kcal/mol), #4 (-3.47 kcal/mol) and #5 (-5.32 kcal/mol). The most stable configuration of NO adsorption on the NLL–ZnONC was represented by the configuration of NO #5 which N atom of NO pointing to a surface Zn atom ($\underline{\text{NO}}\cdots\text{Zn3}$) at a distance of 2.49 Å. There were eight types of adsorption positions on the PRL–ZnONC which were composed of adsorption positions NO #1 (-4.56 kcal/mol), #2 (-3.62 kcal/mol), #3 (-5.35 kcal/mol), #4 (-4.25 kcal/mol), #5 (-4.64 kcal/mol), #6 (-5.29 kcal/mol), #7 (-3.20 kcal/mol) and #8 (-3.71 kcal/mol). The most stable configuration of NO adsorption on the PRL–ZnONC was represented by the configuration of NO #3 which N atom of NO pointing to a surface Zn atom ($\underline{\text{NO}}\cdots\text{Zn2}$) at a distance of 2.54 Å.

The CNL–ZnONS and CCL–ZnONS were in C_{3h} symmetry, the numbers of NO adsorptions on each side of their molecular planes were twenty one and forty five configurations as shown in Figure 4.19(a) and Figure 4.19(a) respectively. There were four types of adsorption positions on the CNL–ZnONS which were composed of adsorption position NO #1 (-5.31 kcal/mol), #2 (-3.34 kcal/mol), #3 (-4.59 kcal/mol) and #4 (-4.73 kcal/mol). The most stable configuration of NO adsorption on the CNL–ZnONS was represented by the configuration of NO #1 which N atom of NO pointing to a surface Zn atom ($\underline{\text{NO}}\cdots\text{Zn1}$) at a distance of 2.56 Å. There were eight types of adsorption positions on the CCL–ZnONS which were composed of adsorption positions NO #1 (-4.03 kcal/mol), #2 (-4.76 kcal/mol), #3 (-4.99

kcal/mol), #4 (-5.03 kcal/mol), #5 (-4.77 kcal/mol), #6 (-5.67 kcal/mol), #7 (-5.82 kcal/mol) and #8 (-5.48 kcal/mol). The most stable configuration of NO adsorption on the CCL-ZnONS was represented by the configuration of NO #1 which N atom of NO pointing to a surface Zn atom ($\text{NO}\cdots\text{Zn1}$) at a distance of 2.56 Å.

The NO adsorptions with pointing N-end towards atoms of the ZnOGLNSs were categorized into two bond types, $[\text{NO}\cdots\text{H}]$ and $[\text{NO}\cdots\text{Zn}]$. The $[\text{NO}\cdots\text{H}]$ bond occurred when the NO adsorption with pointing N-end toward hydroxyl hydrogen of the ZnOGLNSs to which the molecular axis of NO was nearly parallel to the molecular plane. But the $[\text{NO}\cdots\text{H}]$ bond occurred when the NO adsorption with pointing N-end towards Zn atom of the ZnOGLNS to which the molecular axis of NO was nearly perpendicular to the molecular plane.

On the same position of NO adsorptions either on nanoclusters or nanosheets, the adsorption energies of NO of which the N-end pointing towards the nanosheets atoms were more stable than the O-end. The NO adsorptions with pointing N-end towards atoms of the ZnOGLNSs were categorized into two bond types, $[\text{NO}\cdots\text{H}]$ and $[\text{NO}\cdots\text{Zn}]$. The $[\text{NO}\cdots\text{H}]$ bond occurred when the NO adsorption with pointing N-end toward hydroxyl hydrogen of the ZnOGLNSs to which the molecular axis of NO was nearly parallel to the molecular plane. But the $[\text{NO}\cdots\text{H}]$ bond occurred when the NO adsorption with pointing N-end towards Zn atom of the ZnOGLNS to which the molecular axis of NO was nearly perpendicular to the molecular plane.

Table 4.10 Adsorption energies (ΔE_{ads} in kcal/mol) of NO pointing its N-end toward surfaces of ZnONCs and ZnOGLNSs and energy gaps (ΔE_{GAP} in eV) of bare surfaces of ZnONCs, ZnOGLNSs and their NO adsorption complexes, computed at the B3LYP/LanL2DZ level of theory.

ZnOGLNSs/nitric oxide adsorption	ΔE_{ads} (kcal/mol)	E_{GAP} (eV)
AL-ZnONC:		
$\text{NO} + \text{AL-ZnONC} \rightarrow \text{NO/AL-ZnONC}$ (1)	-3.26	2.82
$\text{NO} + \text{AL-ZnONC} \rightarrow \text{NO/AL-ZnONC}$ (2)	-3.17	2.92
NLL-ZnONC:		
$\text{NO} + \text{NLL-ZnONC} \rightarrow \text{NO/NLL-ZnONC}$ (1)	-2.84	2.74
$\text{NO} + \text{NLL-ZnONC} \rightarrow \text{NO/NLL-ZnONC}$ (2)	-3.76	2.99
$\text{NO} + \text{NLL-ZnONC} \rightarrow \text{NO/NLL-ZnONC}$ (3)	-4.49	2.96
$\text{NO} + \text{NLL-ZnONC} \rightarrow \text{NO/NLL-ZnONC}$ (4)	-3.47	2.23
$\text{NO} + \text{NLL-ZnONC} \rightarrow \text{NO/NLL-ZnONC}$ (5)	-5.32	2.92
PRL-ZnONC:		
$\text{NO} + \text{PRL-ZnONC} \rightarrow \text{NO/PRL-ZnONC}$ (1)	-4.56	2.04
$\text{NO} + \text{PRL-ZnONC} \rightarrow \text{NO/PRL-ZnONC}$ (2)	-3.62	1.56
$\text{NO} + \text{PRL-ZnONC} \rightarrow \text{NO/PRL-ZnONC}$ (3)	-5.35	2.11
$\text{NO} + \text{PRL-ZnONC} \rightarrow \text{NO/PRL-ZnONC}$ (4)	-4.25	2.96
$\text{NO} + \text{PRL-ZnONC} \rightarrow \text{NO/PRL-ZnONC}$ (5)	-4.64	2.93
$\text{NO} + \text{PRL-ZnONC} \rightarrow \text{NO/PRL-ZnONC}$ (6)	-5.29	2.80
$\text{NO} + \text{PRL-ZnONC} \rightarrow \text{NO/PRL-ZnONC}$ (7)	-3.20	2.73
$\text{NO} + \text{PRL-ZnONC} \rightarrow \text{NO/PRL-ZnONC}$ (8)	-3.71	3.00
CNL-ZnONS:		
$\text{NO} + \text{CNL-ZnONS} \rightarrow \text{NO/CNL-ZnONS}$ (1)	-5.31	2.87
$\text{NO} + \text{CNL-ZnONS} \rightarrow \text{NO/CNL-ZnONS}$ (2)	-3.34	2.42
$\text{NO} + \text{CNL-ZnONS} \rightarrow \text{NO/CNL-ZnONS}$ (3)	-4.59	3.05
$\text{NO} + \text{CNL-ZnONS} \rightarrow \text{NO/CNL-ZnONS}$ (4)	-4.73	2.91
CCL-ZnONS:		
$\text{NO} + \text{CCL-ZnONS} \rightarrow \text{NO/CCL-ZnONS}$ (1)	-4.03	1.28
$\text{NO} + \text{CCL-ZnONS} \rightarrow \text{NO/CCL-ZnONS}$ (2)	-4.76	2.83
$\text{NO} + \text{CCL-ZnONS} \rightarrow \text{NO/CCL-ZnONS}$ (3)	-4.99	1.77
$\text{NO} + \text{CCL-ZnONS} \rightarrow \text{NO/CCL-ZnONS}$ (4)	-5.03	2.08
$\text{NO} + \text{CCL-ZnONS} \rightarrow \text{NO/CCL-ZnONS}$ (5)	-4.77	2.87
$\text{NO} + \text{CCL-ZnONS} \rightarrow \text{NO/CCL-ZnONS}$ (6)	-5.67	2.62
$\text{NO} + \text{CCL-ZnONS} \rightarrow \text{NO/CCL-ZnONS}$ (7)	-5.82	2.43
$\text{NO} + \text{CCL-ZnONS} \rightarrow \text{NO/CCL-ZnONS}$ (8)	-5.48	3.01

ศูนย์วิทยทรัพยากร
จุฬาลงกรณ์มหาวิทยาลัย

Table 4.11 Bond distances (in Å) between NO atoms and atoms of adsorption sites.

ZnOGLNSs	[<u>NO</u> ...S] ^a		[<u>NO</u> ...S] ^a	
AL-ZnONC:	<u>NO</u> ...Zn1	2.68	<u>NO</u> ...Zn1	2.74
	<u>NO</u> ...H1	2.15	<u>NO</u> ...H1	2.11
NLL-ZnONC:	<u>NO</u> ...Zn1	2.77	<u>NO</u> ...Zn1	2.81
	<u>NO</u> ...H1	2.30	<u>NO</u> ...H1	2.16
	<u>NO</u> ...Zn2	2.52	<u>NO</u> ...Zn2	2.76
	<u>NO</u> ...H4	2.17	<u>NO</u> ...H4	2.41
	<u>NO</u> ...Zn3	2.49	<u>NO</u> ...Zn3	2.66
PRL-ZnONC:	<u>NO</u> ...Zn1	2.51	<u>NO</u> ...Zn1	2.81
	<u>NO</u> ...H1	2.14	<u>NO</u> ...H1	2.14
	<u>NO</u> ...Zn2	2.54	<u>NO</u> ...Zn2	2.67
	<u>NO</u> ...H2	2.31	<u>NO</u> ...H2	2.16
	<u>NO</u> ...Zn3	2.52	<u>NO</u> ...Zn3	2.86
	<u>NO</u> ...Zn4	2.55	<u>NO</u> ...Zn4	2.75
	<u>NO</u> ...Zn5	2.75	<u>NO</u> ...Zn5	2.86
	<u>NO</u> ...H3	2.46	<u>NO</u> ...H3	2.25
CNL-ZnONS:	<u>NO</u> ...Zn1	2.56	<u>NO</u> ...Zn1	2.83
	<u>NO</u> ...H1	2.14	<u>NO</u> ...H1	2.17
	<u>NO</u> ...Zn2	2.68	<u>NO</u> ...Zn2	2.83
	<u>NO</u> ...Zn3	2.63	<u>NO</u> ...Zn3	2.81
CCL-ZnONS:	<u>NO</u> ...H1	2.13	<u>NO</u> ...H1	2.12
	<u>NO</u> ...H2	2.28	<u>NO</u> ...H2	2.13
	<u>NO</u> ...Zn1	2.58	<u>NO</u> ...Zn1	2.81
	<u>NO</u> ...Zn2	2.62	<u>NO</u> ...Zn2	2.78
	<u>NO</u> ...Zn3	2.49	<u>NO</u> ...Zn3	2.81
	<u>NO</u> ...Zn4	2.57	<u>NO</u> ...Zn4	2.81
	<u>NO</u> ...Zn5	2.62	<u>NO</u> ...Zn5	2.81
	<u>NO</u> ...Zn6	2.50	<u>NO</u> ...Zn6	3.02

^a Atom S stands for atomic adsorption site, NO and NO were carbon dioxide molecules pointing their N and O atoms toward atom S in the nanoclusters or nanosheets, respectively. Atomic positions of S atom were shown in Figure 4.1.

4.2.6.2 Adsorption energies of NO pointing with O-end.

The NO adsorption configurations of NO pointing with O-end to adsorption sites of nanoclusters were shown in right side of Figure 4.18 and to adsorption sites of the CNL-ZnONS and CCL-ZnONS nanosheets were shown in Figures 4.18(b) and 4.19(b), respectively.

The number of energy minima of NO adsorptions on the AL-ZnONC of nine configurations was found for each side of its molecular planes. These energy minima were obtained from the structure optimizations of interaction configurations within one third of each side of the AL-ZnONC molecular area and NO adsorptions over the

whole AL–ZnONC molecular area were generated using C_{3h} symmetrical operation. The most stable configuration of NO adsorption on the AL–ZnONC was represented by the configuration of NO #2 of which the adsorption energy was -2.45 kcal/mol (Table 4.13), shows the O atom of NO pointing to a surface Zn atom ($\text{NO}\cdots\text{H1}$) at a distance of 2.11 Å, show in Table 4.11.

As the NLL–ZnONC and PRL–ZnONC nanoclusters were in C_{2v} symmetry, the numbers of NO adsorptions on each side of their molecular planes were nine and sixteen configurations, as shown in the right sides of Figure 4.18(b) and (c), respectively. There were five types of adsorption positions on the NLL–ZnONC which were composed of adsorption position NO #1 (-2.26 kcal/mol), #2 (-2.70 kcal/mol), #3 (-2.60 kcal/mol), #4 (-2.08 kcal/mol) and #5 (-3.03 kcal/mol). The most stable configuration of NO adsorption on the NLL–ZnONC was represented by the configuration of NO #5 which O atom of NO pointing to a surface Zn atom ($\text{NO}\cdots\text{Zn3}$) at a distance of 2.66 Å. There were eight types of adsorption positions on the PRL–ZnONC which were composed of adsorption positions NO #1 (-2.59 kcal/mol), #2 (-3.03 kcal/mol), #3 (-3.36 kcal/mol), #4 (-3.47 kcal/mol), #5 (-2.18 kcal/mol), #6 (-2.73 kcal/mol), #7 (-2.14 kcal/mol) and #8 (-2.53 kcal/mol). The most stable configuration of NO adsorption on the PRL–ZnONC was represented by the configuration of NO #4 which O atom of NO pointing to a surface H atom ($\text{NO}\cdots\text{H2}$) at a distance of 2.16 Å.

The CNL–ZnONS and CCL–ZnONS were in C_{3h} symmetry, the numbers of NO adsorptions on each side of their molecular planes were twenty four and forty five configurations as shown in Figures 4.18(b) and 4.19(b) respectively. There were four types of adsorption positions on the CNL–ZnONS which were composed of adsorption position NO #1 (-3.15 kcal/mol), #2 (-2.98 kcal/mol), #3 (-2.36 kcal/mol) and #4 (-2.78 kcal/mol). The most stable configuration of NO adsorption on the CNL–ZnONC was represented by the configuration of NO #1 which O atom of NO pointing to a surface Zn atom ($\text{NO}\cdots\text{Zn1}$) at a distance of 2.83 Å. There were eight types of adsorption positions on the CCL–ZnONS which were composed of adsorption positions NO #1 (-3.32 kcal/mol), #2 (-3.97 kcal/mol), #3 (-2.81 kcal/mol), #4 (-3.39 kcal/mol), #5 (-2.43 kcal/mol), #6 (-2.87 kcal/mol), #7 (-2.88 kcal/mol) and #8 (-2.42 kcal/mol). The most stable configuration of NO adsorption on the CCL–ZnONC was represented by the configuration of NO #2 which O atom of NO pointing to a surface Zn atom ($\text{NO}\cdots\text{H2}$) at a distance of 2.13 Å.

The NO adsorptions with pointing the O-end toward atoms of the ZnOGLNSs were also categorized into two bond types, $[\text{NO}\cdots\text{H}]$ and $[\text{NO}\cdots\text{Zn}]$. The $[\text{NO}\cdots\text{H}]$ bond occurred when the NO adsorption with pointing O-end toward hydroxyl hydrogen of the ZnOGLNSs to which the molecular axis of NO was nearly parallel to the molecular plane. But the $[\text{NO}\cdots\text{Zn}]$ bond occurred when the NO adsorption with pointing O-end towards Zn atom of the ZnOGLNS to which the molecular axis of NO was nearly perpendicular to the molecular plane.

4.2.6.3 Energy gap

The energy gaps of the clean ZnOGLNSs and their NO pointing with N-end or O-end adsorption complexes were shown in Table 4.10. In all cases, the energy gaps of clean ZnOGLNSs were higher than those values of their corresponding NO adsorption complexes, see Table 4.10 and 4.12. This suggests that the ZnOGLNSs were NO sensitive materials and they would be developed to be NO sensor based on electrical conductivity.



ศูนย์วิทยทรัพยากร
จุฬาลงกรณ์มหาวิทยาลัย

Table 4.12 Adsorption energies (ΔE_{ads} in kcal/mol) of NO pointing its O-end toward surfaces of ZnONCs and ZnOGLNSs and energy gaps (ΔE_{GAP} in eV) of bare surfaces of ZnONCs, ZnOGLNSs and their NO adsorption complexes, computed at the B3LYP/LanL2DZ level of theory.

ZnOGLNSs/nitric oxide adsorption	ΔE_{ads} (kcal/mol)	E_{GAP} (eV)
AL-ZnONC:		6.47
$\text{NO} + \text{AL-ZnONC} \rightarrow \text{NO/AL-ZnONC}$ (1)	-2.25	2.87
$\text{NO} + \text{AL-ZnONC} \rightarrow \text{NO/AL-ZnONC}$ (2)	-2.45	2.94
NLL-ZnONC:		5.32
$\text{NO} + \text{NLL-ZnONC} \rightarrow \text{NO/NLL-ZnONC}$ (1)	-2.26	2.80
$\text{NO} + \text{NLL-ZnONC} \rightarrow \text{NO/NLL-ZnONC}$ (2)	-2.70	2.94
$\text{NO} + \text{NLL-ZnONC} \rightarrow \text{NO/NLL-ZnONC}$ (3)	-2.60	2.64
$\text{NO} + \text{NLL-ZnONC} \rightarrow \text{NO/NLL-ZnONC}$ (4)	-2.08	2.08
$\text{NO} + \text{NLL-ZnONC} \rightarrow \text{NO/NLL-ZnONC}$ (5)	-3.03	2.39
PRL-ZnONC:		4.26
$\text{NO} + \text{PRL-ZnONC} \rightarrow \text{NO/PRL-ZnONC}$ (1)	-2.59	1.66
$\text{NO} + \text{PRL-ZnONC} \rightarrow \text{NO/PRL-ZnONC}$ (2)	-3.03	1.56
$\text{NO} + \text{PRL-ZnONC} \rightarrow \text{NO/PRL-ZnONC}$ (3)	-3.36	1.73
$\text{NO} + \text{PRL-ZnONC} \rightarrow \text{NO/PRL-ZnONC}$ (4)	-3.47	3.00
$\text{NO} + \text{PRL-ZnONC} \rightarrow \text{NO/PRL-ZnONC}$ (5)	-2.18	2.49
$\text{NO} + \text{PRL-ZnONC} \rightarrow \text{NO/PRL-ZnONC}$ (6)	-2.73	2.19
$\text{NO} + \text{PRL-ZnONC} \rightarrow \text{NO/PRL-ZnONC}$ (7)	-2.14	2.67
$\text{NO} + \text{PRL-ZnONC} \rightarrow \text{NO/PRL-ZnONC}$ (8)	-2.53	1.66
CNL-ZnONS:		4.83
$\text{NO} + \text{CNL-ZnONS} \rightarrow \text{NO/CNL-ZnONS}$ (1)	-3.15	2.41
$\text{NO} + \text{CNL-ZnONS} \rightarrow \text{NO/CNL-ZnONS}$ (2)	-2.98	2.87
$\text{NO} + \text{CNL-ZnONS} \rightarrow \text{NO/CNL-ZnONS}$ (3)	-2.36	2.70
$\text{NO} + \text{CNL-ZnONS} \rightarrow \text{NO/CNL-ZnONS}$ (4)	-2.78	2.50
CCL-ZnONS:		3.74
$\text{NO} + \text{CCL-ZnONS} \rightarrow \text{NO/CCL-ZnONS}$ (1)	-3.32	1.35
$\text{NO} + \text{CCL-ZnONS} \rightarrow \text{NO/CCL-ZnONS}$ (2)	-3.97	3.00
$\text{NO} + \text{CCL-ZnONS} \rightarrow \text{NO/CCL-ZnONS}$ (3)	-2.81	1.69
$\text{NO} + \text{CCL-ZnONS} \rightarrow \text{NO/CCL-ZnONS}$ (4)	-3.39	1.70
$\text{NO} + \text{CCL-ZnONS} \rightarrow \text{NO/CCL-ZnONS}$ (5)	-2.43	2.38
$\text{NO} + \text{CCL-ZnONS} \rightarrow \text{NO/CCL-ZnONS}$ (6)	-2.87	2.01
$\text{NO} + \text{CCL-ZnONS} \rightarrow \text{NO/CCL-ZnONS}$ (7)	-2.88	1.84
$\text{NO} + \text{CCL-ZnONS} \rightarrow \text{NO/CCL-ZnONS}$ (8)	-2.42	2.57

4.2.7 Adsorption of nitrous oxide molecule

4.2.7.1 Adsorption energies of N_2O pointing with N-end

The structure optimizations of N_2O adsorptions on the rigid structures of the AL-ZnONC, NLL-ZnONC, and PRL-ZnONC nanoclusters, shown in Figure 4.20 and the CNL-ZnONS, shown in Figure 4.21 and CCL-ZnONS nanosheets, shown in Figure 4.22. The adsorption energy values of the minimum energy structures of N_2O on nanoclusters and nanosheets were shown in Table 4.13. The N_2O adsorption configurations of N_2O pointing with N-end to adsorption sites of nanoclusters were

shown in left side of Figure 4.20 and to adsorption sites of the CNL–ZnONS and CCL–ZnONS nanosheets were shown in Figures 4.21(a) and 4.22(a), respectively.

The number of energy minima of N₂O adsorptions on the AL–ZnONC of six configurations was found for each side of its molecular planes. These energy minima were obtained from the structure optimizations of interaction configurations within one third of each side of the AL–ZnONC molecular area and N₂O adsorptions over the whole AL–ZnONC molecular area were generated using C_{3h} symmetrical operation. The N₂O adsorption on the AL–ZnONC was represented by the configuration of N₂O #1 of which the adsorption energy was –2.86 kcal/mol (Table 4.13), shows the N atom of N₂O pointing to a surface Zn atom (N₂O··H1) at a distance of 2.70 Å, show in Table 4.14.

Due to the NLL–ZnONC and PRL–ZnONC nanoclusters were in C_{2v} symmetry, the numbers of N₂O adsorptions on each side of their molecular planes were five and nine configurations, as shown in the left sides of Figure 4.20(b) and (c), respectively. There were three types of adsorption positions on the NLL–ZnONC which were composed of adsorption position N₂O #1 (–2.68 kcal/mol), #2 (–2.96 kcal/mol) and #3 (–3.80 kcal/mol). The most stable configuration of N₂O adsorption on the NLL–ZnONC was represented by the configuration of N₂O #3 which N atom of N₂O pointing to a surface Zn atom (N₂O··Zn3) at a distance of 2.61 Å. There were five types of adsorption positions on the PRL–ZnONC which were composed of adsorption positions N₂O #1 (–3.01 kcal/mol), #2 (–4.01 kcal/mol), #3 (–2.76 kcal/mol), #4 (–3.00 kcal/mol) and #5 (–2.66 kcal/mol). The most stable configuration of N₂O adsorption on the PRL–ZnONC was represented by the configuration of N₂O #1 which N atom of N₂O pointing to a surface Zn atom (N₂O··Zn1) at a distance of 2.64 Å.

The CNL–ZnONS and CCL–ZnONS were in C_{3h} symmetry, the numbers of N₂O adsorptions on each side of their molecular planes were eighteen and thirty six configurations as shown in Figure 4.21(a) and Figure 4.22(a) respectively. There were three types of adsorption positions on the CNL–ZnONS which were composed of adsorption position N₂O #1 (–3.64 kcal/mol), #2 (–2.71 kcal/mol) and #3 (–2.87 kcal/mol). The most stable configuration of N₂O adsorption on the CNL–ZnONS was represented by the configuration of N₂O #1 which N atom of N₂O pointing to a surface Zn atom (N₂O··Zn1) at a distance of 2.56 Å. There were six types of adsorption positions on the CCL–ZnONS which were composed of adsorption

positions N₂O #1 (-3.87 kcal/mol), #2 (-2.76 kcal/mol), #3 (-2.70 kcal/mol), #4 (-3.39 kcal/mol), #5 (-2.42 kcal/mol) and #6 (-2.70 kcal/mol). The most stable configuration of N₂O adsorption on the CCL-ZnONC was represented by the configuration of N₂O #1 which N atom of N₂O pointing to a surface Zn atom (N₂O...Zn1) at a distance of 2.63 Å.

The N₂O adsorptions with pointing N-end towards atoms of the ZnOGLNSs were [NO...Zn] bond occurred when the N₂O adsorption with pointing N-end towards Zn atom of the ZnOGLNS to which the molecular axis of N₂O was nearly perpendicular to the molecular plane.

The energy gaps (ΔE_{GAP}) of the N₂O adsorptions with pointing N-end towards atoms of the ZnOGLNSs (AL-ZnONC, NLL-ZnONC, PRL-ZnONC, CNL-ZnONS and CCL-ZnONS) were also not much different from their corresponding bare surfaces as shown in Table 4.13.



ศูนย์วิทยทรัพยากร
จุฬาลงกรณ์มหาวิทยาลัย

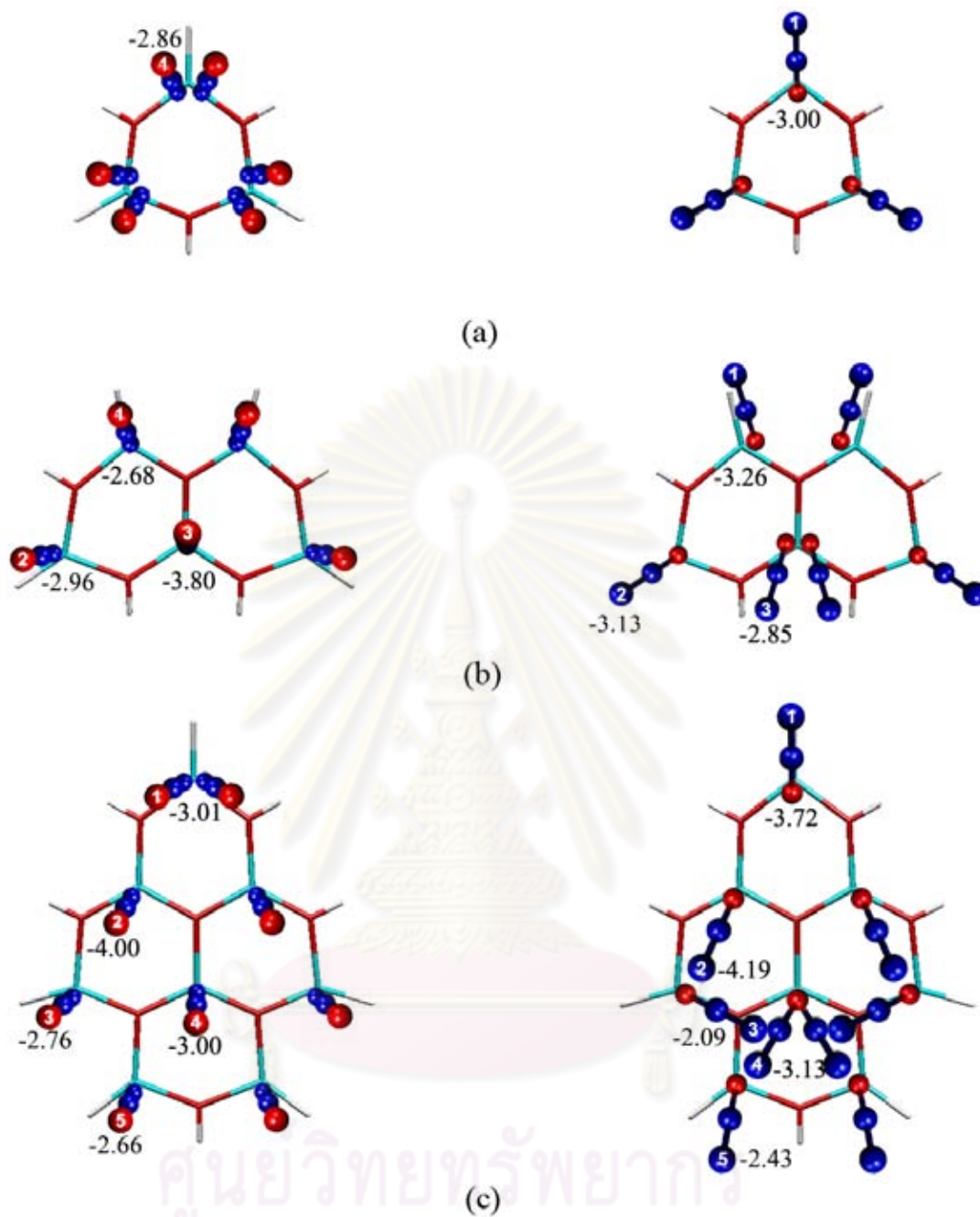


Figure 4.20 Plots of N_2O molecules as minimum energy structures of their adsorptions on (a) the AL-ZnONC ($\text{Zn}_3\text{O}_3\text{H}_6$), (b) NLL-ZnONC ($\text{Zn}_5\text{O}_5\text{H}_8$) and (c) PRL-ZnONC ($\text{Zn}_8\text{O}_8\text{H}_{10}$). Their left and right adsorption maps were N_2O adsorption on ZnONCs by pointing N-end and O-end toward the adsorption sites, respectively. The set of labeled molecules was representative of N_2O interacting with AL-ZnONC (C_{3h}), NLL-ZnONC (C_{2v}) and PRL-ZnONC (C_{2v}). Adsorption energies were presented in kcal/mol.

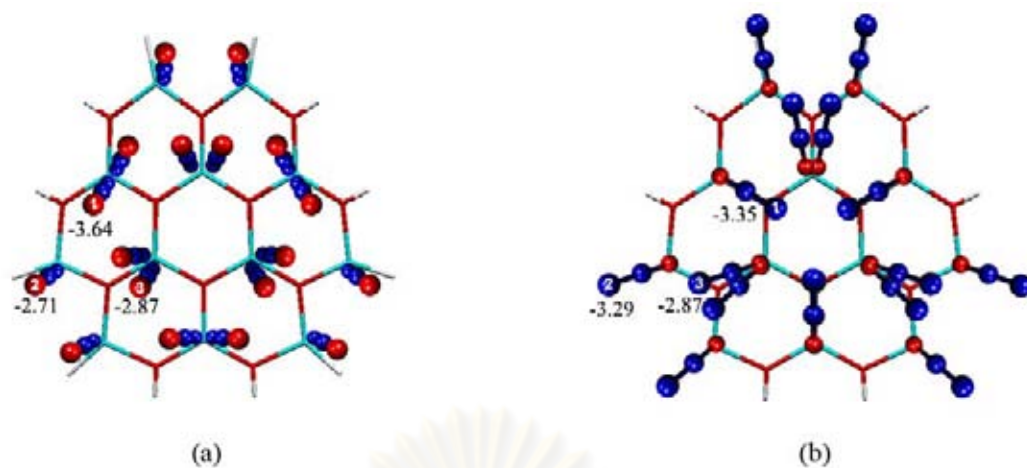


Figure 4.21 Plots of N_2O molecules as minimum energy structures of their adsorptions on CNL-ZnONS ($\text{Zn}_{12}\text{O}_{12}\text{H}_{12}$) as adsorption configurations of N_2O with pointing its (a) N-end and (b) O-end toward the adsorption sites of the CNL-ZnONS. The set of labeled molecules was representative of N_2O adsorption interacting with CNL-ZnONS with C_{3h} symmetry. Adsorption energies were presented in kcal/mol.

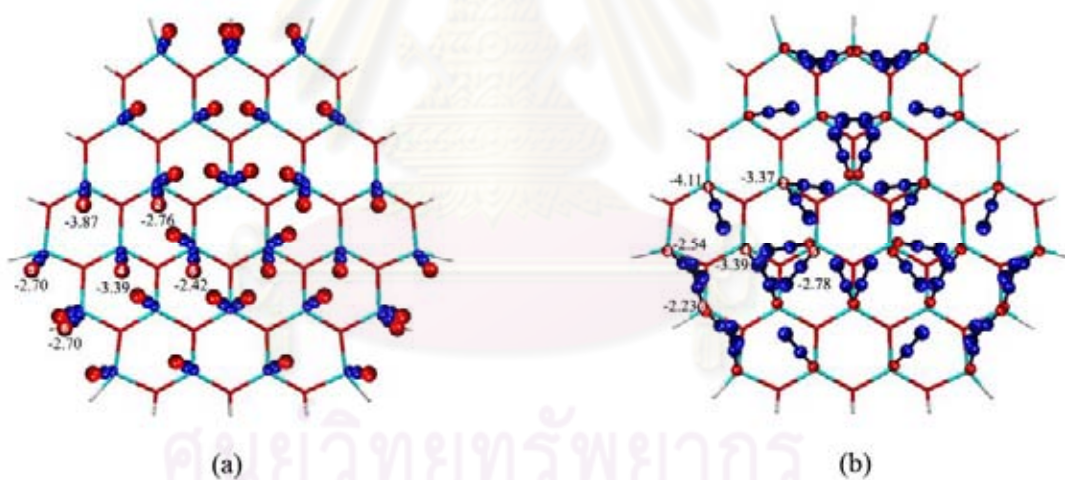


Figure 4.22 Plots of N_2O molecules as minimum energy structures of their adsorptions on CCL-ZnONS ($\text{Zn}_{27}\text{O}_{27}\text{H}_{18}$) as (a) adsorption configurations of N_2O by pointing (a) N-end and (b) O-end toward the adsorption sites. The molecules labeled with numbers represent the N_2O molecule interacting with CCL-ZnONS of molecular symmetry of (C_{3h}). Adsorption energies were presented in kcal/mol.

Table 4.13 Adsorption energies (ΔE_{ads} in kcal/mol) of N_2O pointing its N-end toward surfaces of ZnONCs and ZnOGLNSs and energy gaps (ΔE_{GAP} in eV) of bare surfaces of ZnONCs, ZnOGLNSs and their N_2O adsorption complexes, computed at the B3LYP/LanL2DZ level of theory.

ZnOGLNSs/nitrous oxide adsorption	ΔE_{ads} (kcal/mol)	E_{GAP} (eV)
AL-ZnONC:		6.47
$\text{N}_2\text{O} + \text{AL-ZnONC} \rightarrow \text{N}_2\text{O/AL-ZnONC}$ (1)	-2.86	5.02
NLL-ZnONC:		5.32
$\text{N}_2\text{O} + \text{NLL-ZnONC} \rightarrow \text{N}_2\text{O/NLL-ZnONC}$ (1)	-2.68	4.93
$\text{N}_2\text{O} + \text{NLL-ZnONC} \rightarrow \text{N}_2\text{O/NLL-ZnONC}$ (2)	-2.96	4.71
$\text{N}_2\text{O} + \text{NLL-ZnONC} \rightarrow \text{N}_2\text{O/NLL-ZnONC}$ (3)	-3.80	4.51
PRL-ZnONC:		4.26
$\text{N}_2\text{O} + \text{PRL-ZnONC} \rightarrow \text{N}_2\text{O/PRL-ZnONC}$ (1)	-3.01	3.80
$\text{N}_2\text{O} + \text{PRL-ZnONC} \rightarrow \text{N}_2\text{O/PRL-ZnONC}$ (2)	-4.00	3.86
$\text{N}_2\text{O} + \text{PRL-ZnONC} \rightarrow \text{N}_2\text{O/PRL-ZnONC}$ (3)	-2.76	4.29
$\text{N}_2\text{O} + \text{PRL-ZnONC} \rightarrow \text{N}_2\text{O/PRL-ZnONC}$ (4)	-3.00	4.27
$\text{N}_2\text{O} + \text{PRL-ZnONC} \rightarrow \text{N}_2\text{O/PRL-ZnONC}$ (5)	-2.66	4.22
CNL-ZnONS:		4.83
$\text{N}_2\text{O} + \text{CNL-ZnONS} \rightarrow \text{N}_2\text{O/CNL-ZnONS}$ (1)	-3.64	4.52
$\text{N}_2\text{O} + \text{CNL-ZnONS} \rightarrow \text{N}_2\text{O/CNL-ZnONS}$ (2)	-2.71	4.81
$\text{N}_2\text{O} + \text{CNL-ZnONS} \rightarrow \text{N}_2\text{O/CNL-ZnONS}$ (3)	-2.87	4.62
CCL-ZnONS:		3.74
$\text{N}_2\text{O} + \text{CCL-ZnONS} \rightarrow \text{N}_2\text{O/CCL-ZnONS}$ (1)	-3.87	3.72
$\text{N}_2\text{O} + \text{CCL-ZnONS} \rightarrow \text{N}_2\text{O/CCL-ZnONS}$ (2)	-2.76	3.76
$\text{N}_2\text{O} + \text{CCL-ZnONS} \rightarrow \text{N}_2\text{O/CCL-ZnONS}$ (3)	-2.70	3.76
$\text{N}_2\text{O} + \text{CCL-ZnONS} \rightarrow \text{N}_2\text{O/CCL-ZnONS}$ (4)	-2.95	3.76
$\text{N}_2\text{O} + \text{CCL-ZnONS} \rightarrow \text{N}_2\text{O/CCL-ZnONS}$ (5)	-2.42	3.77
$\text{N}_2\text{O} + \text{CCL-ZnONS} \rightarrow \text{N}_2\text{O/CCL-ZnONS}$ (6)	-2.70	3.73

Table 4.14 Bond distances (in Å) between N₂O atoms and atoms of adsorption sites.

ZnOGLNSs	[<u>N</u> ₂ O...S] ^a		[N ₂ <u>O</u> ...S] ^a	
AL-ZnONC:	<u>N</u> ₂ O...Zn1	2.70	N ₂ <u>O</u> ...Zn1	2.69
NLL-ZnONC:	<u>N</u> ₂ O...Zn1	2.74	N ₂ <u>O</u> ...Zn1	2.79
	<u>N</u> ₂ O...Zn2	2.71	N ₂ <u>O</u> ...Zn2	2.69
	<u>N</u> ₂ O...Zn3	2.61	N ₂ <u>O</u> ...Zn3	2.61
PRL-ZnONC:	<u>N</u> ₂ O...Zn1	2.62	N ₂ <u>O</u> ...Zn1	2.64
	<u>N</u> ₂ O...Zn2	2.64	N ₂ <u>O</u> ...Zn2	2.58
	<u>N</u> ₂ O...Zn3	2.77	N ₂ <u>O</u> ...Zn3	2.83
	<u>N</u> ₂ O...Zn4	2.69	N ₂ <u>O</u> ...Zn4	2.70
	<u>N</u> ₂ O...Zn5	2.77	N ₂ <u>O</u> ...Zn5	2.85
CNL-ZnONS:	<u>N</u> ₂ O...Zn1	2.65	N ₂ <u>O</u> ...Zn1	2.65
	<u>N</u> ₂ O...Zn2	2.77	N ₂ <u>O</u> ...Zn2	2.76
	<u>N</u> ₂ O...Zn3	2.72	N ₂ <u>O</u> ...Zn3	2.70
CCL-ZnONS:	<u>N</u> ₂ O...Zn1	2.63	N ₂ <u>O</u> ...Zn1	2.59
	<u>N</u> ₂ O...Zn2	2.76	N ₂ <u>O</u> ...Zn2	2.72
	<u>N</u> ₂ O...Zn3	2.80	N ₂ <u>O</u> ...Zn3	2.89
	<u>N</u> ₂ O...Zn4	2.72	N ₂ <u>O</u> ...Zn4	2.79
	<u>N</u> ₂ O...Zn5	2.78	N ₂ <u>O</u> ...Zn5	2.82
	<u>N</u> ₂ O...Zn6	2.86	N ₂ <u>O</u> ...Zn6	2.99

^a Atom S stands for atomic adsorption site, N₂O and N₂O were carbon dioxide molecules pointing their N and O atoms toward atom S in the nanoclusters or nanosheets, respectively. Atomic positions of S atom were shown in Figure 4.1.

4.2.7.2 Adsorption energies of N₂O pointing with O-end

The N₂O adsorption configurations of N₂O pointing with O-end to adsorption sites of nanoclusters were shown in right side of Figure 4.20 and to adsorption sites of the CNL-ZnONS and CCL-ZnONS nanosheets were shown in Figures 4.21(b) and 4.22(b), respectively.

The number of energy minima of N₂O adsorptions on the AL-ZnONC of three configurations was found for each side of its molecular planes. These energy minima were obtained from the structure optimizations of interaction configurations within one third of each side of the AL-ZnONC molecular area and N₂O adsorptions over the whole AL-ZnONC molecular area were generated using C_{3h} symmetrical operation. The N₂O adsorption on the AL-ZnONC was represented by the configuration of N₂O #1 of which the adsorption energy was -3.00 kcal/mol (Table

4.15), shows the O atom of N₂O pointing to a surface Zn atom (N₂O···Zn1) at a distance of 2.69 Å, show in Table 4.14.

As the NLL–ZnONC and PRL–ZnONC nanoclusters were in C_{2v} symmetry, the numbers of N₂O adsorptions on each side of their molecular planes were six and nine configurations, as shown in the right sides of Figure 4.20(b) and (c), respectively. There were three types of adsorption positions on the NLL–ZnONC which were composed of adsorption position N₂O #1 (–3.26 kcal/mol), #2 (–3.13 kcal/mol) and #3 (–2.85 kcal/mol). The most stable configuration of N₂O adsorption on the NLL–ZnONC was represented by the configuration of N₂O #1 which O atom of N₂O pointing to a surface Zn atom (N₂O···Zn1) at a distance of 2.79 Å. There were five types of adsorption positions on the PRL–ZnONC which were composed of adsorption positions N₂O #1 (–3.72 kcal/mol), #2 (–4.19 kcal/mol), #3 (–2.09 kcal/mol), #4 (–3.13 kcal/mol) and #5 (–2.43 kcal/mol). The most stable configuration of N₂O adsorption on the PRL–ZnONC was represented by the configuration of N₂O #2 which O atom of N₂O pointing to a surface Zn atom (N₂O···Zn2) at a distance of 2.58 Å.

The CNL–ZnONS and CCL–ZnONS were in C_{3h} symmetry, the numbers of N₂O adsorptions on each side of their molecular planes were fifteen and thirty six configurations as shown in Figures 4.21(b) and 4.22(b) respectively. There were three types of adsorption positions on the CNL–ZnONS which were composed of adsorption position N₂O #1 (–3.35 kcal/mol), #2 (–3.29 kcal/mol) and #3 (–2.87 kcal/mol). The most stable configuration of N₂O adsorption on the CNL–ZnONS was represented by the configuration of N₂O #1 which O atom of N₂O pointing to a surface Zn atom (N₂O···Zn1) at a distance of 2.76 Å. There were six types of adsorption positions on the CCL–ZnONS which were composed of adsorption positions N₂O #1 (–4.11 kcal/mol), #2 (–3.37 kcal/mol), #3 (–2.54 kcal/mol), #4 (–3.39 kcal/mol), #5 (–2.78 kcal/mol) and #6 (–2.23 kcal/mol). The most stable configuration of N₂O adsorption on the CCL–ZnONS was represented by the configuration of N₂O #1 which O atom of N₂O pointing to a surface Zn atom (N₂O···Zn1) at a distance of 2.59 Å.

The N₂O adsorptions with pointing the O–end toward atoms of the ZnOGLNSs were [N₂O···Zn] bond occurred when the N₂O adsorption with pointing O–end towards Zn atom of the ZnOGLNS to which the molecular axis of N₂O was nearly perpendicular to the molecular plane.

Table 4.15 Adsorption energies (ΔE_{ads} in kcal/mol) of N_2O pointing its O-end toward surfaces of ZnONCs and ZnOGLNSs and energy gaps (ΔE_{GAP} in eV) of bare surfaces of ZnONCs, ZnOGLNSs and their N_2O adsorption complexes, computed at the B3LYP/LanL2DZ level of theory.

ZnOGLNSs/nitrous oxide adsorption	ΔE_{ads} (kcal/mol)	E_{GAP} (eV)
AL-ZnONC::		6.47
$\text{N}_2\text{O} + \text{AL-ZnONC} \rightarrow \text{N}_2\text{O/AL-ZnONC}$ (1)	-3.00	5.17
NLL-ZnONC::		5.32
$\text{N}_2\text{O} + \text{NLL-ZnONC} \rightarrow \text{N}_2\text{O/NLL-ZnONC}$ (1)	-3.26	5.21
$\text{N}_2\text{O} + \text{NLL-ZnONC} \rightarrow \text{N}_2\text{O/NLL-ZnONC}$ (2)	-3.13	4.77
$\text{N}_2\text{O} + \text{NLL-ZnONC} \rightarrow \text{N}_2\text{O/NLL-ZnONC}$ (3)	-2.85	4.38
PRL-ZnONC:		4.26
$\text{N}_2\text{O} + \text{PRL-ZnONC} \rightarrow \text{N}_2\text{O/PRL-ZnONC}$ (1)	-3.72	3.90
$\text{N}_2\text{O} + \text{PRL-ZnONC} \rightarrow \text{N}_2\text{O/PRL-ZnONC}$ (2)	-4.19	3.89
$\text{N}_2\text{O} + \text{PRL-ZnONC} \rightarrow \text{N}_2\text{O/PRL-ZnONC}$ (3)	-2.09	4.26
$\text{N}_2\text{O} + \text{PRL-ZnONC} \rightarrow \text{N}_2\text{O/PRL-ZnONC}$ (4)	-3.13	4.29
$\text{N}_2\text{O} + \text{PRL-ZnONC} \rightarrow \text{N}_2\text{O/PRL-ZnONC}$ (5)	-2.43	4.24
CNL-ZnONS:		4.83
$\text{N}_2\text{O} + \text{CNL-ZnONS} \rightarrow \text{N}_2\text{O/CNL-ZnONS}$ (1)	-3.35	4.42
$\text{N}_2\text{O} + \text{CNL-ZnONS} \rightarrow \text{N}_2\text{O/CNL-ZnONS}$ (2)	-3.29	4.86
$\text{N}_2\text{O} + \text{CNL-ZnONS} \rightarrow \text{N}_2\text{O/CNL-ZnONS}$ (3)	-2.87	4.60
CCL-ZnONS:		3.74
$\text{N}_2\text{O} + \text{CCL-ZnONS} \rightarrow \text{N}_2\text{O/CCL-ZnONS}$ (1)	-4.11	3.65
$\text{N}_2\text{O} + \text{CCL-ZnONS} \rightarrow \text{N}_2\text{O/CCL-ZnONS}$ (2)	-3.37	3.68
$\text{N}_2\text{O} + \text{CCL-ZnONS} \rightarrow \text{N}_2\text{O/CCL-ZnONS}$ (3)	-2.54	3.75
$\text{N}_2\text{O} + \text{CCL-ZnONS} \rightarrow \text{N}_2\text{O/CCL-ZnONS}$ (4)	-3.39	3.71
$\text{N}_2\text{O} + \text{CCL-ZnONS} \rightarrow \text{N}_2\text{O/CCL-ZnONS}$ (5)	-2.78	3.73
$\text{N}_2\text{O} + \text{CCL-ZnONS} \rightarrow \text{N}_2\text{O/CCL-ZnONS}$ (6)	-2.23	3.72

The energy gaps (ΔE_{GAP}) of the N_2O adsorptions with pointing O-end towards atoms of the ZnOGLNSs (AL-ZnONC, NLL-ZnONC, PRL-ZnONC, CNL-ZnONS and CCL-ZnONS) were also not much different from their corresponding bare surfaces as shown in Table 4.15.

4.2.8 Adsorption of nitrogen dioxide molecule

4.2.8.1 Adsorption energies of NO_2 pointing with N-end

The B3LYP/LanL2DZ-optimized structures of NO_2 adsorptions on the rigid structures of the AL-ZnONC, NLL-ZnONC, and PRL-ZnONC nanoclusters, shown in Figure 4.23 and the CNL-ZnONS, shown in Figure 4.24 and CCL-ZnONS nanosheets, shown in Figure 4.26. The adsorption energy values of the minimum energy structures of NO_2 on nanoclusters and nanosheets were shown in Table 4.16.

The NO₂ adsorption configurations of NO₂ pointing with N-end to adsorption on the nanoclusters were shown in left side of Figure 4.23 and to adsorption sites of the CNL-ZnONS and CCL-ZnONS nanosheets were shown in Figures 4.24(a) and 4.25(a), respectively.

The number of energy minima of NO₂ adsorptions on the AL-ZnONC of six configurations was found for each side of its molecular planes. These energy minima were obtained from the structure optimizations of interaction configurations within one third of each side of the AL-ZnONC molecular area and NO₂ adsorptions over the whole AL-ZnONC molecular area were generated using C_{3h} symmetrical operation. The most stable configuration of NO₂ adsorption on the AL-ZnONC was represented by the configuration of NO₂ #2 of which the adsorption energy was -2.31 kcal/mol, shows the N atom of NO₂ pointing to a surface Zn atom (NO₂...Zn2) at a distance of 2.75 Å, show in Table 4.17.

The NLL-ZnONC and PRL-ZnONC nanoclusters were in C_{2v} symmetry, the numbers of NO₂ adsorptions on each side of their molecular planes were three and sixteen configurations, as shown in the left sides of Figure 4.23(b) and (c), respectively. There were two types of adsorption positions on the NLL-ZnONC which were composed of adsorption position NO₂ #1 (-1.90 kcal/mol) and #2 (-2.31 kcal/mol). The most stable configuration of NO₂ adsorption on the NLL-ZnONC was represented by the configuration of NO₂ #2 which N atom of NO₂ pointing to a surface Zn atom (NO₂...Zn3) at a distance of 3.06 Å. There were nine types of adsorption positions on the PRL-ZnONC which were composed of adsorption positions NO₂ #1 (-2.30 kcal/mol), #2 (-1.88 kcal/mol), #3 (-2.43 kcal/mol), #4 (-2.90 kcal/mol), #5 (-3.72 kcal/mol), #6 (-3.14 kcal/mol), #7 (-3.93 kcal/mol), #8 (-3.82 kcal/mol) and #9 (-1.27 kcal/mol), The most stable configuration of NO₂ adsorption on the PRL-ZnONC was represented by the configuration of NO₂ #7 which N atom of NO₂ pointing to a surface Zn atom (NO₂...Zn4) at a distance of 2.73 Å.

The CNL-ZnONS and CCL-ZnONS were in C_{3h} symmetry, the numbers of NO₂ adsorptions on each side of their molecular planes were thirty and fifty four configurations as shown in Figure 4.23(a) and Figure 4.24(a) respectively. There were five types of adsorption positions on the CNL-ZnONS which were composed of adsorption position NO₂ #1 (-2.42 kcal/mol), #2 (-3.23 kcal/mol), #3 (-2.89 kcal/mol), #4 (-2.12 kcal/mol) and #5 (-3.95 kcal/mol), The most stable configuration

of NO₂ adsorption on the CNL–ZnONS was represented by the configuration of NO₂ #5 which N atom of N₂O pointing to a surface Zn atom (NO₂···Zn3) at a distance of 2.72 Å. There were ten types of adsorption positions on the CCL–ZnONS which were composed of adsorption positions NO₂ #1 (–2.04 kcal/mol), #2 (–2.77 kcal/mol), #3 (–4.46 kcal/mol), #4 (–3.85 kcal/mol) #5 (–3.91 kcal/mol), #6 (–2.42 kcal/mol), #7 (–3.77 kcal/mol), #8 (–5.08 kcal/mol), #9 (–3.42 kcal/mol) and #10 (–5.54 kcal/mol). The most stable configuration of NO₂ adsorption on the CCL–ZnONC was represented by the configuration of NO₂ #10 which N atom of NO₂ pointing to a surface Zn atom (NO₂···Zn7) at a distance of 2.51 Å.

There were two bond types, types [NO₂···O] and [NO₂···Zn] of all the adsorption energies of NO₂ on the AL–ZnONC, NLL–ZnONC, PRL–ZnONC, CNL–ZnONS and CCL–ZnONS. It shows that bond distances of the bond type [NO₂···O] and [NO₂···Zn], as listed in Table 4.17.

The energy gaps (ΔE_{GAP}) of the NO₂ adsorptions with pointing N–end towards atoms of the ZnOGLNSs (AL–ZnONC, NLL–ZnONC, PRL–ZnONC, CNL–ZnONS and CCL–ZnONS) were also not much different from their corresponding bare surfaces as shown in Table 4.16.

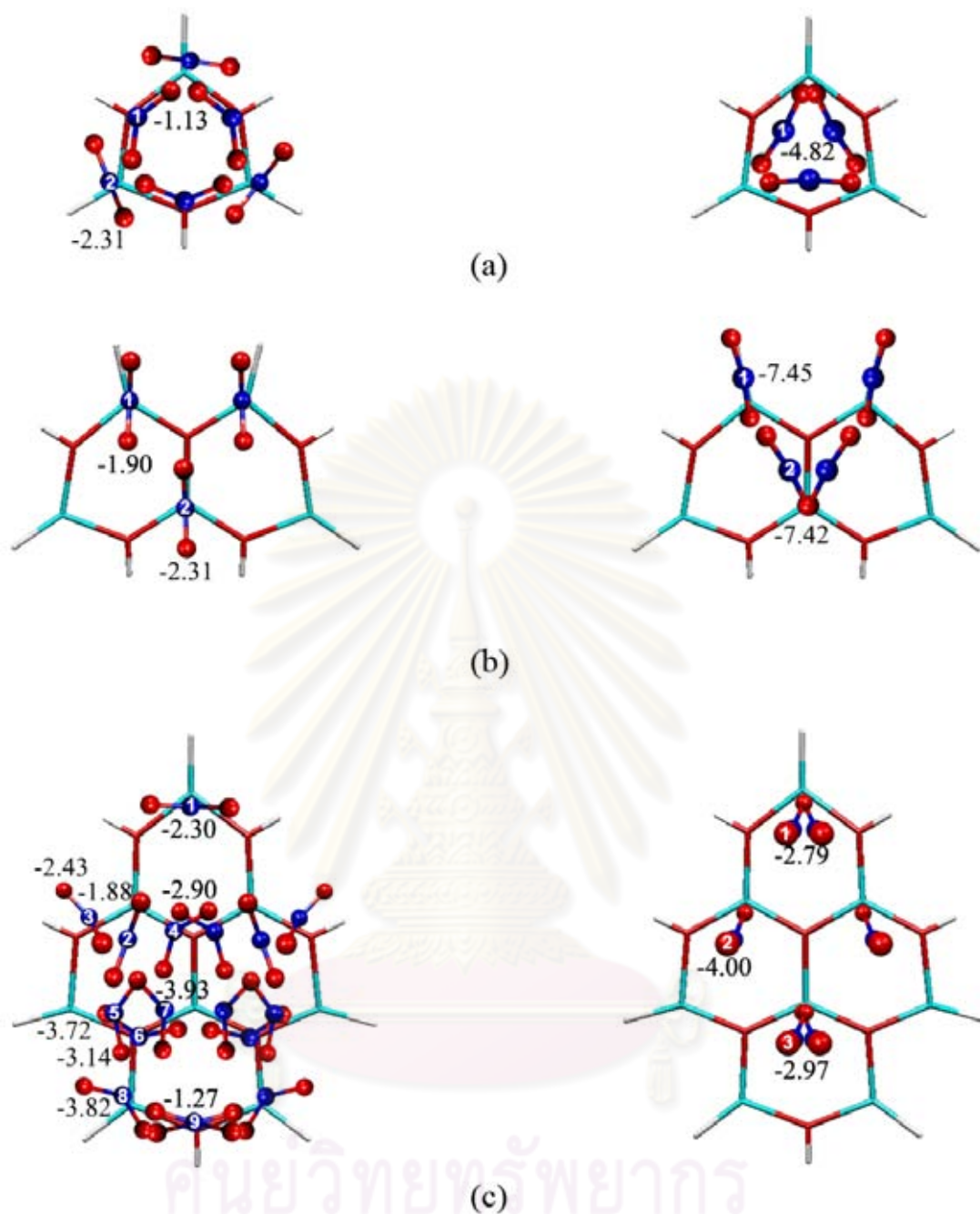


Figure 4.23 Plots of NO_2 molecules as minimum energy structures of their adsorptions on (a) the AL-ZnONC ($\text{Zn}_3\text{O}_3\text{H}_6$), (b) NLL-ZnONC ($\text{Zn}_5\text{O}_5\text{H}_8$) and (c) PRL-ZnONC ($\text{Zn}_8\text{O}_8\text{H}_{10}$). Their left and right adsorption maps were NO_2 adsorption on ZnONCs by pointing N-end and O-end toward the adsorption sites, respectively. The set of labeled molecules was representative of NO_2 interacting with AL-ZnONC (C_{3h}), NLL-ZnONC (C_{2v}) and PRL-ZnONC (C_{2v}). Adsorption energies were presented in kcal/mol.

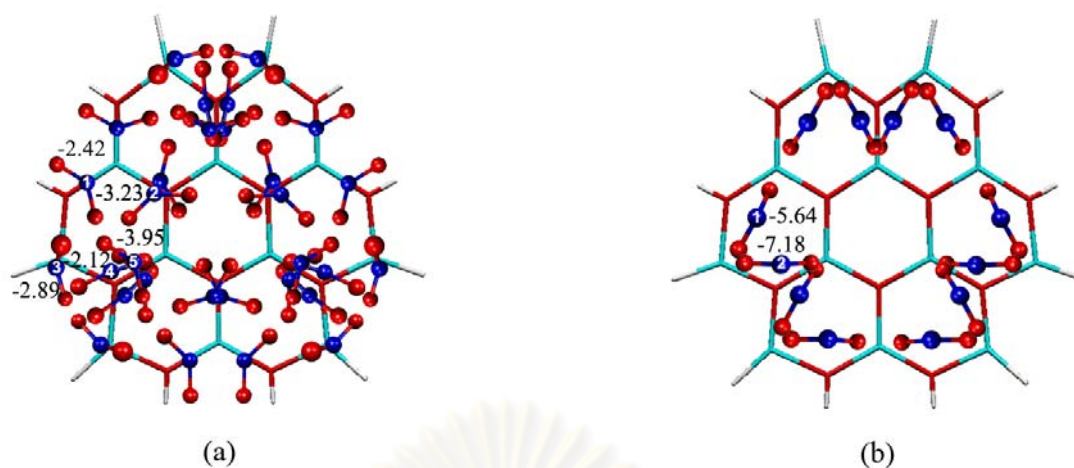


Figure 4.24 Plots of NO_2 molecules as minimum energy structures of their adsorptions on CNL-ZnONS ($\text{Zn}_{12}\text{O}_{12}\text{H}_{12}$) as adsorption configurations of NO_2 with pointing its (a) N-end and (b) O-end toward the adsorption sites of the CNL-ZnONS. The set of labeled molecules was representative of NO_2 adsorption interacting with CNL-ZnONS with C_{3h} symmetry. Adsorption energies were presented in kcal/mol.

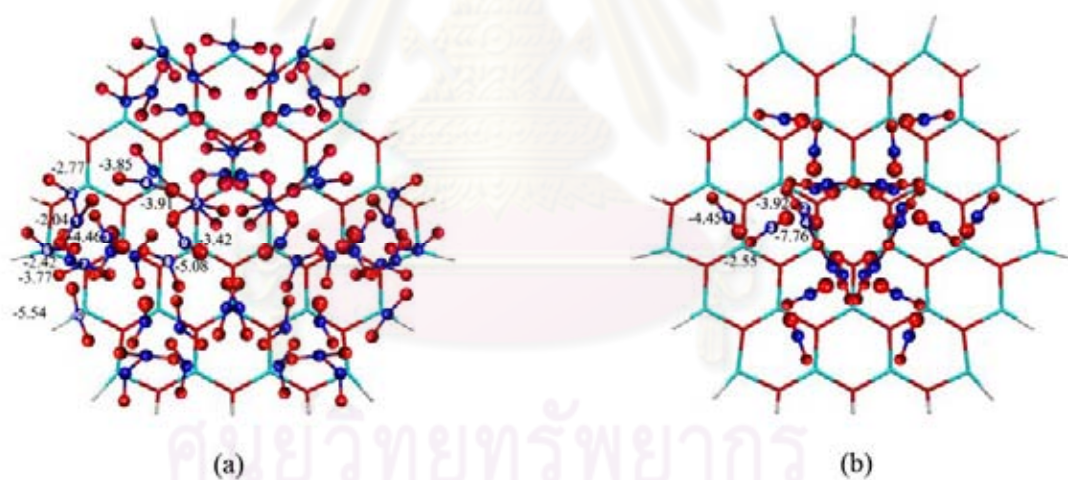


Figure 4.25 Plots of NO_2 molecules as minimum energy structures of their adsorptions on CCL-ZnONS ($\text{Zn}_{27}\text{O}_{27}\text{H}_{18}$) as (a) adsorption configurations of NO_2 by pointing (a) N-end and (b) O-end toward the adsorption sites. The molecules labeled with numbers represent the NO_2 molecule interacting with CCL-ZnONS of molecular symmetry of (C_{3h}). Adsorption energies were presented in kcal/mol.

Table 4.16 Adsorption energies (ΔE_{ads} in kcal/mol) of NO_2 pointing its N-end toward surfaces of ZnONCs and ZnOGLNSs and energy gaps (ΔE_{GAP} in eV) of bare surfaces of ZnONCs, ZnOGLNSs and their NO_2 adsorption complexes, computed at the B3LYP/LanL2DZ level of theory.

ZnOGLNSs/nitrogen dioxide adsorption	ΔE_{ads} (kcal/mol)	E_{GAP} (eV)
AL-ZnONC:		6.47
$\text{NO}_2 + \text{AL-ZnONC} \rightarrow \text{NO}_2/\text{AL-ZnONC}$ (1)	-1.13	3.27
$\text{NO}_2 + \text{AL-ZnONC} \rightarrow \text{NO}_2/\text{AL-ZnONC}$ (2)	-2.31	3.71
NLL-ZnONC:		5.32
$\text{NO}_2 + \text{NLL-ZnONC} \rightarrow \text{NO}_2/\text{NLL-ZnONC}$ (1)	-1.90	3.51
$\text{NO}_2 + \text{NLL-ZnONC} \rightarrow \text{NO}_2/\text{NLL-ZnONC}$ (2)	-1.48	2.92
PRL-ZnONC:		4.26
$\text{NO}_2 + \text{PRL-ZnONC} \rightarrow \text{NO}_2/\text{PRL-ZnONC}$ (1)	-2.30	2.25
$\text{NO}_2 + \text{PRL-ZnONC} \rightarrow \text{NO}_2/\text{PRL-ZnONC}$ (2)	-1.88	2.18
$\text{NO}_2 + \text{PRL-ZnONC} \rightarrow \text{NO}_2/\text{PRL-ZnONC}$ (3)	-2.43	2.16
$\text{NO}_2 + \text{PRL-ZnONC} \rightarrow \text{NO}_2/\text{PRL-ZnONC}$ (4)	-2.90	2.19
$\text{NO}_2 + \text{PRL-ZnONC} \rightarrow \text{NO}_2/\text{PRL-ZnONC}$ (5)	-3.72	2.89
$\text{NO}_2 + \text{PRL-ZnONC} \rightarrow \text{NO}_2/\text{PRL-ZnONC}$ (6)	-3.14	2.83
$\text{NO}_2 + \text{PRL-ZnONC} \rightarrow \text{NO}_2/\text{PRL-ZnONC}$ (7)	-3.93	2.86
$\text{NO}_2 + \text{PRL-ZnONC} \rightarrow \text{NO}_2/\text{PRL-ZnONC}$ (8)	-3.82	3.62
$\text{NO}_2 + \text{PRL-ZnONC} \rightarrow \text{NO}_2/\text{PRL-ZnONC}$ (9)	-1.27	2.80
CNL-ZnONS:		4.83
$\text{NO}_2 + \text{CNL-ZnONS} \rightarrow \text{NO}_2/\text{CNL-ZnONS}$ (1)	-2.42	2.78
$\text{NO}_2 + \text{CNL-ZnONS} \rightarrow \text{NO}_2/\text{CNL-ZnONS}$ (2)	-3.23	2.91
$\text{NO}_2 + \text{CNL-ZnONS} \rightarrow \text{NO}_2/\text{CNL-ZnONS}$ (3)	-2.89	3.26
$\text{NO}_2 + \text{CNL-ZnONS} \rightarrow \text{NO}_2/\text{CNL-ZnONS}$ (4)	-2.12	2.98
$\text{NO}_2 + \text{CNL-ZnONS} \rightarrow \text{NO}_2/\text{CNL-ZnONS}$ (5)	-3.95	3.10
CCL-ZnONS:		3.74
$\text{NO}_2 + \text{CCL-ZnONS} \rightarrow \text{NO}_2/\text{CCL-ZnONS}$ (1)	-2.04	2.15
$\text{NO}_2 + \text{CCL-ZnONS} \rightarrow \text{NO}_2/\text{CCL-ZnONS}$ (2)	-2.77	2.02
$\text{NO}_2 + \text{CCL-ZnONS} \rightarrow \text{NO}_2/\text{CCL-ZnONS}$ (3)	-4.46	2.16
$\text{NO}_2 + \text{CCL-ZnONS} \rightarrow \text{NO}_2/\text{CCL-ZnONS}$ (4)	-3.85	2.02
$\text{NO}_2 + \text{CCL-ZnONS} \rightarrow \text{NO}_2/\text{CCL-ZnONS}$ (5)	-3.91	2.28
$\text{NO}_2 + \text{CCL-ZnONS} \rightarrow \text{NO}_2/\text{CCL-ZnONS}$ (6)	-2.42	2.48
$\text{NO}_2 + \text{CCL-ZnONS} \rightarrow \text{NO}_2/\text{CCL-ZnONS}$ (7)	-3.77	2.70
$\text{NO}_2 + \text{CCL-ZnONS} \rightarrow \text{NO}_2/\text{CCL-ZnONS}$ (8)	-5.08	2.48
$\text{NO}_2 + \text{CCL-ZnONS} \rightarrow \text{NO}_2/\text{CCL-ZnONS}$ (9)	-3.42	2.13
$\text{NO}_2 + \text{CCL-ZnONS} \rightarrow \text{NO}_2/\text{CCL-ZnONS}$ (10)	-5.54	3.51

Table 4.17 Bond distances (in Å) between NO₂ atoms and atoms of adsorption sites.

ZnOGLNSs	[NO...S] ^a		[NO ₂ ...S] ^a	
AL-ZnONC:	<u>NO</u> ₂ ...O1	3.19	<u>NO</u> ₂ ...Zn1	2.67
	<u>NO</u> ₂ ...Zn1	2.75	—	—
NLL-ZnONC:	<u>NO</u> ₂ ...Zn1	2.85	<u>NO</u> ₂ ...Zn1	2.32
	<u>NO</u> ₂ ...Zn3	3.06	<u>NO</u> ₂ ...Zn3	2.45
PRL-ZnONC:	<u>NO</u> ₂ ...Zn1	2.73	<u>NO</u> ₂ ...Zn1	2.71
	<u>NO</u> ₂ ...Zn2	3.05	<u>NO</u> ₂ ...Zn2	2.62
	<u>NO</u> ₂ ...O2	2.99	<u>NO</u> ₂ ...Zn4	2.72
	<u>NO</u> ₂ ...O3	2.84	—	—
	<u>NO</u> ₂ ...O4(I)	2.77	—	—
	<u>NO</u> ₂ ...O4(II)	2.70	—	—
	<u>NO</u> ₂ ...Zn4	2.73	—	—
	<u>NO</u> ₂ ...Zn5	2.61	—	—
CNL-ZnONS:	<u>NO</u> ₂ ...O5	3.31	—	—
	<u>NO</u> ₂ ...Zn1	2.89	<u>NO</u> ₂ ...Zn1	2.63
	<u>NO</u> ₂ ...O2	2.78	<u>NO</u> ₂ ...Zn3	2.52
	<u>NO</u> ₂ ...Zn2	2.73	—	—
	<u>NO</u> ₂ ...O3	3.16	—	—
CCL-ZnONS:	<u>NO</u> ₂ ...Zn3	2.72	—	—
	<u>NO</u> ₂ ...O1	3.27	<u>NO</u> ₂ ...Zn1	2.71
	<u>NO</u> ₂ ...Zn1	2.85	<u>NO</u> ₂ ...Zn2	2.83
	<u>NO</u> ₂ ...Zn4	2.96	<u>NO</u> ₂ ...O2	3.42
	<u>NO</u> ₂ ...Zn2	2.95	<u>NO</u> ₂ ...Zn5	2.55
	<u>NO</u> ₂ ...O3	2.78	—	—
	<u>NO</u> ₂ ...Zn3	2.97	—	—
	<u>NO</u> ₂ ...O4	2.69	—	—
	<u>NO</u> ₂ ...O5	2.63	—	—
	<u>NO</u> ₂ ...Zn6	3.04	—	—
<u>NO</u> ₂ ...Zn7	2.51	—	—	

^a Atom S stands for atomic adsorption site, NO₂ and NO₂ were carbon dioxide molecules pointing their N and O atoms toward atom S in the nanoclusters or nanosheets, respectively. Atomic positions of S atom were shown in Figure 4.1.

4.2.8.2 Adsorption energies of NO₂ pointing with O-end

The NO₂ adsorption configurations of NO₂ pointing with O-end to adsorption sites of nanoclusters were shown in right side of Figure 4.23 and to adsorption sites of the CNL-ZnONS and CCL-ZnONS nanosheets were shown in Figures 4.24(b) and 4.25(b), respectively.

The number of energy minima of NO₂ adsorptions on the AL-ZnONC of three configurations was found for each side of its molecular planes. These energy minima were obtained from the structure optimizations of interaction configurations within

one third of each side of the AL–ZnONC molecular area and NO₂ adsorptions over the whole AL–ZnONC molecular area were generated using C_{3h} symmetrical operation. The N₂O adsorption on the AL–ZnONC was represented by the configuration of NO₂ #1 of which the adsorption energy was –4.82 kcal/mol (Table 4.18), shows the O atom of NO₂ pointing to a surface Zn atom (NO₂···Zn1) at a distance of 2.67 Å, show in Table 4.17.

As the NLL–ZnONC and PRL–ZnONC nanoclusters were in C_{2v} symmetry, the numbers of NO₂ adsorptions on each side of their molecular planes were four and six configurations, as shown in the right sides of Figure 4.23(b) and (c), respectively. There were two types of adsorption positions on the NLL–ZnONC which were composed of adsorption position NO₂ #1 (–7.45 kcal/mol) and #2 (–7.42 kcal/mol). The most stable configuration of NO₂ adsorption on the NLL–ZnONC was represented by the configuration of NO₂ #1 which O atom of NO₂ pointing to a surface Zn atom (N₂O···Zn1) at a distance of 2.32 Å. There were three types of adsorption positions on the PRL–ZnONC which were composed of adsorption positions NO₂ #1 (–2.79 kcal/mol), #2 (–4.00 kcal/mol) and #3 (–2.97 kcal/mol). The most stable configuration of NO₂ adsorption on the PRL–ZnONC was represented by the configuration of NO₂ #2 which O atom of N₂O pointing to a surface Zn atom (N₂O···Zn2) at a distance of 2.62 Å.

The CNL–ZnONS and CCL–ZnONS were in C_{3h} symmetry, the numbers of NO₂ adsorptions on each side of their molecular planes were twelve and twenty four configurations as shown in Figures 4.24(b) and 4.25(b) respectively. There were two types of adsorption positions on the CNL–ZnONS which were composed of adsorption position NO₂ #1 (–5.64 kcal/mol) and #2 (–7.18 kcal/mol). The most stable configuration of NO₂ adsorption on the CNL–ZnONC was represented by the configuration of N₂O #2 which O atom of NO₂ pointing to a surface Zn atom (N₂O···Zn3) at a distance of 2.52 Å. There were four types of adsorption positions on the CCL–ZnONS which were composed of adsorption positions NO₂ #1 (–4.45 kcal/mol), #2 (–3.92 kcal/mol), #3 (–2.55 kcal/mol) and #4 (–7.76 kcal/mol). The most stable configuration of NO₂ adsorption on the CCL–ZnONC was represented by the configuration of NO₂ #4 which O atom of NO₂ pointing to a surface Zn atom (NO₂···Zn5) at a distance of 2.55 Å. The adsorption energies were of NO₂ on the AL–ZnONC, NLL–ZnONC, PRL–ZnONC, CNL–ZnONS and CCL–ZnONS as shown in

Figure 4.18. It shows that bond distances of the bond type $[\text{NO}_2\cdots\text{O}]$ and $[\text{NO}_2\cdots\text{Zn}]$, as listed in Table 4.17.

Table 4.18 Adsorption energies (ΔE_{ads} in kcal/mol) of NO_2 pointing its O-end toward surfaces of ZnONCs and ZnOGLNSs and energy gaps (ΔE_{GAP} in eV) of bare surfaces of ZnONCs, ZnOGLNSs and their NO_2 adsorption complexes, computed at the B3LYP/LanL2DZ level of theory.

ZnOGLNSs/nitrogen dioxide adsorption	ΔE_{ads} (kcal/mol)	E_{GAP} (eV)
AL-ZnONC:		
$\text{NO}_2 + \text{AL-ZnONC} \rightarrow \text{NO}_2/\text{AL-ZnONC}$ (1)	-4.82	6.47
NLL-ZnONC:		
$\text{NO}_2 + \text{NLL-ZnONC} \rightarrow \text{NO}_2/\text{NLL-ZnONC}$ (1)	-7.45	5.32
$\text{NO}_2 + \text{NLL-ZnONC} \rightarrow \text{NO}_2/\text{NLL-ZnONC}$ (2)	-7.42	4.02
PRL-ZnONC:		
$\text{NO}_2 + \text{PRL-ZnONC} \rightarrow \text{NO}_2/\text{PRL-ZnONC}$ (1)	-2.79	3.37
$\text{NO}_2 + \text{PRL-ZnONC} \rightarrow \text{NO}_2/\text{PRL-ZnONC}$ (2)	-4.00	4.26
$\text{NO}_2 + \text{PRL-ZnONC} \rightarrow \text{NO}_2/\text{PRL-ZnONC}$ (3)	-2.97	1.86
CNL-ZnONS:		
$\text{NO}_2 + \text{CNL-ZnONS} \rightarrow \text{NO}_2/\text{CNL-ZnONS}$ (1)	-5.64	1.90
$\text{NO}_2 + \text{CNL-ZnONS} \rightarrow \text{NO}_2/\text{CNL-ZnONS}$ (2)	-7.18	2.32
CCL-ZnONS:		
$\text{NO}_2 + \text{CCL-ZnONS} \rightarrow \text{NO}_2/\text{CCL-ZnONS}$ (1)	-4.45	4.83
$\text{NO}_2 + \text{CCL-ZnONS} \rightarrow \text{NO}_2/\text{CCL-ZnONS}$ (2)	-3.92	2.81
$\text{NO}_2 + \text{CCL-ZnONS} \rightarrow \text{NO}_2/\text{CCL-ZnONS}$ (3)	-2.55	3.20
$\text{NO}_2 + \text{CCL-ZnONS} \rightarrow \text{NO}_2/\text{CCL-ZnONS}$ (4)	-7.76	3.74
		2.10
		2.16
		2.04
		2.31

The energy gaps (ΔE_{GAP}) of the NO_2 adsorptions with pointing O-end towards atoms of the ZnOGLNSs (AL-ZnONC, NLL-ZnONC, PRL-ZnONC, CNL-ZnONS and CCL-ZnONS) were also not much different from their corresponding bare surfaces as shown in Table 4.18. The most stable configuration of all gases adsorbed on CCL-ZnONS are shown in Table A-1.

CHAPTER V

5.1 Conclusions

A theoretical study on the adsorption of gaseous oxygen, carbon monoxide, nitric oxide, nitrogen dioxide, nitrous oxide, ammonia, hydrogen and water molecules on the ZnO nanoclusters (ZnONCs) and ZnO nanosheets (ZnONSs) i.e. ZnO nanoclusters of aromatic-like (AL-ZnONC, $Zn_3O_3H_6$), naphthalene-like (NLL-ZnONC, $Zn_5O_5H_8$), pyrene-like PRL-like (PRL-ZnONC, $Zn_8O_8H_{10}$), and ZnO nanosheets of coronene-like (CNL-ZnONS, $Zn_{12}O_{12}H_{12}$) and circumcoronene-like (CCL-ZnONS, $Zn_{27}O_{27}H_{18}$) for all possible configurations was investigated at the B3LYP/LanL2DZ level of theory. All the results can be concluded as follows:

1. The O_2 is chemisorbed on the hydride adsorption site of the ZnOGLNSs edge and physisorbed over the plane of ZnOGLNSs.
2. The adsorption of various gases (CO, H_2 , H_2O , NH_3 , NO, NO_2 and N_2O) on ZnOGLNSs is physisorbed.
3. The energy gaps of ZnOGLNSs are largely reduced after the adsorptions of O_2 , NO or NO_2 on these ZnOGLNSs.
4. The ZnOGLNSs are sensitive material for O_2 , NO and NO_2 and could be developed as sensor based on electrical conductivity.

5.2 Suggestion for future work

Due to the knowledge of molecular gas adsorption on metal oxides lead to find efficient way for gas sensor and economic way to convert harmful gas into harmless gas. Thus, co-adsorption between molecular gases such as CO and N_2O conversion to N_2 and CO_2 on ZnO nanosheets could be studied. Moreover, the mechanism of the reactions for absorbed molecules taking place on the ZnO nanosheets unknown and is an interesting subject remain for further study.

REFERENCES

- [1] Wander, A., and Harrison, N.M. An *Ab Initio* study of hydrogen adsorption on ZnO(10 $\bar{1}$ 0). J. Phys. Chem. B 105 (2001): 6191–6193.
- [2] Andres, J.B.L., Longo, J.E., and Taft, I.C.A. H₂O and H₂ interaction with ZnO surfaces: A MNDO, AM1, and PM3 theoretical study with large cluster models. J. Quantum Chem. 57 (1996): 861–870.
- [3] Martins, J.B.L., Taft, C.A., and Andres, E.J. *Ab Initio* study of CO and H₂ interaction with ZnO surfaces using a small cluster model. J. Mol. Struct. Theochem 398 (1997): 457–466.
- [4] Martins, J.B.L., Taft, C.A., and Lie, S.K.E. Lateral interaction of CO and H₂ molecules on ZnO surfaces: An AM1 study. J. Mol. Struct. Theochem 528 (2000): 161–170.
- [5] Becker, T., et al. Interaction of hydrogen with metal oxides: The case of the polar ZnO(000 $\bar{1}$) surface. Surf. Sci. 486 (2001): 502–506.
- [6] Gay, R.R., Nodine, M.H., Henrich, V.E., Zeiger, H.J., and Solomon, E.I. Photoelectron study of the interaction of carbon monoxide with zinc oxide. J. Am. Chem. Soc. 102 (1980): 6752–6761.
- [7] Nakazawa, M., and Somorjai, G.A. Coadsorption of water and selected aromatic molecules to model the adhesion of epoxy resins on hydrated surfaces of zinc oxide and iron oxide. Appl. Surf. Sci. 84 (1995): 309–323.
- [8] Kumashiro, M.R., Matsuda, T., and Kuroda, Y. Calorimetric study of water two-dimensionally condensed on the homogeneous surface of a solid. Thermochim. Acta 253 (1995): 221–233.
- [9] Calzolari, A., and Catellani, A. Water adsorption on nonpolar ZnO($\bar{1}$ 0 $\bar{1}$ 0) surface: A microscopic understanding. J. Phys. Chem. C 113 (2009): 2896–2902.
- [10] Hotan, W., Gopel, W., and Haul, R. Advanced gas sensing: the electroadsorptive effect and related techniques. Surf. Sci. 83 (1979): 162–180.

- [11] Martins, J.B.L., Longo, E., Salmon, O.D.R., Espinoza, V.A.A., and Taft, C.A. The interaction of H₂, CO, CO₂, H₂O and NH₃ on ZnO surfaces: an oniom study. Chem. Phys. Lett. 400 (2004): 481–486.
- [12] Breedon, M., Spencer, M.J.S., and Yarovsky, I. Adsorption of NO and NO₂ on the ZnO(21̄1̄0) surface: A DFT study. Surf. Sci. 603 (2009): 3389–3399.
- [13] Prades, J.D., Cirera, A., and Morante, J.R. *Ab Initio* calculations of NO₂ and SO₂ chemisorption onto non-polar ZnO surfaces. Sens. Actuators B 142 (2009): 179–184.
- [14] Spencer, M.J.S., Wong, K.W.J., and Yarovsky, I. ZnO nanostructure-based sensors: Density functional theory modelling of the gas-sensor interaction. Mater. Chem. Phys. 119 (2010): 505–514.
- [15] Na, S.-H., and Park, C.-H. First-principles study of the surface of wurtzite ZnO and ZnS—implications for nanostructure formation. J. Korean Phys. Soc. 54 (2009): 867~872.
- [16] Tang, Q., Li, Y., Zhou, Z., Chen, Y., and Chen, Z. Tuning electronic and magnetic properties of wurtzite ZnO nanosheets by surface hydrogenation. ACS Appl. Mater. Inter. 8 (2010): 2442–2447.
- [17] Tu, Z.C., and Hu, X. Elasticity and piezoelectricity of zinc oxide crystals, single layers, and possible single-walled nanotubes. Phys. Rev. B 74 (2006): 035434–035440.
- [18] Yi, G.-C., Wang, C., and Park, W.I. ZnO nanorods: synthesis, characterization and applications. Semicond. Sci. Technol. 20 (2005): 22–34.
- [19] Wang, N., Cai, Y., and Zhang, R.Q. Growth of nanowires. Mater. Sci. Eng. R 60 (2008): 1–51.
- [20] Lieber, C.M., and Wang, Z.L. Functional nanowires. MRS Bull. 32 (2007): 99–104.
- [21] Jiang, Z.-Y., et al. Molten salt route toward the growth of ZnO nanowires in unusual growth directions. J. Phys. Chem. B 109 (2005): 23269–23273.
- [22] Lao, C.S., et al. Formation of double-side teathed nanocombs of ZnO and self-catalysis of Zn-terminated polar surface. Chem. Phys. Lett. 417 (2006): 358–362.

- [23] Peng, Y., and Bao, L. Controlled-synthesis of ZnO nanorings. Front. Chem. China 4 (2008): 458–463.
- [24] She, G.W., Zhang, X.H.W., Shi, S., Fan, X., and Chang J.C. Electrochemical/chemical synthesis of highly-oriented single-crystal ZnO nanotube arrays on transparent conductive substrates. J. C. Electrochem. Commun. 9 (2007): 2784–2788.
- [25] She, G.W., et al. Controlled synthesis of oriented single-crystal ZnO nanotube arrays on transparent conductive substrates. Appl. Phys. Lett. 92 (2008): 053111/1–053111/3.
- [26] Li, Q.H., Liang, Y.X., Wan, Q., and Wang, T.H. Oxygen sensing characteristics of individual ZnO nanowire transistors. Appl. Phys. Lett. 85 (2004): 6389–6391.
- [27] Fan, Z., Wang, D., Chang, P.C., Tseng, W.Y., and Lu, J.G. ZnO nanowire field-effect transistor and oxygen sensing property ZnO nanowire field-effect transistor and oxygen sensing property. Appl. Phys. Lett. 85 (2004): 5923–5925.
- [28] Wang, H.T., et al. Hydrogen-selective sensing at room temperature with ZnO nanorods. Appl. Phys. Lett. 86 (2005): 243503–243505.
- [29] Kang, B.S., et al. Hydrogen and ozone gas sensing using multiple ZnO nanorods. Appl. Phys. A 80 (2005): 1029–1032.
- [30] Rout, C.S., Kulkarni, G.U., and Rao, C.N.R. Room temperature hydrogen and hydrocarbon sensors based on single nanowires of metal oxides. J. Phys. D: Appl. Phys. 40 (2007): 2777–2782.
- [31] Xu, J.Q., Chen, Y.P., Chen, D.Y., and Shen, J.N. Hydrothermal synthesis and gas sensing characters of ZnO nanorods. Sens. Actuators, B 113 (2006): 526–531.
- [32] Xu, J.Q., Chen, Y.P., Li, Y.D., and Shen, J.N. Gas sensing properties of ZnO nanorods prepared by hydrothermal method. J. Mater. Sci. 40 (2005): 2919–2921.
- [33] Wang, J.X., et al. Hydrothermally grown oriented ZnO nanorod arrays for gas sensing applications. Nanotechnology 17 (2006): 4995–4998.
- [34] Park, J.-H., Choi, H.-J., Choi, Y.-J., Sohn, S.-H., and Park, J.-G. Ultrawide ZnO nanosheets. J. Mater. Chem. 14 (2004): 35–36.

- [35] Tu, Z.C. First-principles study on physical properties of a single ZnO monolayer with graphene-like structure. J. Comput. Theor. Nanosci. 7 (2010): 1182–1186.
- [36] Morkoç, H., and Özgür, Ü. Zinc oxide: fundamentals, materials and device technology. Wiley–VCH Verlag, GmbH & Co, 2009.
- [37] Meyer, B., and Marx, D. First-principles study of CO adsorption on ZnO surfaces. J. Phys.: Condens. Matter 15 (2003): 89–94.
- [38] Zhang, Y., Wu, S.Q., Wen, Y.H., and Zhu, Z.Z. Surface-passivation-induced metallic and magnetic properties of ZnO graphitic sheet. Appl. Phys. Lett. 96 (2010): 223113–223116.
- [39] He, A.L., Wang, X.Q., Wu, R.Q., Lu, Y.H., and Feng, Y.P. Adsorption of an Mn atom on a ZnO sheet and nanotube: a density functional theory study. J. Phys.: Condens. Matter 22 (2010): 175501–175508.
- [40] Levine, N. Quantum chemistry. 6th edition. Pearson prentice hall, 2010.
- [41] Cramer, C.J. Essentials of computational chemistry: theories and models 2nd edition. Singapore: John Wiley and Sons, 2004.
- [42] Engel, T., and Reid, P. Physical chemistry. Pearson benjamin chummings, 2009.
- [43] Lewars, E. Computational chemistry. Canada: Trent University, 2003.
- [44] Frisch, M.J., et al. Gaussian 03, revision D.02, gaussian Inc. wallingford. CT, 2006.
- [45] Kong, S., Shenderovich, G., and Vener, M.V. Density functional study of the proton transfer effect on vibrations of strong (short) intermolecular O–H···N/O⁻···H–N⁺ hydrogen bonds in aprotic solvents. J. Phys. Chem. A 114 (2010): 2393–2399.
- [46] Wang, Z.L., et al. Semiconducting and piezoelectric oxide nanostructures induced by polar surfaces. Adv. Funct. Mater. 14 (2004): 943–956.



APPENDIX

ศูนย์วิทยทรัพยากร
จุฬาลงกรณ์มหาวิทยาลัย

APPENDIX A

Table A–1 Adsorption energies (ΔE_{ads} in kcal/mol) of various gases on CCL–ZnONS and energy gaps (ΔE_{GAP} in eV) of their corresponding adsorption complexes as the most stable configuration, compared to the bare surface of CCL–ZnONS, computed at the B3LYP/LanL2DZ level of theory.

CCL–ZnONS/gas adsorption	ΔE_{ads} (kcal/mol)	ΔE_{GAP} (eV)
<i>CCL–ZnONS:</i>		3.74
$\text{O}_2 + \text{CCL–ZnONS} \rightarrow \text{O}_2/\text{CCL–ZnONS}$	–38.83	2.95
$\underline{\text{CO}} + \text{CCL–ZnONS} \rightarrow \underline{\text{CO}}/\text{CCL–ZnONS}$	–5.83	3.70
$\underline{\text{CO}} + \text{CCL–ZnONS} \rightarrow \underline{\text{CO}}/\text{CCL–ZnONS}$	–4.07	3.56
$\underline{\text{H}_2\text{O}} + \text{CCL–ZnONS} \rightarrow \underline{\text{H}_2\text{O}}/\text{CCL–ZnONS}$	–14.08	3.76
$\underline{\text{NH}_3} + \text{CCL–ZnONS} \rightarrow \underline{\text{NH}_3}/\text{CCL–ZnONS}$	–14.08	3.76
$\text{H}_2 + \text{CCL–ZnONS} \rightarrow \text{H}_2/\text{CCL–ZnONS}$	–0.96	3.75
$\underline{\text{NO}} + \text{CCL–ZnONS} \rightarrow \underline{\text{NO}}/\text{CCL–ZnONS}$	–5.82	2.43
$\underline{\text{NO}} + \text{CCL–ZnONS} \rightarrow \underline{\text{NO}}/\text{CCL–ZnONS}$	–3.97	3.00
$\underline{\text{N}_2\text{O}} + \text{CCL–ZnONS} \rightarrow \underline{\text{N}_2\text{O}}/\text{CCL–ZnONS}$	–3.87	3.72
$\underline{\text{N}_2\text{O}} + \text{CCL–ZnONS} \rightarrow \underline{\text{N}_2\text{O}}/\text{CCL–ZnONS}$	–4.11	3.65
$\underline{\text{NO}_2} + \text{CCL–ZnONS} \rightarrow \underline{\text{NO}_2}/\text{CCL–ZnONS}$	–5.54	3.51
$\underline{\text{NO}_2} + \text{CCL–ZnONS} \rightarrow \underline{\text{NO}_2}/\text{CCL–ZnONS}$	–7.76	2.31

ศูนย์วิทยทรัพยากร
จุฬาลงกรณ์มหาวิทยาลัย

VITAE

- Name:** Miss BENJAWAN KAEWRUKSA
- Date of Birth:** November 8th, 1985
- Place of Birth:** Ubonratchathani, Thailand
- Address:** 104 Tessaban 64 Road, Ubonratchathani 34190, Thailand
- Telephone:** 087-2545820
- E-mail address:** miney_bow@hotmail.com
- Educations:**
- | | |
|-----------|---|
| 2009–2011 | M.Sc. (Physical Chemistry), Chulalongkorn University, Thailand |
| 2005–2008 | B.Sc. (Chemistry), Burapha University, Thailand |
| 2001–2004 | Leu Kumharn Warinchamlarp high school, Ubonratchathani, Thailand |
| 1998–2000 | Tessaban Warin Wichachart secondary school, Ubonratchathani, Thailand |
| 1992–1997 | Tessaban Warin Wichachart primary school, Ubonratchathani, Thailand |
- Presentations:**
- [1] Benjawan Kaewruksa, Vithaya Ruangpornvisuti, Theoretical investigation of gas-sensing properties of ZnO nanosheets (Poster Session): The 34th Congress on Science and Technology of Thailand (STT 36), October 26–28 2010 at Bangkok International Trade and Exhibition Centre (BITEC), Bangkok, Thailand.
- [2] Benjawan Kaewruksa, Vithaya Ruangpornvisuti, Potential energy surfaces for oxygen adsorption on various ZnO nanosheets (Poster Session): Pure and Applied Chemistry International Conference (PACCON 2011), January 5–7 2011 at the Miracle Grand Hotel, Bangkok, Thailand.
- Publication:**
- Kaewruksa, B., and Ruangpornvisuti, V. Theoretical study on the adsorption behaviors of H₂O and NH₃ on hydrogen-terminated ZnO nanoclusters and ZnO graphene-like nanosheets. J. Mol. Struct. In Press.